A SIMPLE ICE PHASE PARAMETERIZATION

By

Mark Argyle Stephens

Atmospheric Science
PAPER NO.
319

US ISSN 0067-0340

DEPARTMENT OF ATMOSPHERIC SCIENCE
COLORADO STATE UNIVERSITY
FORT COLLINS, COLORADO

A SIMPLE ICE PHASE PARAMETERIZATION

by

Mark Argyle Stephens

Research Supported by the

National Science Foundation
under grant
ATM77-09770

Department of Atmospheric Science
Colorado State University
Fort Collins, Colorado

December, 1979

Atmospheric Science Paper No. 319

ABSTRACT OF THESIS

A SIMPLE ICE PHASE PARAMETERIZATION

A two variable ice parameterization was developed for use in three-dimensional models of cumulonimbus clouds and mesoscale squall lines. Bulk water techniques were employed to simulate the growth and decay of snow crystals and of graupel in order to keep the use of computer resources to a minimum. An externally specified concentration of ice crystals was used to initiate snow. Graupel was assumed to follow the Marshall-Palmer distribution with a constant total concentration. Microphysical growth processes for snow included initiation from the vapor at liquid water saturation, riming, melting, vapor deposition and conversion of rimed crystals into graupel. The graupel microphysical processes that were modeled included raindrop freezing by contact with snow crystals, accretion of raindrops, vapor deposition, riming of cloud droplets and melting. Both types of ice were allowed to precipitate.

Sensitivity tests and internal consistency checks on the parameterization were done using a one-dimensional, time-dependent cloud model. Results suggested that the parameterization should simulate adequately the ice phase evolution in higher dimensional models. The parameterization is most suitable for modeling studies in which the major emphasis is on exploring the dynamic consequences of the ice

phase rather than exploratory studies in cloud microphysics. Several deficiencies of the parameterization were commented on, specifically: the use of an externally specified snow concentration and its influence on the conversion of snow into graupel. Comments were also made on how local changes in the snow concentration brought about by seeding, ice multiplication and aggregation could be handled in higher dimensional models.

Mark Argyle Stephens
Department of Atmospheric Science
Colorado State University
Fort Collins, Colorado 80523
Fall, 1979

ACKNOWLEDGMENTS

The author would like to express his appreciation to Dr. William R. Cotton for his valuable suggestions, guidance and encouragement. The author is also indebted to Mr. Gregory J. Tripoli for his untiring assistance and advice, and to Mr. Richard L. Hughes for many fruitful discussions. The efforts of Mrs. Bonnie Tripoli and Mrs. Lucy McCall in figure drafting and Ms. Polly Laun Cletcher in typing and preparation of the manuscript are deeply appreciated.

This research was supported by National Science Foundation Grant #ATM77-09770. Computer time was provided by the National Center for Atmospheric Science facility, Boulder, Colorado.

TABLE OF CONTENTS

TABLE OF CONTENTS (continued)

TABLE OF CONTENTS (continued)

LIST OF FIGURES

LIST OF FIGURES (continued)

LIST OF SYMBOLS

Symbol	Explanation	Value	Units
C	Capacitance analoque of vapor deposition		cm
C_D	Drag coefficient		
C_m	Fraction of snow mixing ratio used for conversion	1×10^{-2}	
C_{pd}	Specific heat of dry air at constant pressure	1.005×10^{7}	erg gm^{-1} K^{-1}
C_w	Specific heat of water vapor at constant pressure	4.186×10^{7}	erg gm^{-1} K^{-1}
D	Diameter of ice particle		cm
$\overline{D}$	Mean diameter of graupel distribution		cm
D_c	Mean diameter of cloud droplets		cm
d_g	Density of a graupel particle		gm cm^{-3}
d_ℓ	Density of liquid water	1.0	gm cm^{-3}
D_r	Diameter of a raindrop		cm
$\overline{D}_r$	Mean diameter of the rain distribution	0.054	cm
E_{gr}	Coallescence/collection riming efficiency of graupel		
$\overline{E}_{gr}$	Characteristic riming efficiency of graupel distribution		
$\hat{E}_{fr}$	Characteristic riming efficiency for snow		
e_{si}	Saturation vapor pressure over a flat ice surface		dynes cm^{-2}
e_{sw}	Saturation vapor pressure over a flat water surface		dynes cm^{-2}
$f(Re)$	Ventilation function		

LIST OF SYMBOLS (Continued)

Symbol	Explanation	Value	Units
$f(Re)_g$	Ventilation function for graupel		
G	Acceleration of gravity	980.0	cm s^{-2}
G(T,p)	Function of temperature and pressure for vapor deposition on ice		gm s^{-1} cm^{-2}
K	Molecular thermal conductivity of air	2360.0	erg cm^{-1} s^{-1} K^{-1}
K_v	Graupel velocity factor		$cm^{\frac{1}{2}}$ s^{-1}
$L_{\ell i}$	Latent heat of freezing		erg gm^{-1}
L_{vi}	Latent heat of sublimation	2.837×10^{10}	erg gm^{-1}
$\bar{m}$	Mean mass of graupel distribution		gm
m_f	Mass of an individual snow crystal		gm
$m_g(D)$	Mass of graupel particle as a function of diameter		gm
$m_r(D_r)$	Mass of a raindrop as a function of diameter		gm
MF	Total mass flux of graupel		gm cm^{-2} s^{-1}
N(D)	Marshall-Palmer distribution for graupel		cm^{-4}
N_{of}	Total concentration of snow at 0C	10^{-8}	cm^{-3}
N_{og}	Slope intercept of graupel distribution		cm^{-4}
N_{or}	Slope intercept of raindrop distribution		cm^{-4}
$N_r(D_r)$	Marshall-Palmer distribution for rain		cm^{-4}
N_{tc}	Total concentration of cloud droplets		cm^{-3}
N_{tf}	Total concentration of snow		cm^{-3}
N_{tg}	Total concentration of graupel	10^{-4}	cm^{-3}

Symbol	Explanation	Value	Units
p	Total pressure of air		dynes cm^{-2}
P_{oo}	Pressure of air at sea level	10^6	dynes cm^{-2}
q_c	Cloud water mixing ratio		gm gm^{-1}
q_f	Snow ice mixing ratio		gm gm^{-1}
q_g	Graupel ice mixing ratio		gm gm^{-1}
q_r	Rainwater mixing ratio		gm gm^{-1}
q_{si}	Ice saturation mixing ratio		gm gm^{-1}
q_{sw}	Water saturation mixing ratio		gm gm^{-1}
q_v	Water vapor mixing ratio		gm gm^{-1}
R_a	Gas constant for dry air	2.878×10^6	cm^2 s^{-1} K^{-1}
Re	Reynold's number for an ice particle		
S_{fglac}	Source of snow mixing ratio from ice saturation thermodynamics		gm gm^{-1} s^{-1}
S_{fmelt}	Sink of snow mixing ratio due to melting		gm gm^{-1} s^{-1}
S_{fnich}	Source of initial snow mixing ratio		gm gm^{-1} s^{-1}
S_{frim}	Source of snow mixing ratio from riming of cloud droplets		gm gm^{-1} s^{-1}
S_{fvdep}	Source of snow mixing ratio from vapor deposition		gm gm^{-1} s^{-1}
S_{gconv}	Source of graupel mixing ratio from conversion of snow crystals		gm gm^{-1} s^{-1}
S_{gmelt}	Sink of graupel mixing ratio due to melting		gm gm^{-1} s^{-1}
S_{grcol}	Source of graupel mixing ratio from rain drop collection		gm gm^{-1} s^{-1}

Symbol	Explanation	Value	Units
S_{grfrz}	Source of graupel mixing ratio from raindrop freezing by snow crystal contact		gm gm^{-1} s^{-1}
S_{grim}	Source of graupel mixing ratio from riming of cloud droplets		gm gm^{-1} s^{-1}
S_{gvdep}	Source of graupel mixing ratio from vapor deposition		gm gm^{-1} s^{-1}
SS	Ice supersaturation		
STK(D)	Potential flow Stokes number		
STK_E	Characteristic Stokes number for graupel		
T	Cloud temperature		K
T_f	Freezing point of water	273.16	K
v_f	Snow terminal velocity		cm s^{-1}
$v_g(D)$	Graupel terminal velocity		cm s^{-1}
$\bar{v}_g$	Mass weighted terminal velocity of graupel		cm s^{-1}
$v_r(D_r)$	Raindrop terminal velocity		cm s^{-1}
$\bar{v}_r$	Mass weighted terminal velocity of rain		cm s^{-1}
w	Vertical velocity		cm s^{-1}
β	Exponential factor of snow concentration	0.6	K^{-1}
$\Gamma( )$	Gamma function		
δt	Current model time step		s
ε	Ratio of molecular weights of water to air	0.622	
λ	Slope of graupel Marshall-Palmer distribution		cm^{-1}

Symbol	Explanation	Value	Units
λ_r	Slope of rain Marshall-Palmer distribution	18.52	cm^{-1}
μ	Dynamic viscosity of air		$gm\ cm^{-1}\ s^{-1}$
π	Ratio of the circumference of a circle to its diameter	3.14159	
ρ_a	Density of dry air		$gm\ cm^{-3}$
ρ_c	Cloud water content		$gm\ cm^{-3}$
ρ_f	Snow ice content		$gm\ cm^{-3}$
ρ_g	Graupel ice content		$gm\ cm^{-3}$
ρ_r	Rainwater content		$gm\ cm^{-3}$
ρ_v	Water vapor content		$gm\ cm^{-3}$
ψ	Diffusivity of water vapor in air		$cm^2\ s^{-1}$

1.0 INTRODUCTION

The ice phase plays an important role in convective dynamics. The freezing of water drops and the deposition of water vapor onto ice particles both contribute to latent heat release to enhance cloud growth. Due to the fact that large ice particles (e.g., hail) do not easily break up and they do not deform with their major axis against the flow as do rain drops, ice particles fall at higher terminal velocities. They thus can play a dominant role in altering the distribution of total water, and subsequently the formation and extent of downdrafts as well as the amount of precipitation at the ground. Indeed, observations by Knight et al.(1974) show graupel and hail to be the main source of hydrometeor formation in Great Plains thunderstorms. Current attempts toward the beneficial modification of cumulus clouds utilize the freezing of the supercooled liquid phase to obtain increases in the amount of precipitation on the ground or to suppress the formation of hail.

If computer models are to simulate the dynamics and microphysics of convective clouds and convective mesoscale systems faithfully, the ice phase must be included. The purpose of this thesis is to develop an ice phase parameterization for use in three-dimensional time dependent models of cumulus clouds; specifically, the larger, cumulonimbus thunderstorms and mesoscale squall lines.

2.0 LITERATURE REVIEW

Modeling of the ice phase in convective clouds has, for the most part, depended on the use of the computer. Even the investigation of the growth of individual snow crystals can become too complex for an analytical study and certainly the study of the effects on the dynamics of ice (and vice versa) within thunderstorm systems demands use of all computer resources available today. Indeed, the investigation of ice in convective clouds has grown with the availability of computer resources. Not that the computer is the dominant restraint on research into the ice phase. The complex nature of clouds of any sort coupled with the difficulties (and expense) in obtaining field data severely limits the ability to compare computer results on hypothetical ice phase processes with what actually occurs in nature. The study of the ice phase still is in its infancy.

Although the full use of computer resources is necessary for some studies into the ice phase, much research has been done using models which are less restrictive on computer resources. The investigation of individual snow crystals (e.g., hexagonal plates, columns, dendrites, etc.) can be done by simulating their growth at a constant level in the atmosphere. Such studies concentrate on the environmental factors influencing the shape, mass and growth rates of snow crystals and not the effects such crystals have on the environment. An important factor arising from these investigations is the time at which a snow crystal becomes big enough to rime. In continental precipitatation regimes, where the availability of large supercooled liquid drops which can be

frozen is virtually absent, snow crystal riming into spherically shaped particles (i.e., graupel) is the only means of initiating precipitation.

Jayaweera (1971) predicted the growth of snow crystals at constant temperature, pressure and liquid water saturation. Using empirical studies on the shapes of snow crystals nucleated and grown at a certain temperature, he then could calculate the rate of crystal growth as a function of time and temperature by assuming Fickian diffusion (a balance between the rates of heat and mass transfer) and the analogue between the electrostatic potential field surrounding a changed body and the vapor field surrounding a snow crystal. Although riming was not allowed, using data taken by Ono (1969) on the size threshold where crystals began to rime (about 300μm), Jayaweera grew crystals to riming size in 3.3 min and 8.3 min for hexagonal plates grown at -11 and -18C, respectively, and 6.7 min for columns.

Koenig (1971), using similar assumptions on crystal shape and growth in a constant environment, produced crystals which could begin to rime in an average time of two to six minutes, in agreement with Jayaweera. Koenig also reduced his computed data into a parameterization of the growth rate as a function of temperature and crystal mass. His parameterization could then be used to investigate snow crystal growth for larger scales in the atmosphere for models which cannot compute the growth of individual snow crystals directly.

By using an empirical numerical approximation of snow crystal growth along the major and minor axes which depended only on the environmental temperature and the time after nucleation, Hindman and Johnson (1972) investigated the time needed to grow snow crystals to riming size and the time to grow crystals into graupel and hail within

a field of supercooled cloud droplets. The onset of riming was studied in a more natural way than the two previous papers by assuming a distribution of cloud droplets, a crystal fall velocity, and an efficiency of riming. The riming threshold was crossed when growth along the axis growing both by diffusion plus accretion increased that axis by 1 μm over that of growth by diffusion alone. The threshold times were somewhat less than those found for Koenig or Jayaweera, taking one to three minutes, and were little affected by changes in the cloud water content. Graupel formed when the two axes became equal and took from three to ten minutes at cloud water contents of 1gm m^{-3}.

Steady state (streamline) computer models of convective flow have been used extensively in the study of the growth of hail. Again, such models investigated the growth of individual or groups of particles and not the effects of the ice phase on the dynamics. Although not considered ice parameterizations per se, they were useful in giving information on the growth of hail which any ice parameterization developed for convective clouds should tend to duplicate. Many different environments, hail embryo release points within the domain and concentrations of hail (including a concentration of one) have been tried using these one-dimensional models. The only growth mechanism in the following papers was by cloud droplet riming.

Gokhale and Rao (1969) assumed hail embryos to be produced by the freezing of raindrops at the top of a cloud and followed the growth of the hailstone by liquid water accretion until it reached the melting level. List, et al., (1968) studied the effects of differing concentrations of hailstones by ejecting them into the flow at the OC

isotherm and studied their growth during ascent. Charlton and List (1972) also studied hail size distributions by ejecting into the flow embryos at the OC isotherm, but allowed the liquid water content (LWC) to be depleted by the growing stones. All these models concluded two important points about the growth of hail: that large hail (>1cm in diameter) could be grown in a short amount of time (ten to twenty minutes) without complex trajectories and without large LWC (disputing the claim of the Russian hail suppression studies, c.f. Sulakvelidze, et al., 1967).

Using a two-dimensional streamline model based on field data of LWC and velocities as measured by aircraft and radar, English (Chisholm and English, 1973) attempted to produce hail of a similar size as found on the ground. The individual hailstones were allowed to grow by cloud droplet riming by simulating both wet and dry growth regimes based on a calculation of the surface temperature of the stone, a more realistic way of differentiating between wet and dry growth than had been used previously. She found that while in the main updraft, the embryos, growing by collection of supercooled water, reached a height where their size and assumed concentration produced a radar echo. They continued to grow by falling along the sides of the updraft, forming a precipitation cascade. This was consistent with radar studies of the convective storms used in the study in which there was a weak echo region (WER), consisting of the main updraft, bounded by regions of higher reflectivity. English could grow hail three to six centimeters in diameter (within the range found on the ground) in nine to twenty-eight minutes from a simple up-down trajectory.

Understanding the nature of hailstone growth was a first step in studying hail suppression concepts. Using vertical profiles of velocity, Young (1975) followed a non-precipitating parcel containing 550 differing size categories of condensate. Snow crystals were represented by 400 categories with the rest divided between cloud droplets, rain and graupel. The model was used to study two hail suppression concepts: Hail embryo competition and complete glaciation of updrafts. Young concluded that natural hail embryo formation was most likely to occur in cells with low updraft speeds (3-4m s^{-1}) since the residence time of the particles from which embryos arose was long enough to produce millimeter sized hail embryos. Seeding such a cell to increase the number of embryos must produce a narrow size spectrum in order for competition to be effective, or else preferential growth would be given to those stones having the largest diameters. The spectrum must remain narrow after the cell either increases in strength, or feeds into a main updraft. Thus embryo competition was determined to be a more expedient method of hail suppression in storms growing hail in simple up-down trajectories, e.g. multicell storms, but could produce an increase in storms with complex hail trajectories. For such storms, e.g. supercell, the complete glaciation of embryo forming cells adjacent to the main updraft was determined to be a way to produce a decrease in hail.

Streamline models by their very nature are incapable of simulating the influence of the ice phase on the dynamics. The first step in such a simulation can be made by one dimensional lagrangian models (1DL) which give temperature and vertical velocity profiles with height by following the ascent of a parcel in the atmosphere. Since in using such

a model one is following a single point, realistic precipitation fall-out cannot be accomplished.

Simpson and Wiggert (1969) used a 1DL model to investigate the effects of latent heat released by seeding on cumulus clouds. At the time their model was formulated, there was a dearth of information on the ice phase and its simulation was primitive. Both rain and ice followed inverse exponential (Marshall-Palmer) distributions and both grew from the cloud water by autoconversion and collection. To simulate seeding, an ice initialization began at the -4C isotherm. Seeding was accomplished by linearly decreasing a pre-specified percent of the cloud water between the -4 and -8C isotherms, thus rapidly releasing latent heat. Within this temperature range, the cloud linearly transformed from water to ice saturation. Precipitation of rain and ice was accomplished by setting the amount of water dropped out of the parcel as equal to the time taken by the parcel to rise an increment of height divided by the time taken by a volume median diameter particle to fall one cloud radius. Thus, precipitation amount was correlated, somewhat, to the updraft speed and a characteristic fall speed of rain or ice.

The difference in the amount of water precipitated and in the cloud top height was found for seeded and non-seeded runs. The main effect of seeding supercooled cumuli in the tropics (the soundings used came from Miami, Florida) was through the alteration of cloud dynamics and thus an alteration in the water carried and precipitated. Defining favorable seeding conditions as an increase in precipitation brought about by seeding, the authors concluded that favorable conditions arose, for clouds having natural cloud top heights around 6 and

7 km, when the model demonstrated large vertical growth differences occurring between simulated seeded and non-seeded runs. When this difference is low and when natural clouds already exhibit large vertical growth (around 8 to 10km) then conditions were unfavorable for seeding and precipitation tended to be 'hung up' in the cloud in the form of ice.

Cotton (1972) also developed a parcel model to investigate, in a more sophisticated and realistic way than Simpson and Wiggert, the effects of seeding. Ice was divided into two basic types: Snow crystals and frozen rain (graupel). Due to better field data, Cotton could divide the snow crystals into 21 classes based on temperature to include hexagonal plates, dendrites, and prism-type crystals. Graupel, as well as rain, was considered to follow the Marshall-Palmer distribution while snow crystals were considered mono-disperse with a specified external concentration, based on the nucleation temperature of depositional nuclei, giving an order of magnitude increase to the concentration for every 4C drop in temperature. Important ice phase processes included were cloud droplet riming onto ice, vapor deposition and the freezing of supercooled raindrops by activation of a heterogeneous nucleant, or from contact with a snow crystal. Ice saturation thermodynamics were permitted when the cloud water became zero at temperatures below freezing. For rain and graupel, precipitation was accomplished by dropping out of the parcel that portion of the distribution with diameters producing fall speeds greater than the updraft speed of the parcel. By changing the parameters of the snow crystal concentration, seeding was simulated with an increase in the number of crystals present at a

given temperature. Cotton found that the main effect of seeding maritime clouds was to increase the cloud top height and that the principal mechanism responsible for this enhancement was the increased freezing of raindrops from crystal contact. Clouds containing small amounts of rain were dynamically insensitive to moderate increases of snow crystals.

In a model developed by Danielsen, et al., (1972) to study the growth of hail, parcels were released from the surface every 30 seconds. Thus, this model could be considered a hybrid between Lagrangian and one-dimensional time dependent models. Its advantage over the previous parcel models was in the precipitation process; precipitation falling out of a parcel could influence parcels below it. The model would have tended toward a steady-state except for the influence of the precipitation and the varying water loading produced by growing hydrometeors. Hail and liquid water (cloud and rain) were divided into differing mass categories (40 for hail and 31 for liquid water) and growth was simulated stochastically, as opposed to the bulk water techniques used by Simpson and Wiggert, and by Cotton. Hail was initialized by the probability of a liquid water drop freezing by homogeneous and heterogeneous freezing. Growth of hail continued by stochastic collection and by vapor deposition. Only the cloud radius at the ground, mixing coefficients and the cloud droplet distribution were arbitrarily specified in initializing the model. By varying the initial cloud droplet distribution, its subsequent effects on hail were investigated. The authors found that hail number and mass were increased by the the presence of large liquid drops in the initial droplet distribution. They also found, confirming previous results from the streamline models

reviewed above, that large LWC were not necessary to produce large hail and that ice, not water, collected above the updraft maximum. Indeed, hail growth was restricted to updraft speeds large enough to support a growing hail embryo, but not large enough to sweep it above the updraft maximum and thus out of the major growth region. Hail growth depended on updraft speeds, the initial droplet distribution, the surface mixing ratio (increases in this quantity producing increases in the size of the liquid drops through condensation), and the height above cloud base at which liquid drops began to freeze. All these factors combined to control the time and level in the cloud where collection of liquid drops by hail became the dominant growth process.

The importance of including a time dependency for simulating the ice phase was demonstrated in the one-dimensional time dependent (1DT) model of Weinstein (1970). Weinstein studied the effects of seeding on precipitation and cloud dynamics in a similar fashion to Simpson and Wiggert. He simulated seeding by simultaneous freezing of all cloud water at pre-selected temperatures (-4 to -10C) and times. Rainwater was not included in the freezing process. Weinstein found that seeding did not produce a one-to-one correspondence between cloud top height increases due to seeding and increases in the amount of precipitation. Not only was the temperature at which seeding was done important, but also the time of seeding. Low seeding temperatures (around -10C) succeeded in producing vertical velocity increases high in the cloud which tended to decouple the updraft from the bottom part of the cloud. Rain was then carried upward and 'hung up' in this region of lessened condensate production (relative to the lower reaches of the domain where the difference between ice saturation and water vapor were

greater). Thus, precipitation was decreased, even though the model responded with cloud top height increases, due to the low growth rates and a greater distance needed to reach the ground. Should seeding have been done during the decay stage of the cloud, part of the latent heat release due to freezing went into overcoming the deaccelerating updraft and resulted in a decrease in precipitation when compared to seeding during the active stages of cloud growth.

One-dimensional time-dependent models do not simulate well the dynamics of convective clouds. Their less restrictive use of computer resources, as opposed to higher dimensional time-dependent models, allow many more runs to be made for parameterization testing purposes. For example, Wisner, et al., (1972) developed a hail parameterization which was eventually used in a two-dimensional time-dependent (2DT) model (c.f. Orville and Kopp, 1977, below). One-dimensional models also allow a better simulation of the microphysics since one often has the computer resources needed to include more variables.

Scott and Hobbs (1977) presented a 1DT model whose emphasis was on the microphysics. Liquid water, snow and graupel were divided into many different size categories. The only initial microphysical inputs needed were the spectrum of cloud condensation nuclei, snow crystal depositional nuclei, and the probability that a liquid drop would freeze by containing an active heterogeneous nucleant. Snow crystals grew by vapor deposition and by riming cloud droplets. Their mass and number were also increased by the Hallett and Mossop (1974) ice multiplication process. Graupel was produced by the freezing of large drops (by either heterogeneous nucleation or by contact with a snow crystal) and grew

by liquid water accretion and by vapor deposition. Aggregation of snow crystals and the formation of graupel by snow crystals riming into spherical ice particles were also included.

They found that the predominant ice particle in the maritime simulation was graupel, which contained greater than 50% of the total ice mass and 10% of the total condensate. On the other hand, for the continental cloud simulation, ice as a whole contained only 0.01% of the total condensate with graupel greater in mass (but not in number) than snow crystals. This difference in the two precipitation regimes resulted from the greater number of large liquid drops formed in the maritime cloud. Graupel produced from the freezing of these large drops could begin to rime immediately. By contrast, in the continental cloud the time lag between snow crystal production and snow crystal riming resulted in a delay in graupel formation. Since the ice multiplication process was dependent on drops greater than 23 μm, the difference in the drop spectrum between maritime and continental clouds also controls the increase in the snow crystal concentration. For the continental cloud, the concentration of snow crystals increased little while the maritime cloud produced increases of 20-60% prior to sixty minutes of cloud integration time. The authors found that production of splinters by ice multiplication depended on there being enough time for the graupel to grow large enough to fall through the updraft into the major ice multiplication region (-3 to -8C). Once this occurred, a chain reaction was created whereby the graupel accreted liquid drops to create ice splinters. These splinters then grew by vapor deposition into snow crystals large enough to be accreted by large liquid drops which, in turn, were frozen into graupel.

Seeding was accomplished by supplying 10 μm spherical crystals to the cloud in concentrations of 1 to 250 per liter at various times and heights. The authors found large increases in graupel were produced by seeding at the top of the maritime cloud and at the bottom of the continental cloud. Seeding at the top of the maritime cloud froze large drops which then reached a balance level within the updraft. They eventually grew big enough to fall through the updraft and reach the -3 to -8C ice multiplication region, thereby further increasing the graupel via the cycle described above. By seeding at the bottom of the continental cloud, the crystals thus introduced grew primarily by riming into larger graupel particles.

From the above discourse, one can notice the great emphasis on the microphysical aspect of cumulus clouds and not on the dynamics. Scott and Hobbs themselves point out that emphasis should be placed on trends and relative changes of the microphysics. A 1DT model cannot simulate rotations or complex trajectories as seen in natural clouds. Indeed, Cotton (1975) pointed out that 1DT models are incapable of simultaneously predicting consistent correct LWC and cloud top height. It then seems necessary to investigate cumulus clouds using higher dimensional models. The interaction between the microphysics and the dynamics is important in modeling cumulus convection. Unfortunately, both make heavy demands on computer resources in order to obtain a proper simulation. In using two- or three-dimensional time-dependent models on present day computers, one is faced with two choices: Emphasize the dynamics by parameterizing the microphysics, or emphasize the microphysics by restricting the dynamics.

Takahashi (1976) developed an axisymmetric two-dimensional time-dependent (2DT) model simulating the ice phase using stochastic growth equations for the microphysics similar to those of Scott and Hobbs (1977), with the exception of snow crystal aggregation. Takahashi allowed drop freezing by Brownian, thermophoretic and diffusiophoretic collection of contact nucleants and also included the Hallett and Mossop (1974) ice multiplication process. He used a total of 135 size classes to describe spherical hydrometeors (liquid drops, graupel and hail) and 105 classes to describe snow crystals (assumed to be disk-shaped). The emphasis here was clearly on the microphysics. In order to be able to integrate the extensive microphysical equations, the domain was quite small: 6km in height and 2km in radius with 200m spacing between grid points giving a total of 341 points. Such a small domain precluded realistic simulation of the dynamics.

Orville and Kopp (1977), on the other hand, placed their emphasis on simulating a large hail storm using a 2DT slab-symmetric model. Their domain was a 20km square grid with 200m spacing between grid points. It contained substantially more grid points (10201) than did Takahashi. With such a large number of grid points, the microphysics were limited to only four variables: Non-precipitating liquid water (cloud droplets), precipitating water (rain), non-precipitating ice (cloud ice) and precipitating ice (hail). Rain and hail were both assumed to have an inverse exponential distribution (Marshall-Palmer) with constant slope intercepts.

Cloud ice was used to control glaciation and was initialized by the freezing of all cloud water advected above the -35C isotherm. Hail

formed from heterogeneous raindrop freezing and by a simulated Bergeron precipitation process of cloud droplet riming onto an implicit number of snow crystals and by the use of Koenig's (1971) parameterization of snow crystal vapor depositional growth. The number of snow crystals was given by Fletcher's (1969) concentration of depositional ice nuleants which gave an order of magnitude increase to the concentration for every 4C drop in temperature. Wet and dry growth of hail from liquid water accretion was the major source of hail mass. Other microphysical processes included were cloud ice accretion by hail, autoconversion of cloud water to rain, cloud droplet accretion by rain, melting of hail and cloud ice, rain evaporation and hail sublimation.

Koenig (1977) also used an axisymmetric 2DT model to investigate the ice multiplication process using the Hallett and Mossop scheme. His domain was larger than that of Takahashi being 9km in height and 6km in radius with 200m spacing between grid points, a total of 1426 points. Although integration was done over a smaller number of grid points than those used by Orville and Kopp, Koenig uses only six microphysical variables: cloud water, rainwater, type A ice (produced by depositional nucleants and ice splinters), type B ice (produced by the freezing of large liquid drops), and the concentrations of type A and B ice. Rain was formed from cloud water by autoconversion and continued to grow by cloud droplet accretion. Type A ice was initiated by assuming the activation of depositional nucleants, dependent on temperature, given as a rate of increase to the concentration of type A ice and by the formation of ice splinters from the ice multiplication process. Type B ice was initiated by raindrop freezing from contact with type

A ice. Vapor deposition and cloud droplet riming processes were done separately, for ice types A and B, by using the parameterization developed by the author (Koenig, 1972). Melting of ice and the evaporation of liquid water were also included.

Koenig did not stress the importance of recycling hydrometeors in the formation of graupel as did Takahashi (c.f, below), although some recycling must have occurred. Instead, he concentrated on the increases in the type A ice concentration from ice multiplication and the processes which led to complete glaciation of the cloud. Due mainly to the creation of large precipitating drops (rain) for the maritime cloud simulation (which had a lower concentration of cloud droplets and thus a higher autoconversion rate), type B ice formed early in the integration by rainwater freezing from contact with type A ice. A similar chain reaction to that found by Scott and Hobbs (1977) was predicted. These large ice particles rimed cloud droplets to produce ice splinters by the multiplication process which, in turn, were collected by rain to freeze into more type B ice. The multiplication process thus produced large increases in type A ice concentration. Koenig found an increase to this concentration due to type A ice crystals falling from regions of lower temperatures into the ice multiplication area (-3 to -8C). The continental cloud simulation, with its lower production of rain by autoconversion, did not produce as large an increase as did the maritime cloud. Thus, the ice multiplication process, according to Koenig, was dependent on the formation of large drops. It was also dependent on the updraft speed; high vertical velocities would sweep the type A ice and any splinters produced into the upper reaches of the cloud and away

from the main ice multiplication region. Thus, ice multiplication brought about large increases to the type A ice concentration after the vertical velocity had begun to decrease, hence, during the decay stages of the cloud. This also had an effect on the rate of glaciation. The large amounts of type B ice formed by the ice multiplication cycle rapidly collected both rain and cloud drops. The cloud became glaciated within the ice multiplication region and spread to other parts of the cloud and eventually caused the complete freezing of all liquid water. Thus, the rapidity of glaciation depended on the presence of high concentrations of both small and large drops and on the ice multiplication process.

Takahashi found that, during the early growth stages of the cloud, snow crystals were advected upward into the top portions of the cloud, fell with the downdraft and were recycled back into the updraft, a similar process as found by Koenig. This allowed the crystals to have a longer riming time than would have occurred without recycling. They eventually became large enough to be considered graupel, which formed mainly along side the updraft. This graupel strengthened the downdraft and was also recycled back into the updraft. Those graupel particles which were recycled above the melting level produced ice splinters as they rimed with cloud droplets (the ice multiplication process). At -5C, recycling of snow crystals and the production of ice splinters increased the snow crystal concentration three orders of magnitude higher than given by the number of depositional nucleants. Graupel which fell below the melting level created drops which broke up to form relatively large-sized drizzle. Some of this was recycled back into

the updraft and accreted cloud droplets to form large drops. These drops were, in turn, accreted by graupel to form relatively large hail. The main conclusion drawn by Takahashi was the importance of recycling in the creation of hail in a cumulus cloud.

As mentioned before, the main emphasis in Orville and Kopp was on the natural simulation of a hail storm. Their large domain and the use of slab-symmetry allows a more realistic circulation to form. While both Takahashi's and Koenig's circulation was restricted by their use of small domains and their assumptions of axisymmetry to a circular pattern (updraft in the center and downdraft closer to the side), Orville and Kopp's initial circulations took the form of a cycle of small cumuli cells which grew upwards until they spread out underneath a mid-level inversion. Under the influence of continued surface heating, used to initialize the clouds (a momentum impulse was used to initiate the 2DT axisymmetric models), coupled with the continuing moistening below the inversion the circulation finally broke through to create a vigorous storm circulation. Precipitation formed, small amounts of which were stripped by the updraft to be swept into the divergent zone at the top of the storm to form a radar overhang lower in the cloud. A cascade of precipitation also formed along side the main updraft. Both these phenomena were observed in nature as was the gust front created by the cooling and water loading of hydrometeors. The gust front was crucial to the continuation of the circulation. Its movement out of the domain signaled the demise of the storm. There was recycling of both rain and hail; falling rain was advected into the updraft from below, while hail was advected from above.

One can easily note the differences between these 2DT models. All the authors point out similarities between results obtained in the model with observations in the field. Takahashi and Koenig both note that their models were capable of obtaining observed increases in snow crystal concentrations by the use of the Hallett and Mossop ice multiplication scheme and by the recycling of crystals from above. Orville and Kopp found their model predicted many observed dynamically induced features, e.g., radar overhang, the formation of pedestal and shelf clouds, gust front, etc. Little insight in microphysical processes not already 'built in' to the parameterizations could be obtained since there was no evolution of particle spectrum. Likewise, Takahashi and Koenig could not draw many conclusions on the effects of the microphysics on the dynamics; mainly because their domains were too limited in extent and their assumption of axisymmetry restricted the circulation to an updraft at the center and downdraft at the side. Indeed, Takahashi's great emphasis on the effects of recirculation of snow crystals in the formation of graupel may have been somewhat unjustified. Hydrometeors were forced into a recycling pattern due to the pattern of the circulation. On the other hand, it was important to note that, regardless of the restricted circulation, snow crystals were able to present themselves for a recirculation process, e.g., they did not cease to exist by melting or sublimation.

Using Takahashi's microphysics in a 2DT slab-symmetric model (or better yet, a 3DT model) would quantify the effects of recycling in a more realistic manner. It must be pointed out that to do so in a domain the size of Orville and Kopp's cannot be done using present day

computers and it is quite likely that a complete dynamical and microphysical simulation of a large, mesoscale hail storm cannot be done in the near future.

As yet, no descriptions of three-dimensional time-dependent (3DT) models of cumulus convection containing the ice phase have been published. The importance of including the effects of ice in such models was demonstrated by Miller (1978) who developed a 3DT cumulus model containing only liquid microphysical parameterizations. A first attempt by Miller to simulate a steady, long-lived circulation over London, England failed to produce the observed storm duration, rainfall amount and outflow pattern at the surface, even though the computed circulation produced deep, moist convection. Miller then used the arbitrary procedure of doubling the raindrop fall velocity to simulate the fallout of hail. This so altered the computed flow field that the observed storms activity was well simulated. It should be pointed out that this did not allow latent heat release due to the ice phase to occur and that there was no way to specify in which regions within the cloud the raindrop fall velocity should have been doubled. Even though the observed storms activity was apparently simulated by increasing the rain terminal velocity, this might well have been a fortuitous result. Certainly, more credence and confidence in the model's results would have resulted by explicitly including the ice phase.

It is, therefore, the objective of this thesis to develop a simple ice phase parameterization which can simulate some of the most important effects of the ice phase on convective storm dynamics.

3.0 FORMULATION OF THE PARAMETERIZATION

From the above review, what then are the important aspects of the ice phase to be included in a 3DT model of cumulus convection? The main restraint placed on the extent of parameterization of the ice phase is on the size of the domain to be used in simulating the convective activity. The ice phase parameterization developed here is to be used in a model whose domain will be large enough to allow the simulation of a large thunderstorm in three dimensions (c.f., Cotton and Tripoli, 1978). This greatly restricts the number of variables containing the effects of ice and makes substantial parameterization of the ice phase necessary.

An ice phase parameterization, similar to that of Orville and Kopp (1977), is developed using at most two ice microphysical variables and bulk water techniques. The important ice phase particles considered are snow and graupel (or hail). The inclusion of some form of snow crystal is important. Snow crystals, due to their relatively high concentration, are the major ice particles controlling ice saturation thermodynamics analogous to the role of cloud droplets in dominating the condensation process. Snow crystals also initiate precipitating ice (graupel) by riming into large quasi-spherical particles and by the contact freezing of raindrops. Graupel (or hail) is the dominant sink of cloud water for the ice phase, releasing latent heat and producing substantial ice loading. Its high fall speed is expeditious in obtaining precipitation at the ground. Indeed, graupel can often be the only means of achieving precipitation in cold-base continental cloud regimes, e.g., Great Plains thunderstorms (Knight et al., 1974).

The important ice phase processes to be used in formulating the parameterization are:

1. Snow crystal initation by external specification of primary ice crystal concentrations which have been activated by depositional nucleation or condensation/freezing or by freezing of cloud droplets.
2. Graupel initiation by rimed snow crystals.
3. Graupel initation by the freezing of supercooled raindrops. from snow crystal contact.
4. Rain accretion by graupel.
5. Cloud droplet riming onto ice particles.
6. Vapor deposition and sublimation.
7. Melting of ice particles.

Ice multiplication, specifically the Hallett and Mossop (1974) scheme, will not be explicitly modeled, even though its importance in graupel production and rapidity of glaciation have been demonstrated by several authors (Scott and Hobbs, 1977; Takahashi, 1976; Koenig, 1977). This is due mainly to the restriction of the number of prognostic variables used. How ice multiplication might be simulated in higher dimensional models will be discussed in a later section.

3.1.0 Snow

Snow crystals will be represented by hexagonal plates only. This is done for several reasons. At each grid point in the model, the only information known about snow crystals will be their ice mixing ratio (or ice content); no record of crystal type or by what process the

crystal obtained its mass and shape can be kept. Since the initial shape of the crystal is determined by the environmental temperature (and perhaps the amount of ice supersaturation), advection of the ice mass into a region of different temperature would change the shape of the crystal. The equations describing mass versus crystal shape for hexagonal plates are more tractable; only a diameter versus mass is needed to obtain a vapor depositional rate, whereas an additional equation giving length versus mass is needed for column-shaped crystals. Another consideration is that in their 1DT cumulus model, which included both hexagonal plates and columns, Scott and Hobbs (1977) found that 90% of the graupel obtained from snow crystal riming originated as hexagonal plates. Assuming only hexagonal plates can imply an overestimate of the riming rate for snow crystals, since column-shaped crystals present a smaller surface area for riming.

3.1.1 Concentration of snow crystals

The assumed concentration will be a mono-disperse collection of homogeneous snow crystals (e.g., hexagonal plates). Thus, only the total concentration of the crystals need be given. The concentration is an externally defined function and can be constant or dependent on temperature, ice saturation, or, perhaps, seeding effects. For testing purposes, the concentration will be assumed equal to the number of depositional nucleants given by the equation derived by Fletcher (1969):

$$N_{tf} = N_{of} e^{\beta(T_f - T)} \qquad (3.1)^*$$

---

*All units, unless otherwise specified, are c.g.s.

where $N_{of} = 10^{-8} cm^{-3}$ and $\beta = 0.6K^{-1}$, as given by Fletcher. These values produce an order of magnitude increase to the concentration for approximately every 4C decrease in temperature.

3.1.2 Equations of mass versus diameter

From the concentration and snow ice content, the mass of an individual snow crystal is

$$m_f = \rho_f / N_{tf} = q_f \rho_a / N_{tf} \tag{3.2}$$

Equations of mass versus diameter of the plate are derived from observations of hexagonal plates. The diameter is used to obtain rates of vapor deposition and riming. Three types of crystals are included: Unrimed hexagonal plates, lightly rimed hexagonal plates and graupel-like snow of hexagonal type. Following the a priori decision that riming will produce the larger, more massive crystals, the type of crystal assumed to exist at a grid point is determined by m_f. Decisions are based on smoothness of transition between the types and by the limits of crystal mass found by observation. For an m_f below 1.7×10^{-7} gm, the equations for unrimed hexagonal plates are (Hobbs, et al., 1972):

$$D = 51.5\ m_f^{\frac{1}{2}} \tag{3.3}$$

$$v_f = 304.0\ D \tag{3.4}$$

where D is the diameter and v_f the terminal velocity.

For masses greater than 1.7×10^{-7} gm, but less than 1×10^{-5} gm, the equations for lightly rimed plates are (Hobbs, et al., 1972):

$$D = 19.2\, m_f^{\frac{1}{2}} \tag{3.5}$$

$$v_f = 1250.0\, D \tag{3.6}$$

For masses greater than 1×10^{-5} gm, the equations pertaining to graupel-like snow of hexagonal type are (Locatelli and Hobbs, 1974):

$$D = 8.89\, m^{0.417} \tag{3.7}$$

$$v_f = 153.0\, D^{0.25} \tag{3.8}$$

Since the terminal fall speeds are valid at a pressure of one atmosphere (e.g., $p_{oo} = 10^6$ dynes cm^{-2}) a factor of

$$(p_{oo}/p)^{\frac{1}{2}}$$

is multiplied to the right hand side of (3.4), (3.6) and (3.8) to take into account the decreased resistance of the air at lower pressures.

3.1.3 Initiation

The ice phase is initiated whnever the cloud becomes water saturated and the temperature is below freezing. This is done by assuming the existence of spherical particles grown from the vapor whose diameter is 12.9μm, which gives an initial mass of approximately 1×10^{-9} gm. This is converted into a rate:

$$\frac{d\rho_f}{dt} = \frac{d}{dt}\,(m_f N_{tf})$$

or, by using the continuity equations of air and ice,

$$\frac{dq_f}{dt} = \frac{1}{\rho_a} \frac{d\rho_f}{dt}$$

$$\simeq \frac{1 \times 10^{-9}}{\rho_a \delta t} N_{tf}$$

where δt is the current time step.

With the Fletcher concentration, large numbers of snow crystals can exist at low temperatures such that the rate just given will exceed the amount of water actually available for ice crystal growth. The rate is therefore compared to the amount of water vapor above ice saturation and the minimum is taken to initialize the ice phase:

$$S_{fnich} = \min (1 \times 10^{-9} N_{tf}/\rho_a, q_v - q_{si})/\delta t \qquad (3.9)$$

3.1.4 Vapor deposition

Once an initial mass has been formed, continued growth is by the process of vapor deposition. Riming will not take place during the first stages of vapor deposition, the crystals being too small in dimension to have any significant collection efficiency. Once the crystal dimension has passed some critical value (see section 3.1.5 below), riming, due to the release of the latent heat of freezing, has a significant effect on the vapor deposition rate. Vapor deposition is simulated by use of the electrostatic analogue of capacitance to describe the field of vapor around the crystal. A heat and mass balance is then obtained to describe the rate of change of the mass of a

single crystal as (see Cotton, 1970 for a complete derivation):

$$\frac{dm_f}{dt} = 4\pi C\, SS\, G(T,p) f(Re) - \frac{L_{vi} L_{li} G(T,p)}{K T^2} \left.\frac{dm_f}{dt}\right|_{rime} \tag{3.10}$$

where SS is the supersaturation with respect to ice

$$SS = q_v/q_{si} - 1 \tag{3.11}$$

f(Re) is the ventilation factor, a function of the Reynolds number, simulating the increased vapor source due to the crystal's fall speed:

$$Re = \rho_a D v_f/\mu \tag{3.12}$$

$$f(Re) = 1 + 0.229(Re)^{\frac{1}{2}} \tag{3.13}$$

and the capacitance C, for hexagonal plates, is

$$C = D/\pi$$

G(T,p) is

$$G(T,p) = \frac{1}{\frac{\varepsilon L_{vi}^2}{K R_a T^2} + \frac{R_a T}{\varepsilon \Psi e_{si}}} \tag{3.14}$$

and $\left.\frac{dm_f}{dt}\right|_{rime}$ is the rate of riming of an individual snow crystal. (3.10) is converted to give the time rate of change to the snow mixing ratio as:

$$S_{fvdep} = 4\, D\, SS\, G(T,p) f(Re)/\rho_a - \frac{L_{vi} L_{li} G(T,p)}{K T^2} S_{frim} \tag{3.15}$$

where S_{frim} is the rate of riming given in section 3.1.5 below.

3.1.5 Riming

In the presence of supercooled cloud droplets, riming can take place and in general will supercede the rate of vapor deposition as the main source of mass for the ice phase. Significant riming takes place only when the crystal has achieved a critical dimension. From observations of hexagonal plates, Ono (1969) reported that significant amounts of frozen cloud droplets were found on the plates once the diameter of the plate surpassed 300μm. Using an analytical model to calculate efficiencies, Pitter and Pruppacher (1974) gave this diameter as 160μm for a plate collecting 10μm cloud droplets. An hexagonal plate cutoff diameter is chosen to be 200μm giving a mass cutoff, from (3.3) of 1.5×10^{-7} gm. Riming is also not allowed when the cloud water falls below 10^{-5} gm gm^{-1}, so as to save time by not calculating an insignificant rate.

The riming rate for a single snow crystal mass is derived by assuming the crystal falls through a volume containing cloud droplets, coalescing with any droplet the crystal comes in contact with. This rate, assuming zero or insignificant fall speeds for cloud droplets, is

$$\frac{dm_f}{dt} = Av_f E_{fr} \rho_c \tag{3.16}$$

where A is the crystal area presented perpendicular to the flow

$$A = \pi D^2/4$$

and E_{fr} is the riming collection efficiency for a hexagonal plate relative to a cloud drop with the coalescence efficiency being assumed one. The change to the mixing ratio of snow becomes

$$S_{frim} = N_{tf}\pi D^2 v_f \hat{E}_{fr} q_c/4 \tag{3.17}$$

The characteristic efficiency $\hat{E}_{fr}$ for plates riming small cloud droplets cannot be obtained in a straightforward manner. Pitter and Pruppacher (1974) present their results in the form of graphs of E_{fr} as a function of plate diameter and to the ratio of terminal velocities of a sphere to oblate spheroid (the assumed shape of the plates) for various plate diameters. Since their riming efficiency are estimates not in simple functional form, it was decided to use a more convenient expression for this ice parameterization scheme. The efficiencies will be obtained by assuming a sphere of diameter equivalent to a hexagonal plate and Stokes flow about the plate. The Stokes number for a sphere is (Langmuir, 1948 and Byers, 1965)

$$STK(D) = d_\ell D^2 v_f/9\mu D \tag{3.18}$$

where the cloud droplet diameter is given by

$$D_c = (6\rho_c/\pi d_\ell N_{tc})^{1/3} \tag{3.19}$$

The efficiency $\hat{E}_{fr}$, assuming potential flow, is

$$\hat{E}_{fr} = \left(\frac{STK(D)}{STK(D)+0.5}\right)^2 \tag{3.20}$$

3.1.6 Melting

Complete melting of a snow crystal is assumed to occur once the temperature becomes greater than freezing. The melted mass is assumed to be in the form of cloud droplets and is therefore converted into

cloud water. The snow crystal velocity is set to zero. The rate of snow crystal melting is

$$S_{fmelt} = -q_f/\delta t \qquad (3.21)$$

3.1.7 Ice saturation thermodynamics

It is assumed that the model cloud remains at ice saturation when the temperature is below freezing, the cloud water is zero and the vapor deposition rate (3.15) consumes 75% of the difference between the water vapor and ice saturation mixing ratios during a given time step. The conditions under which the cloud follows an ice adiabat are:

$$|S_{fvdep}\ \delta t| \geqslant 0.75\ |q_v - q_{si}|$$

$$q_c = 0$$

$$T \leqslant 0C$$

Thus the vapor deposition rate for snow must always be computed. Once the conditions for ice saturation are met, a flag is set to communicate with other parts of the program.

Ice saturation thermodynamics are done in a two stage process (see Appendix I for derivations of the following equations): A rate of ice deposition (the ice saturation adiabat) and an isobaric adjustment on snow, water vapor, temperature and cloud water. The rate of ice saturation is done in the snow routine and is given by

$$S_{fglac} = \frac{Gwq_{si}}{R_a T}\left(\frac{\varepsilon L_{vi}}{C_{pd}T} - 1\right) \Big/ \left(1 + \frac{\varepsilon L_{vi}^2 q_{si}}{C_{pd} R_a T^2}\right) \tag{3.22}$$

Once all variables have been updated at the end of a time step, the snow, water vapor, cloud water and temperature are isobarically adjusted to ice saturation:

$$\begin{aligned}
\delta q_f &= \frac{q_v - q_{si}}{1+B} - \frac{L_{\ell i} q_c}{L_{vi}(1+1/B)} + q_c \\
\delta q_v &= -\frac{q_v - q_{si}}{1+B} + \frac{L_{\ell i} q_c}{L_{vi}(1+1/B)} \\
\delta q_c &= -q_c \\
\delta T &= \frac{L_{vi}}{C_{pd}} \delta q_f - \frac{L_{\ell i}}{C_{pd}} \delta q_c
\end{aligned} \tag{3.23}$$

where $B = \varepsilon L_{vi}^2 q_{si} / (C_{pd} T^2 R_a)$.

This adjustment is made until the temperature change is less than 10^{-4}C after which the water vapor mixing ratio is set exactly to ice saturation.

3.2.0 Graupel

By graupel is meant any spherically shaped ice particle. Graupel can thus come from the freezing of raindrops or by the riming of snow crystals into round ice particles and includes low density particles up to the high density (d_g = 0.9gm cm^{-3}) hailstones.

3.2.1 Graupel particles and the Marshall-Palmer distribution

The number of graupel particles per diameter increment N(D) will be assumed inverse exponentially distributed in the form of the so-called Marshall-Palmer (1948) distribution

$$N(D) = N_{og} e^{-\lambda D} \tag{3.24}$$

where N_{og} is the slope intercept of the distribution and λ is the slope. Observations of the distribution of graupel and hail have shown the tendency of these ice particles to approximate an inverse exponential distribution both from sampling done in the air (Jones, 1959; Musil, et al., 1978) and on the ground (Federer and Waldvogel, 1975; Douglas, 1964). From an analytical standpoint, the Marshall-Palmer distribution is easily integrable as opposed to other distributions proposed to describe graupel.

The total number of particles of the distribution can be found by an integration of the distribution

$$\begin{aligned} N_{tg} &= \int_0^\infty N(D)\, dD \\ &= N_{og}/\lambda \end{aligned} \tag{3.25}$$

The total graupel content ρ_g is found by taking the mass weighted mean of the distribution

$$\rho_g = \int_0^\infty N(D)\, m_g(D)\, dD$$

$$= \pi \Gamma(4)\, N_{og} d_g / 6\lambda^4$$

$$= \pi\, d_g N_{og} / \lambda^4$$

where $\Gamma(\ )$ is the gamma function and d_g is the density of the particle. The slope of the distribution is then

$$\lambda = (\pi\, d_g N_{og} / \rho_g)^{1/4} \tag{3.26}$$

or using (3.25)

$$\lambda = (\pi\, d_g N_{tg} / \rho_g)^{1/3} \tag{3.27}$$

The mean diameter $\overline{D}$ is given by

$$\overline{D} = \frac{1}{N_{tg}} \int_0^\infty D\, N(D)\, dD \tag{3.28}$$

$$= 1/\lambda$$

The mean mass* $\bar{m}$ is given by

$$\bar{m} = \frac{1}{N_{tg}} \int_0^\infty m_g(D)\, N(D)\, dD$$

$$= \rho_g / N_{tg} \qquad (3.29)$$

$$= q_g \rho_a / N_{tg}$$

From (3.25) and the specification of the density d_g along with either (3.26) or (3.27), one can see that the distribution can be completely described by assigning a value to either λ, N_{tg} or N_{og}. A constant λ has been used for describing a rain Marshal-Palmer distribution (Manton and Cotton, 1977) by assuming that the process of breakup coupled with coalescence between drops and accretion of cloud droplets will keep the slope constant. No such balance exists for graupel. A constant N_{og}, used by Orville and Kopp (1977), was found to produce too fast a melting rate due to the inability to simulate melting of the smaller graupel particles first. By choosing N_{tg} to be a constant, this problem will

---

*The mean mass is not the mass of the mean diameter. They are related by the equation

$$\bar{m} = \pi d_g \bar{D}^3$$

not be eliminated, but the rate of melting will be slowed since it can be shown that for a constant N_{og}

$$\frac{d \ln \rho_g}{d \ln \bar{D}} = 4$$

while for a constant N_{tg}

$$\frac{d \ln \rho_g}{d \ln \bar{D}} = 3$$

A constant N_{tg} will be used to complete the distribution.

3.2.2 Value of the total concentration

The value of the total concentration N_{tg} is taken from observation. Using hailstones collected on the ground by farmers, Douglas (1964) found that the slope of the assumed inverse-exponential distribution was a constant whose value was around $2.93 cm^{-1}$, contrary to the above discussion. The total concentration is a function of the ice content as $N_{tg} = 3.41 \rho_g$. For an assumed ice content of $1 gm\ m^{-3}$, N_{tg} has a value of $3.41 \times 10^{-6} cm^{-3}$, smaller than the values found by Federer and Waldvogel (1975) and Musil, et al., (1978) and is probably due to the melting of the stones collected and, more importantly, by the complete melting of the smaller graupel particles before being collected by the farmers. A better representation of the distribution on the ground was obtained by Federer and Waldvogel by using foam rubber impact platforms coupled with hail/rain mass separaters to obtain water contents of both rain and hail precipitation. Assuming an inverse-exponential distribution, the

best fit of their data gives values of λ and N_{og} as $4.2cm^{-1}$ and $1.2x10^{-4}cm^{-4}$, respectively, giving an N_{tg} of $2.86x10^{-5}cm^{-3}$. The values of λ ranged from $3.3cm^{-1}$ to $6.4cm^{-1}$ and those of N_{og} from $1.5x10^{-5}cm^{-4}$ to $5.2x10^{-4}cm^{-4}$. Combining these values to obtain a total concentration gives a maximum range for N_{tg} of $2.34x10^{-6}cm^{-3}$ to $1.58x10^{-4}cm^{-3}$. Musil, et al., (1978) sampled graupel particles in the cloud itself using an image recorder (the two-dimensional PMS), a foil impactor and a one-dimensional hail spectrometer. The 2-D PMS is accurate for particles whose maximum dimension is greater than 30μm and less than 2mm, and can therefore be assumed to sample small graupel composed of lightly rimed snow crystals and frozen raindrops. Taking typical values from the graph of the data presented in their report, one obtains a λ of $7.68cm^{-1}$. Using the maximum ice content for this device ($0.3gm\ m^{-3}$), one obtains a value for N_{tg} of $2.14x10^{-4}cm^{-3}$. From foil impact and 1-D hail spectrometer data, one can obtain a λ of $0.88cm^{-1}$. Using the maximum ice content for these two samplers ($0.2gm\ m^{-3}$, which appears rather low for hail), the value of N_{tg} is $4.82x10^{-8}cm^{-3}$.

There appears to be a choice of what value to use for the total concentration: The higher values of N_{tg} imply that the bulk of the graupel content is composed of the lightly rimed snow crystals and/or frozen raindrops, or that the graupel content is composed of heavier particles of lower total concentration (e.g., hail). It will be assumed that the smaller, more numerous spherical ice particles will represent the distribution of graupel, and that the value of N_{tg} is chosen to be $10^{-4}cm^{-3}$. N_{tg} can always be lowered should one want to model the fewer, heavier hail particles.

3.2.3 Density and equations for terminal velocity

Three different types of spherical ice particles will be used to represent graupel: Light graupel, heavy graupel and hail. Three types are used in an attempt to simulate the progression of rimed snow crystals or frozen raindrops collecting rain or cloud drops and thereby growing into hail. Also, since the observations show a decreasing total concentration with increasing mean diameter (or mean mass), three types of graupel particles will allow the total concentration to vary for each particle. Should this be the case, one will note from (3.29) that three differing masses will result corresponding to the three types of graupel particles. Only one type is assumed present at a grid point, the type being decided by the mean mass of the distribution for that specific particle. Thus, as in snow, it will be assumed that growth determines which type of graupel particle exists at any particular grid point in a cloud model. For graupel mean masses below 10^{-3}gm, light graupel is assumed to dominate the graupel ice content. Using the equations for hexagonal graupel from Locatelli and Hobbs (1974), which is spherically shaped, the derived density is

$$d_g = 0.1 \text{gm cm}^{-3} \tag{3.30}$$

and the terminal velocity is

$$v_g(D) = 594\ D^{0.46}(p_{oo}/p)^{\frac{1}{2}} \tag{3.31}$$

where the factor containing the pressure on the right hand side of (3.31) allows for changes in air resistance with pressure and hence of fall speed. For light graupel mean masses greater than 10^{-3}gm, the graupel

ice content is considered to be heavy graupel with a density of

$$d_g = 0.6 \text{gm cm}^{-3} \tag{3.32}$$

Assuming a balance between the weight of the particle and the aerodynamic drag, and a constant drag coefficient C_D (c.f., Manton and Cotton, 1977 for a similar derivation of the terminal velocity of a raindrop), a fall speed of

$$v_g(D) = (4\, d_g\, G\, D/3\rho_a C_D)^{\frac{1}{2}} \tag{3.33}$$

where C_D is assumed to have a value of 0.45.

Hail will occur for heavy graupel mean masses greater than $2\text{x}10^{-2}$gm, implying hailstones with diameters greater than 0.88cm have concentrations of 1m^{-3} or less. The density of hail is assumed to be

$$d_g = 0.9 \text{gm cm}^{-3} \tag{3.34}$$

and the terminal velocity is given by (3.33) with an assumed increased drag of 0.6 (Wisner, et al., 1972). The velocities used to calculate the advection of the graupel ice content will be mass weighted. The total mass flux of graupel, using (3.33) is given by

$$MF = \int_0^\infty m_g(D)\, v_g(D)\, N(D)\, dD$$

integration gives

$$MF = \frac{\Gamma(4.5)}{6} N_{tg} \bar{m}\, v_g(\bar{D}) \tag{3.35}$$

The mass flux is related to the mass weighted velocity by

$$\bar{v}_g = MF/\rho_g$$

or

$$\bar{v}_g = \frac{\Gamma(4.5)}{6} v_g(\bar{D}) \tag{3.36}$$

for heavy graupel and hail. Due to the different exponent to the diameter in (3.31) for light graupel, a different weight is obtained

$$\bar{v}_g = \frac{\Gamma(4.46)}{6} v_g(\bar{D}) \tag{3.37}$$

Due to this difference in exponent between the velocities of light and heavy graupel (or hail), there arises a difference in the weights for the source and sink derivations which follow. In all calculations, neglect of this difference amounts to a percent error of under 2%, which is in all likelihood within the error inherent in the terminal velocity equations associated with the assumptions of perfectly round ice particles, etc. Therefore, this difference will be ignored by assuming that velocity has the form

$$v_g(D) = K_v D^{\frac{1}{2}} \tag{3.38}$$

$$K_v = \begin{cases} (4\, d_g\, G/3\rho_a C_D)^{\frac{1}{2}} & ; \text{ heavy graupel or hail} \\ 594.\ (p_{oo}/p)^{\frac{1}{2}} & ; \text{ light graupel} \end{cases}$$

3.2.4 Initiation

Initial graupel ice contents will occur from the conversion of rimed snow crystals to graupel or by raindrop freezing by contact with snow crystals. The conversion will be shown in section 3.2.11.

3.2.5 Raindrop freezing by contact with snow crystals.

When supercooled raindrops are intermixed with snow crystals in a cloud, significant amounts of rain drops can be frozen from contact with snow crystals which act as efficient freezing nucleants. As reported in Cotton (1972), the freezing of rain drops by this process, for a maritime cloud regime, had a dominating influence on the rate of increase to graupel ice content and on the time of glaciation of the parcel.

The rain distribution follows from Manton and Cotton (1977) who assume a Marshall-Palmer distribution with constant slope ($\lambda_r = 18.52 cm^{-1}$)

$$N_r(D_r) = N_{or} e^{-\lambda_r D_r} \tag{3.39}$$

The terminal velocity for rain, similar to that of heavy graupel, is

$$v_r(D_r) = (4\, d_\ell\, G D_r / 3\rho_a\, C_D)^{\frac{1}{2}} \tag{3.40}$$

where $C_D = 0.587$.

Similar to graupel, the following quantities are obtained:

Mean diameter

$$\overline{D}_r = 1/\lambda_r \tag{3.41}$$

mass weighted velocity

$$\bar{v}_r = \frac{\Gamma(4.5)}{6} v_r(\bar{D}_r) \tag{3.42}$$

and the rain water content

$$\rho_r = \pi d_\ell N_{or} / \lambda_r^4 \tag{3.43}$$

The time rate of change to the rain water content, for raindrop freezing by crystal contact is

$$\frac{d\rho_r}{dt} = \int_o^\infty \frac{d}{dt} \left[m_r(D_r)\ N_r(D_r) \right]$$

Assuming the collection of a single crystal increases the mass of a raindrop insignificantly

$$\frac{d\rho_r}{dt} = \int_o^\infty m_r(D_r)\ \frac{dN_r}{dt}(D_r)\ dD_r \tag{3.44}$$

As the rain distribution sweeps out snow crystals through a volume V of

$$V = \frac{\pi}{4} D_r^2\ |v_r(D_r) - v_f|$$

collecting N_{tf} crystals onto $N_r(D_r)$ raindrops per diameter increment, with an assumed collection/coalescence efficiency of one, the time rate of change to the rain distribution is

$$\begin{aligned} \frac{dN_r}{dt} &= V N_{tf}\ N_r(D_r) \\ &= -\frac{\pi}{4} D_r^2\ |v_r(D_r) - v_f|\ N_{tf}\ N_r(D_r) \end{aligned} \tag{3.45}$$

Combining (3.44) and (3.45) gives

$$\frac{d\rho_r}{dt} = -\int_0^\infty m_r(D_r)\ \frac{\pi}{4}\ D_r^2\ \ |v_r(D_r) - v_f|\ N_{tf} N_r(D_r)\ dD_r$$

$$= -\frac{\pi^2}{24}\ d_\ell\ N_{tf}\ N_{or} \int_0^\infty D_r^5\ \left|\left(\frac{4d_\ell G}{3\rho_a C_D}\right)^{\frac{1}{2}}\ D_r^{\frac{1}{2}} - v_f\right|\ e^{-\lambda_r D_r}\ dD_r$$

Assuming that $v_r(D_r) > v_f$ and taking the absolute value signs outside the integral gives

$$\frac{d\rho_r}{dt} = -\frac{\pi^2}{24}\ d_\ell\ N_{tf}\ N_{or} \left|\left(\frac{4d_\ell G}{3\rho_a C_D}\right)^{\frac{1}{2}}\ \overline{D}_r^{6.5}\ \Gamma(6.5) - \overline{D}_r^{6}\ \Gamma(6)\ v_f\right|$$

substituting for $\overline{v}_r$ (3.42) and ρ_r (3.43) into the above, with some rearrangement, gives

$$\frac{d\rho_r}{dt} = -\pi\ N_{tf}\ \overline{D}_r^{2}\ |6.1875\ \overline{v}_r - 5v_f|\rho_r \qquad (3.46)$$

The time rate of change of graupel mixing ratio is then

$$S_{grfrz} = \pi\ N_{tf}\ \overline{D}_r^{2}\ |6.1875\ \overline{v}_r - 5v_f|\ q_r \qquad (3.47)$$

3.2.6 Vapor deposition

Following (3.10) for the vapor deposition on a single ice crystal mass and using a capacitance for spherical particles of C = D/2, the time rate of change of a mass m_g is

$$\frac{dm_g}{dt} = 2\pi D \; SS \; G(T,p) \; f(Re) \tag{3.48}$$

where the riming term of (3.10) has been dropped for graupel by assuming that riming and vapor deposition will be mutually exclusive. Since vapor deposition does not change the concentration, the time rate of change of graupel ice content is

$$\frac{d\rho_g}{dt} = \int_0^\infty \frac{dm_g}{dt} N(D) \, dD$$

$$= \int_0^\infty 2\pi D \; SS \; G(T,p) \left[1 + 0.229 \left(\frac{\rho_a D v_g(D)}{\mu} \right)^{\frac{1}{2}} \right] N(D) \, dD \tag{3.49}$$

where (3.12) and (3.13) have been used for f(Re) with appropriate substitutions made for graupel. Substituting (3.24) for N(D) and using the velocity relationship of (3.38), (3.49) becomes

$$\frac{d\rho_g}{dt} = \int_0^\infty 2\pi D \; SS \; G(T,p) \left[1 + 0.229 \left(\frac{\rho_a D K_v D^{\frac{1}{2}} \Gamma(\frac{1}{2})}{\mu} \right) \right] N_{og} e^{-\lambda D} dD$$

$$= 2\pi \; SS \; G(T,p) \; N_{og} \left[\int_0^\infty D e^{-\lambda D} dD + \int_0^\infty 0.229 \left(\frac{\rho_a K_v}{\mu} \right)^{\frac{1}{2}} D^{\frac{1}{4}} D^{\frac{1}{2}} D e^{-\lambda D} dD \right]$$

$$= 2\pi \; SS \; G(T,p)(N_{og}\bar{D})\bar{D}\left[1+0.229\;\Gamma(2.75)\left(\frac{\rho_a K_v \bar{D}^{\frac{1}{2}}\bar{D}}{\mu}\right)^{\frac{1}{2}}\right]$$

$$= 2\pi \; G(T,p)\; N_{tg}\bar{D}\; f(Re)_g \tag{3.50}$$

where

$$f(Re)_g = 1 + 0.229\;\Gamma(2.75)(\rho_a \bar{D}\; v_g(\bar{D})/\mu)^{\frac{1}{2}}$$

Writing $f(Re)_g$ in terms of the mass weighted velocity (3.36) gives

$$f(Re)_g = 1 + 0.229\;\Gamma(2.75)(6/\Gamma(4.5))^{\frac{1}{2}}\;(\rho_a \bar{D}\; \bar{v}_g/\mu)^{\frac{1}{2}} \tag{3.51}$$

Using continuity on (3.50) to obtain the time rate of change of graupel mixing ratio and multiplying out the numerical factors in (3.51) gives the set of equation describing vapor deposition onto the graupel distribution

$$\left.\begin{aligned} f(Re)_g &= 1 + 0.265\;(\rho_a \bar{D}\; \bar{v}_g/\mu)^{\frac{1}{2}} \\ S_{gvdep} &= 2\pi \; SS \; N_{tg}\bar{D}\; G(T,p)\; f(Re)_g/\rho_a \end{aligned}\right\} \tag{3.52}$$

3.2.7 Riming

As mentioned under the section describing vapor deposition onto graupel, riming will be assumed to preclude vapor deposition. When conditions for riming are met, here defined as a cloud water mixing ratio greater than 10^{-5}gm gm^{-1} and a mean mass greater than 10^{-6}gm

(corresponding approximately to a mean diameter of 200μm, see section 3.1.5), it will be assumed that riming will dominate the increase in mass to the graupel ice content over and above that for vapor deposition.

The derivation for riming of cloud droplets onto graupel follows the same assumptions as for snow crystals in section 3.1.5. The time rate of change of mass due to riming is

$$\frac{dm_g}{dt} = \frac{\pi}{4} D^2 v_g(D)\ E_{gr} \rho_c \tag{3.53}$$

Integrating the above equation to obtain the change to graupel ice content gives

$$\frac{d\rho_g}{dt} = \int_0^\infty N(D)\ \frac{dm_g}{dt}\ dD$$

$$= \int_0^\infty N(D)\ \frac{\pi}{4} D^2 v_g(D)\ E_{gr} \rho_c\ dD$$

Substituting for N(D) from (3.24) and using the equation set (3.38) for velocity gives

$$\frac{d\rho_g}{dt} = \int_0^\infty \frac{\pi}{4} D^2 K_v D^{\frac{1}{2}}\ E_{gr} \rho_c\ N_{og}\ e^{-\lambda D} dD \tag{3.54}$$

By assuming an average efficiency of riming $\overline{E}_{gr}$, the above equation can be integrated to give

$$\frac{d\rho_g}{dt} = \frac{\pi}{4}\ \overline{E}_{gr}\ N_{og}\ \overline{D}\ K_v \overline{D}^{\frac{1}{2}}\ \Gamma(3.5)\ \overline{D}^2 \rho_c$$

$$= \frac{\pi}{4} \bar{E}_{gr} N_{tg} v_g(\bar{D}) \bar{D}^2 \rho_c \Gamma(3.5) \tag{3.55}$$

Writing the above in terms of the mass weighted velocity (3.36) gives

$$\frac{d\rho_g}{dt} = \frac{\pi}{4} \bar{E}_{gr} N_{tg} 6 \frac{\Gamma(3.5)}{\Gamma(4.5)} \bar{v}_g \bar{D}^2 \rho_c$$

$$= \frac{3}{7} \pi \bar{E}_{gr} N_{tg} \bar{v}_g \bar{D}^2 \rho_c \tag{3.56}$$

There remains to define the average collection efficiency $\bar{E}_{gr}$, which will be derived assuming potential flow about the ice sphere

$$STK(D) = d_\ell D_c^2 \; v_g(D)/9\mu D \tag{3.57}$$

$$E_{gr} = \left(\frac{STK(D)}{STK(D) + 0.5} \right)^2 \tag{3.58}$$

where D_c, the cloud droplet diameter, is given by (3.19). One can see the necessity of defining an average collection efficiency by substituting (3.58) into (3.54). No analytical solution to the integration exists. Direct integration of (3.58) to derive an average efficiency leads to similar results. One must then find a typical diameter, D_E, to use in calculating the Stokes number. A typical diameter can be found by noticing that the riming equation (3.54) depends on $D^2 D^{\frac{1}{2}}$:

$$D_E^2 \, D_E^{\frac{1}{2}} = \frac{1}{N_{tg}} \int_0^\infty D^2 D^{\frac{1}{2}} \, N(D) \, dD$$

$$D_E = \left(\Gamma(3.5)\right)^{0.4} \bar{D}$$

$$= 1.62\ \bar{D} \qquad (3.59)$$

It will be assumed that replacing D with D_E in (3.57) is more representative a Stokes number for use in computing an average efficiency than an average Stokes number. (3.57) then gives

$$STK(D_E) = d_\ell\ D_c^2\ v(D_E)/9\mu D_E$$

Substituting (3.59) into the above, and writing the velocity in terms of $\bar{v}_g$ gives the Stokes number used to compute $\bar{E}_{gr}$

$$STK_E = 0.405\ d_\ell\ \bar{D}_c^2\ \bar{v}_g/9\mu\bar{D}$$

The complete set of equations describing the riming of cloud droplets onto graupel, converting ice mass density into ice mixing ratio, is

$$\left.\begin{aligned} D_c &= (6\rho_c/\pi d_\ell N_{tc})^{1/3} \\ STK_E &= 0.405\ d_\ell\ D_c^2\ \bar{v}_g/9\mu\bar{D} \\ \bar{E}_{gr} &= \left(\frac{STK_E}{STK_E + 0.5}\right)^2 \\ S_{grim} &= \frac{3}{7}\pi\ \bar{E}_{gr}\ N_{tg}\ \bar{v}_g\ \bar{D}^2\ q_c \end{aligned}\right\} \qquad (3.60)$$

3.2.8 Raindrop collection by graupel

Raindrop freezing onto graupel is an important source of ice growth (second in magnitude to riming of cloud droplet for similar ice and liquid contents). The time rate of change of a graupel particle of mass m_g falling through a collection of rain drops having a Marshall-Palmer distribution (c.f. section 3.2.5) is

$$\frac{dm_g}{dt} = \int_0^\infty \frac{\pi}{4}(D + D_r)^2 \, |v_r(D_r) - v_g(D)| \, \frac{\pi}{6} D_r^3 d_\ell \, E(D_r \backslash D) N_r(D_r) dD_r \tag{3.61}$$

where $E(D_r \backslash D)$ is the efficiency of collection/coalescence. This efficiency will be assumed to have a value of one, a good assumption as it can be shown that for a graupel mean diameter greater than the mean diameter for rain (which is a constant of 0.054 cm) the Stokes number

$$STK(\bar{D}, \bar{D}_r) = d_\ell |v_r(\bar{D}_r) - v(\bar{D})| \bar{D}_r^2 / 9\mu\bar{D}$$

will produce an efficiency (assuming potential flow) very close to one. Even for a graupel mean diameter producing a near zero efficiency, the rain collection rate would also be near zero due to the velocity factor in (3.61). The time rate of change to the graupel ice content is

$$\frac{d\rho_g}{dt} = \int_0^\infty N(D) \, \frac{dm_g}{dt} \, dD$$

$$= \iint_0^\infty \frac{\pi}{4}(D + D_r)^2 |v_r(D_r) - v_g(D)| \frac{\pi}{6} D_r^3 d_\ell N(D) N_r(D_r) dD_r dD \tag{3.62}$$

where $E(D_r \backslash D)$ has been assumed equal to 1.

The absolute value signs about the velocity difference in the above equation makes integration difficult. To circumnavigate this problem, the factor will be approximated and taken out of the integral signs as the absolute value of the difference of the mass weighted terminal velocities (Wisner, et al., 1972), giving

$$\frac{d\rho_g}{dt} = |\bar{v}_r - \bar{v}_g| \int_0^\infty \int_0^\infty \frac{\pi}{4}(D + D_r)^2 \frac{\pi}{6} D_r^3 d_\ell N_r(D_r) N(D) \, dD_r dD$$

Substitution of (3.39) and (3.24) into the above gives

$$\frac{d\rho_g}{dt} = \frac{\pi^2}{24} d_\ell N_{or} N_{og} |\bar{v}_r - \bar{v}_g| \int_0^\infty \int_0^\infty (D^2 + 2DD_r + D_r^2) D_r^3 e^{-\lambda_r D_r} e^{-\lambda D} \, dD_r dD$$

Integrating over D_r first and then over D gives

$$\frac{d\rho_g}{dt} = \frac{\pi^2}{24} d_\ell N_{or} N_{og} |\bar{v}_r - \bar{v}_g| \int_0^\infty \left(\Gamma(4)\bar{D}_r^4 D^2 + 2\Gamma(5)\bar{D}_r^5 D + \Gamma(6)\bar{D}_r^6\right) e^{-\lambda D} dD$$

$$= \pi^2 d_\ell N_{or} N_{og} |\bar{v}_r - \bar{v}_g| (0.5\bar{D}_r^4 \bar{D}^3 + 2\bar{D}_r^5 \bar{D}^2 + 5\bar{D}_r^6 \bar{D})$$

using (3.43) and (3.25) gives

$$\frac{d\rho_g}{dt} = \pi |\bar{v}_r - \bar{v}_g| \rho_r N_{tg} (0.5\bar{D}^2 + 2\bar{D}_r \bar{D} + 5\bar{D}_r^2) \qquad (3.63)$$

The source of graupel ice mixing ratio then becomes

$$S_{grcol} = \pi |\bar{v}_r - \bar{v}_g| q_r N_{tg} (0.5\bar{D}^2 + 2\bar{D}_r \bar{D} + 5\bar{D}_r^2) \qquad (3.64)$$

3.2.9 Melting

In a liquid free atmosphere whose temperature is above freezing, the heat required to melt a graupel particle comes from two sources: Heat conducted to the particle from the surrounding air and conduction of heat by water vapor condensing onto the particle. For these two processes, the time rate of change of mass is (Mason, 1956)

(3.65)

$$\frac{dm_g}{dt}\Big|_{gas} = -\frac{1}{L_{\ell i}}\left[2\pi DK(T-T_{sfc}) + 2\pi DL_{vi}\,\Psi(\rho_v-\rho_{vsfc})\right]\left[1+0.226(Re)^{\frac{1}{2}}\right]$$

where T_{sfc} and ρ_{vsfc} are the temperature and water vapor density, respectively, at the surface of the graupel particle.

When liquid water is present, there is an additional term for the transfer of heat to the graupel from the accreted water (Wisner, et al., 1972).

$$\frac{dm_g}{dt}\Big|_{liq} = -\frac{1}{L_{\ell i}} C_w(T-T_{sfc})\left[\frac{\pi}{4}E_{gr}v_g(D)D^2\rho_c + \int_0^{\infty} E(D_r\backslash D)\left|v_r(D_r) - v_g(D)\right| \frac{\pi D_r^3}{6}\, d_\ell N_r(D_r)dD_r\right] \tag{3.66}$$

The above equation can be integrated over the distribution of graupel to give the time rate of change of graupel ice content. Using (3.60) and (3.64) gives

$$\frac{d\rho_g}{dt}\Big|_{liq} = -\frac{1}{L_{\ell i}} C_w(T-T_{sfc})\rho_a(S_{grim} + S_{grcol}) \tag{3.67}$$

Integration of (3.65) over the graupel distribution (see section 3.2.6 for a similar derivation) gives

$$\frac{d\rho_g}{dt}\Big|_{gas} = -\frac{1}{L_{\ell i}}\left[2\pi K(T-T_{sfc}) + 2\pi L_{vi}\,\Psi(\rho_v-\rho_{vsfc})\right]\bar{D}\,N_{tg}f(Re)_g \tag{3.68}$$

where $f(Re)_g$ is taken from equation set (3.50).

Adding (3.67) and (3.68), assuming that surface temperature of the particle is at 0C and that the surface water vapor density ρ_{vsfc} is liquid water saturated, and dividing by the density of air gives

$$S_{gmelt} = -\frac{1}{L_{\ell i}}\left[2\pi K(T-T_f)/\rho_a + 2\pi L_{vi}\,\Psi(q_v-q_{sw})\right]\bar{D}\,N_{tg}f(Re)_g$$

$$-\frac{1}{L_{\ell i}}\left[C_w(T-T_f)(S_{grim}+S_{grcol})\right] \tag{3.69}$$

In a liquid free environment with low water vapor mixing ratios and temperatures slightly warmer than the melting point, graupel particles can sublimate heat to the environment which lowers their surface temperatures below $0^{\circ}C$. Should this occur, the term in equation (3.69) containing q_v-q_{sw} is set to zero.

3.2.10 Ice saturation thermodynamics

Control of glaciation will not be done by graupel. Once a region is ice saturated, rates of change of graupel are not computed. Only the characteristic fall speed for the graupel distribution is diagnosed.

3.2.11 Conversion of snow to graupel

In the absence of rain drop freezing by snow crystal contact, the only means of initialization of graupel ice is through the conversion of snow crystals into graupel. The rate of conversion will be based on the rate of riming of snow crystals. Since the total concentration of snow crystals is externally specified and not explicity modeled, no elegant means of conversion can be contrived. If the total concentration varied with crystal diameter (e.g., an inverse exponential), then one might convert all the mass contained in those crystals whose diameters are greater than a prespecified 'conversion diameter' into graupel. Since this is not the case, a method of conversion, conflicting with a constant total snow concentration, must be found. This is done by assuming, should the amount of snow crystal rimed mass exceed a pre-specified fraction C_m of the snow mixing ratio, that all the rimed snow mass will be converted. This riming conversion is given as a rate of increase to the graupel ice mixing ratio as

$$S_{gconv} = S_{frim}\, H(S_{frim} - C_m q_f/\delta t) \tag{3.70}$$

where S_{frim} is the riming rate of the snow given by (3.17) and H(x), the heavyside step function, is zero for $x < 0$ and one for $x \geq 0$.

Preliminary runs with the parameterization in a 1DT cloud model were used to find a value of C_m. It was found that a sharp cutoff existed above which virtually no conversion occurred and below which conversion occurred. For the continental sounding used, that value was 2.5×10^{-2}. The current value of C_m to be used in testing the parameterization is 10^{-2}.

There is an upper limit to the diameter, and thus to the mass, of an individual snow crystal given by observation beyond which the equations of diameter versus mass and terminal velocity versus diameter are no longer valid. For graupel-like snow of hexagonal type, (3.7) and (3.8), this mass upper limit m_{max} has been set at 10^{-3}gm, which gives a diameter of 5mm and a fall speed (at sea level) of 1.29m s^{-1}. Any value of the snow ice mixing ratio in excess of this mass will be subtracted off. This maximum mass conversion is formulated into a rate as follows:

$$q_{fmax} = m_{max} N_{tf} / \rho_a \tag{3.71}$$

$$S_{gconv} = \max(0, (q_f - q_{fmax})/\delta t) \tag{3.72}$$

which is then added to (3.70) to give a total conversion rate of

$$S_{gconv} = \max(0,(q_f - q_{fmax})/\delta t) + S_{frim}\, H(S_{frim} - C_m q_f/\delta t) \tag{3.73}$$

Once substantial graupel ice ($q_g \sim 10^{-5}$gm gm^{-1}) has been established, the changes due to this graupel ice should dominate the ice phase. It is hoped that the mass of crystals will remain below the 10^{-3}gm threshold while the riming conversion rate builds the graupel ice up to a point where conversion does not significantly increase the graupel ice mixing ratio.

4.0 ICE PROCESSES NOT INCLUDED

4.1.0 Heterogeneous freezing of liquid water

Bigg (1953) investigated the freezing of supercooled water by suspending millimeter sized drops between two immiscible fluids and then by lowering the temperature of the fluids in increments and counting the number of drops frozen per degree of supercooling. For his experiment, Bigg used laboratory distilled water, water passed through an ion-exchange column, and water condensed onto a hydrophylic surface from a beaker of hot water; he did not use water collected from a cloud. Using his results to predict the freezing of rainwater in a cloud model, as done by Cotton (1972) and by Orville and Kopp (1977), cannot be considered a valid approximation of the in cloud freezing process. Using both 'Bigg's freezing' and raindrop freezing by contact with a snow crystal, Cotton (1972) found that the snow crystal contact freezing mechanism dominated rain drop freezing. Scott and Hobbs (1977), who used crystal contact freezing and the experimental results of Vali (1968, 1973) describing immersion freezing nuclei, not only found that the freezing of raindrops was dominated by crystal contact, but that only 1% of the total drops frozen came from containing an active freezing nucleant.

4.2.0 Graupel accretion of snow crystals

The accretion of snow crystals by graupel, as used by Orville and Kopp (1977), gives an equation similar to that of the riming of cloud droplets onto graupel. The difference is low collection/coalescence

efficiency whose value is assumed by Orville and Kopp to be 0.1 for dry growth due to the assumed low coalescence between the two ice particles. During wet growth, for which the efficiency is 1.0, accretion of snow crystals will equal that of cloud droplet riming for equal snow and cloud contents. Wet growth occurs mainly between the 0C and -15C isotherms, where the number of snow crystals assumed for this parameterization is not normally large, and such concentrations would not produce a significant rate of increase to the graupel mass.

4.3.0 Wet growth of graupel

Wet growth of hail or graupel is not included in the model, but can be added at a later time following procedures described by Musil (1970).

4.4.0 Aggregation and ice multiplication

Aggregation and ice multiplication both change the number of snow crystals, a physical impossibility in the current parameterization since the number of snow crystals is externally defined and not predicted. Aggregation of snow crystals is perhaps important in cumulus clouds due to the increased surface area made available for cloud droplet riming, giving a more rapid conversion of snow crystals into graupel. By far the more important of the two processes is ice multiplication. Using the results of Hallett and Mossop (1974), in which small ice splinters are thrown off by riming ice crystals, several authors (Scott

and Hobbs, 1977; Takahashi, 1976; Koenig, 1977) show results from their cloud models confirming observations of an increase in the number of snow crystals over and above that given by ice depositional nucleants. By riming and an increased freezing of raindrops, this increase in the number of snow crystals increases the number of graupel by a significant amount. Unless the total concentration for snow crystals is carried as a variable, no ice multiplication process can be realistically simulated, which is a definite shortcoming in this limited, degree-of-freedom parameterization of ice processes. How the effects of ice multiplication might be handled in future uses of this parameterization will be discussed in section 9.0.

5.0 PARAMETERIZATION SUMMARY AND FLOW

The parameterization divides the ice phase into two basic types: Snow (in this case, hexagonal plates) and graupel. The sources and sinks for each basic type are contained in two separate subroutines, the only direct interaction being a conversion of snow crystals to graupel and a flag indicating ice saturation. Each subroutine produces time rates for the changes of water vapor, cloud liquid water and rainwater due to the ice phase as well as ice particle terminal velocities for use in computing advection and turbulent diffusion by the main cloud model. For each variable, the sum of these rates will give the total change to the respective ice variable. Also included is a small subroutine containing the isobaric ice saturation adjustment routine. Figure 1 diagrams the following summary to the two variable ice phase parameterization.

5.1.0 Snow

At the start of each pass through the snow subroutine, the snow crystal concentration as a function of temperature is found from (3.1), or from some other external definition. If the temperature is above freezing, total melting of the snow ice occurs as given by (3.21), and the fall speed is set to zero. Given an initial mixing ratio of snow and a temperature below freezing, the individual mass of a snow crystal is found from the snow ice mixing ratio and the total concentration N_{tf} by using (3.2). This mass is then used in determining which type of hexagonal plate will supply the diameter and terminal

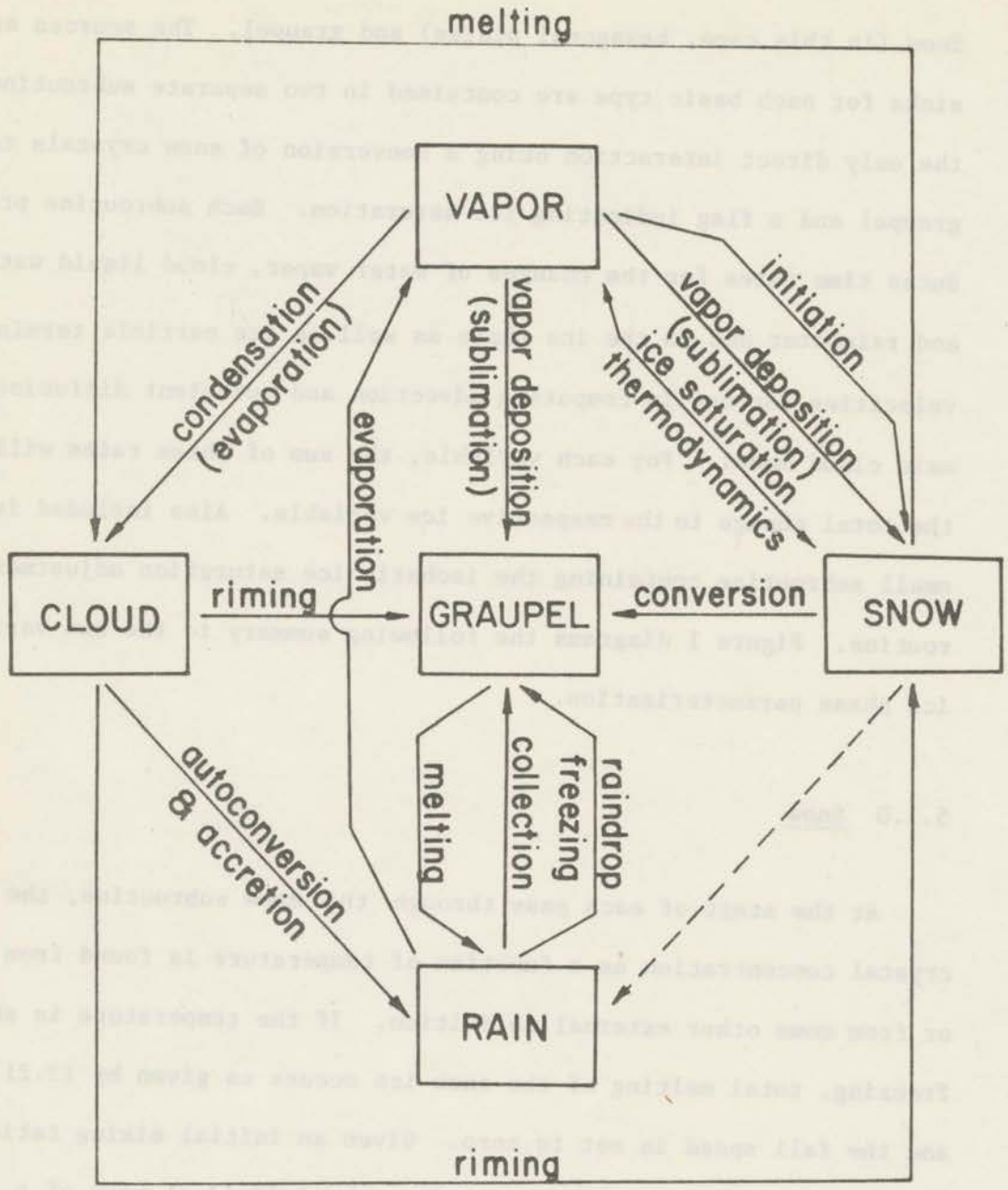

Figure 1. Diagram of microphysical processes. Arrows denote direction of mass transfer. Parentheses denote negative rate. Dotted line depicts interaction between rain and snow for the freezing of raindrops by snow crystal contact.

velocity ((3.3) through (3.8)) used to compute the rates of vapor deposition and riming. Vapor deposition is always computed and is found from (3.15). A decision is then made as to whether ice saturation thermodynamics are followed using the criteria outlined in section 3.1.7. Should the region be determined ice saturated, the vapor deposition rate is then equal to the rate of ice saturation, a flag is set and the rate of change of ice saturation is computed from (3.22). The isobaric adjustments (3.23) are calculated out of the snow subroutine, after all other chnages to the variables have been made. If the region is determined not to be ice saturated, then riming is done if the mass of an individual snow crystal is greater than 10^{-6} gm and the cloud water is greater than 10^{-5} gm gm^{-1} (c.f., section 3.1.5). If the riming rate is greater than zero then a check is made to see if snow should be converted to graupel following the criteria of section 3.2.11. The last routine done by the snow subroutine is a check to see if the snow crystal mass is greater than the maximum mass allowed for a crystal (10^{-3} gm). If such is the case, enough snow ice content is 'converted' into graupel following (3.72) to set the snow crystal mass to 10^{-3} gm.

5.2.0 Graupel

Initial mass for graupel comes from two processes: Conversion from snow and raindrop freezing by contact with snow crystals. Rain drop freezing by snow crystal contact (3.47) is always done when both rain and snow are present together at a grid point.

Once there is an initial graupel mass, the mean mass is obtained from the mixing ratio of graupel and the total concentration (3.29).

Following section 3.2.3, the mean mass then determines the mean diameter and mass weighted fall speed of the graupel distribution. The sources and sinks of graupel can then be computed.

Vapor deposition (3.52) is done given the conditions for cloud water and mean mass as for snow with an extra condition on rainwater If significant rain water ($q_r > 10^{-5}$ gm gm^{-1}), along with too low an amount of cloud water exists, and the mean mass is above the riming threshold, then rain collection will give a higher rate than will vapor deposition; thus, vapor deposition is done if the temperature is below freezing and the mean mass is less than 10^{-6}gm, or if the mean mass is greater than 10^{-6}gm, but both cloud water and rain water are less than 10^{-5}gm gm^{-1}. Riming is computed should the mean mass be greater than 10^{-6}gm and the cloud water be greater than 10^{-5}gm gm^{-1}, and is given by (3.60). If the mean mass is greater than 10^{-6}gm, and the rainwater is greater than 10^{-5}gm gm^{-1}, then the rain collection rate is calculated from (3.64). Should the temperature be above freezing, the melting rate is calculated from (3.69) and the riming and rain collection rates are set to zero. If the cloud is glaciated, the characteristic fall speed $\bar{v}_g$ of the graupel distribtuion is determined, but no rates are calculated except for rain drop freezing from snow crystal contact.

6.0 MODEL AND SOUNDINGS USED TO TEST THE PARAMETERIZATION

6.1.0 Model

A one-dimensional time-dependent model is used to test the parameterization. Its advantages over the simpler lagrangian model is in its resolution of mass fluxes and the ability to simulate the simultaneous occurrence of differing growth and decay processes (e.g., melting and glaciation) within the domain of the model. Although a 1DT model cannot simulate cumulus convection well (c.f., Cotton, 1975), it does have several advantages over higher dimensional time-dependent models. The equations for advection and diffusion used are simpler, making it easier to rewrite the model for testing purposes to include the effects of ice. The most important reason is that a 1DT model uses many fewer computer resources and therefore allows many more runs for sensitivity tests and parameter changes than do two- or three-dimensional time-dependent models.

6.1.1 Description of model used

The model is similar to the one developed by Cotton (1975) with equations for the effects of rain and ice (both graupel and snow) added. The microphysical relationship between cloud and rain water (e.g., autoconversion and accretion) follows that of Manton and Cotton (1977).

The thermodynamic and dynamic equations are developed using the assumptions of axisymmetry, a hydrostatic base state, the Boussinesq approximation and pressure equilibrium between cloud and environment.

These equations, and those describing the conversion of mass for water vapor cloud, rain and ice mixing ratios, are averaged in the radial direction to give predictions on the cloud scale mean. First order turbulent parameterization is used with a turbulent eddy viscosity coefficient proportional to the magnitude of the deformation tensor. Simple entrainment is also used to simulate mixing with the environment.

The equations are numerically integrated, using fourth order centered in space and Matsuno (1966) time differencing schemes, on a staggered finite-difference grid with 100m spacing between the variables.

6.1.2 Initiation of the model

An environmental sounding (pressure, temperature and dew point temperature) is read and interpolated to the 100m grid spacing. The first fifty millibars next to the surface are assumed well mixed with the temperature adiabatic and the water vapor equal to an average water vapor mixing ratio through the layer. These values are then used to find a cloud condensation level (CCL). Below the CCL, (i.e., cloud base), for both environmental and cloud soundings, the temperature is made adiabatic and the vapor mixing ratio is a constant equal to the average used in determining the CCL. Above and equal to the CCL, the cloud domain is water saturated to a depth equal to that of the mixed layer below the CCL, but no greater than 3km; the temperature is left unchanged and equal to that of the environment. Above the saturated region, there is no initial difference between cloud and environment. All other microphysical and dynamic variables, with the exception of water vapor, are initiated to zero.

In order to obatin a stable cloud base for the first moments of the integration, water vapor is added to five grid points centered about cloud base at a rate of 10^{-5} gm gm^{-1} s^{-1} per grid point during the first 500 seconds.

6.2.0 Soundings

Two thermodynamic soundings were selected to test the parameterization. One, taken from a maritime airmass supporting deep convective warm-base clouds (Miami), allows the development of cloud water, rain water and vertical velocity fields at temperatures greater than freezing. The other, a continental airmass sounding (South Park) supporting deep convective cold-base clouds, permits very little warm cloud precipitation processes (e.g., coalescence and accretion) and therefore depends on the ice phase for precipitation development. These two soundings, therefore, represent distinctly different precipitation regimes, mainly due to the presence (or absence) of a supercooled rainwater field and its subsequent effects on the ice phase.

The difference in rainwater formation is attained in the model by changes in the total number of cloud droplets which in turn affects the autoconversion rate (the parameterization of cloud droplets coalescing into precipitation sized drops). High cloud droplet concentrations raise the autoconversion threshold on cloud water necessitating high cloud water mixing ratios before autoconversion can take place. This concentration (N_{tc}) is chosen to be 300 cm^{-3} and 1500 cm^{-3} for maritime and continental soundings, respectively. The latter allows a rainwater field to develop well before the cloud reaches the 0C isotherm, while the former permits very little, if any, autoconversion.

6.2.1 South Park

South Park is, for the most part, a flat valley located high in the Colorado Rockies. Here extensive data was acquired during the South Park Area Cumulus Experiment (SPACE) whose base site was near Fairplay, Colorado. The sounding used was taken on the 19 of July, 1977 at 0550 MDT, a day on which good convective activity occurred (hail and gusty winds were reported later on in the afternoon). The environmental sounding is shown in Fig. 2 by the solid lines. Also on this figure are the initial cloud saturation field and the adiabatic well-mixed layer, both depicted by the dotted lines. The horizontal line is the cloud base produced by the model at 5.03km MSL (2.1km above the ground level) and a temperature of 0.1C.

6.2.2 Miami

This maritime sounding is derived from a composite of soundings obtained during the Florida Area Cumulus Experiment (FACE) near Miami and the central base site. The day, 17 of July, 1973, had extensive, well-developed, deep moist convective activity occurring throughout most of the period. As one can see from Fig. 3, which is the same as Fig. 2 for Miami, cloud base is produced at 0.8km MSL and a temperature of 22.8C.

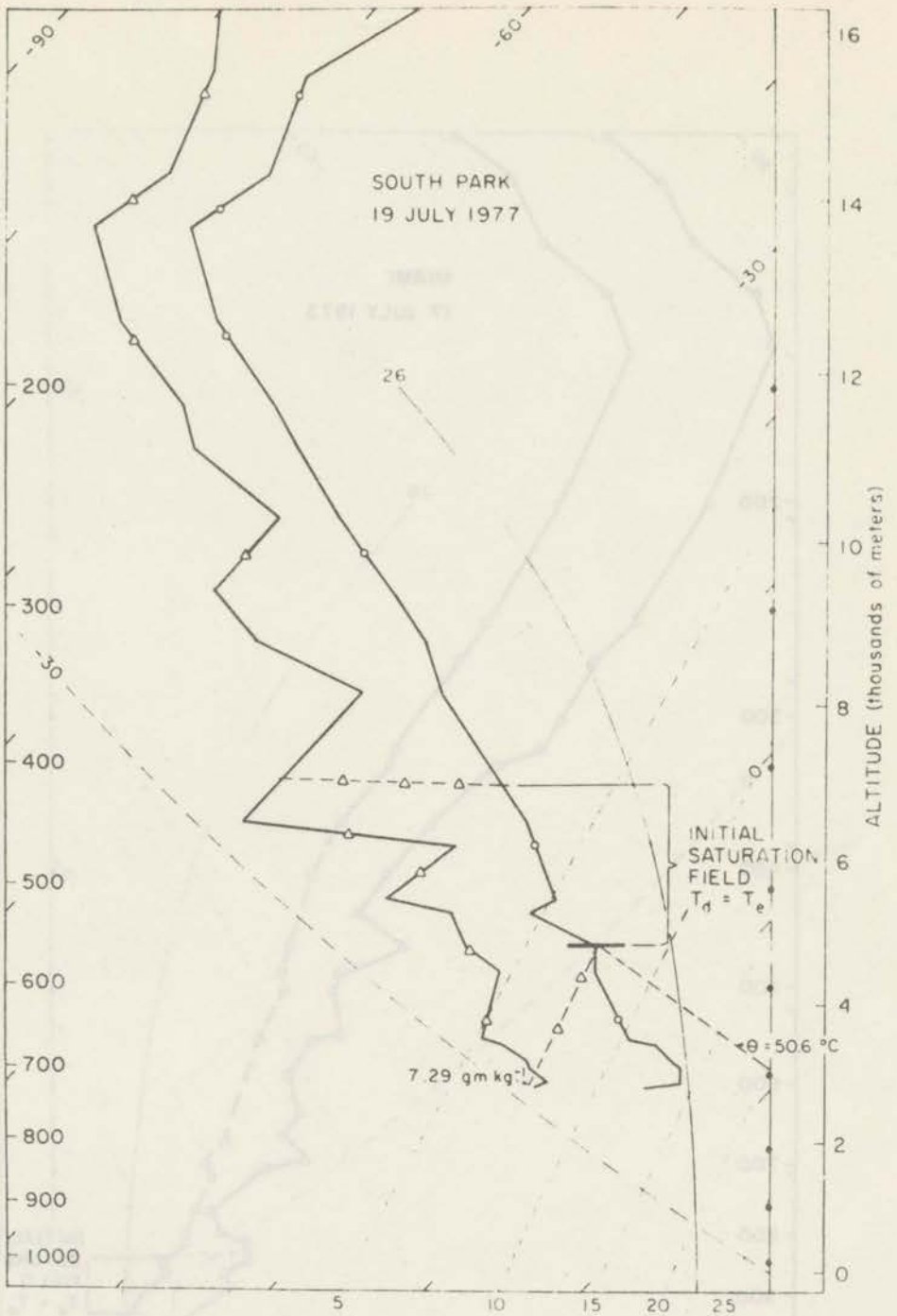

Figure 2. Skew-T, log-P plot of thermodynamic sounding (solid line) taken at 0550 MDT on 19 July 1977 at South Park, Colorado. Dotted lines show adiabatic well-mixed layer and the brackets delineate the saturation field (dew point temperature, T_d, equals environmental temperature, T_e), both of which are used to initiate the cloud circulation. Also shown by the horizontal line is the model produced cloud base.

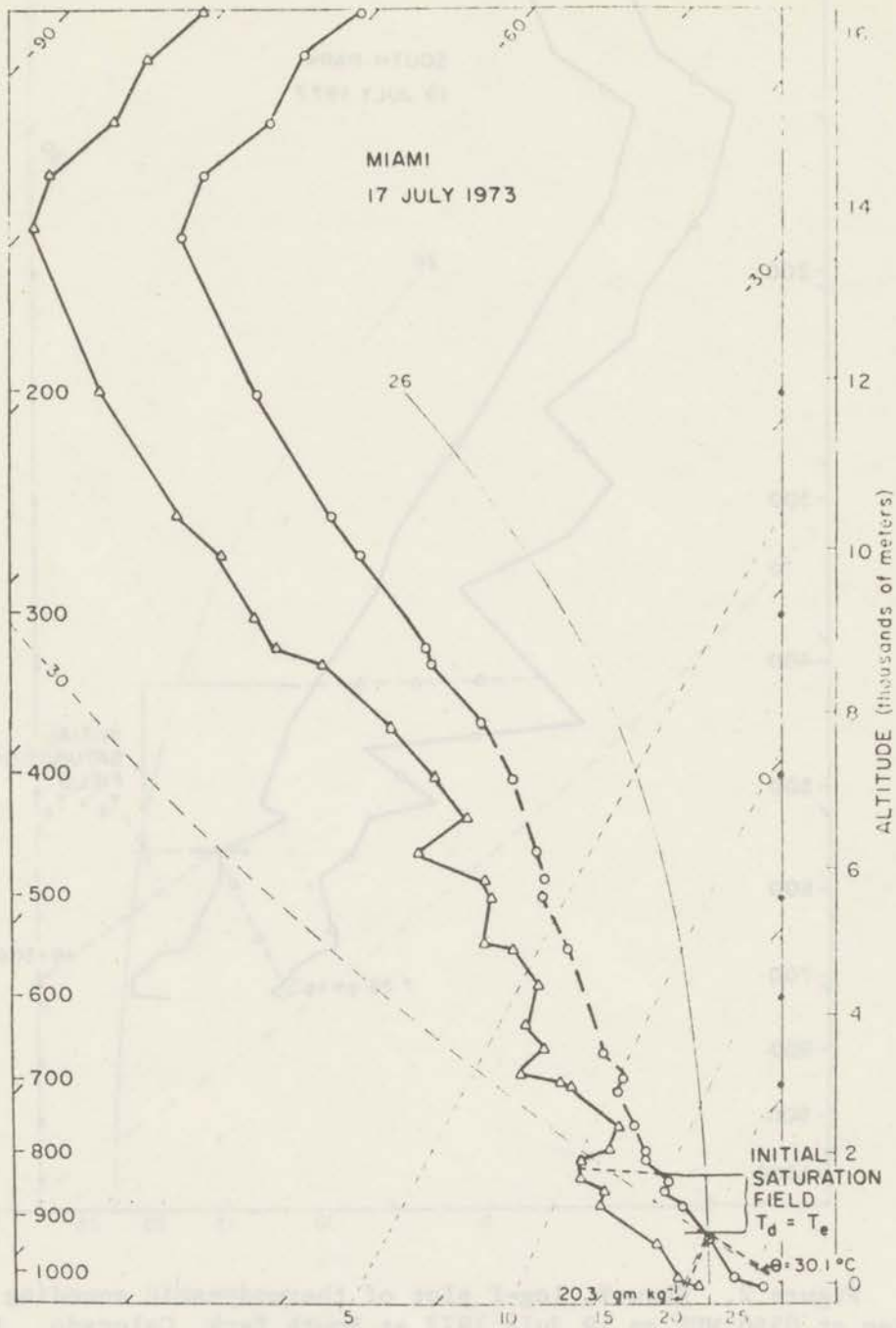

Figure 3. Same as Fig. 2 for the composite sounding taken on 17 July 1973 near Miami, Florida.

7.0 RESULTS

The 1DT cumulus cloud model was run at the National Center for Atmospheric Research (N.C.A.R.) on the CRAY I computer. All fields were printed at intervals of five minutes up to thirty minutes simulated time*, and thereafter at intervals of ten minutes. Total amounts of all water and ice contents (e.g., variables were summed over the whole domain) and source and sink terms were printed every one minute. All runs were integrated out to sixty minutes.

No attempt will be made to compare model results with data taken from the real world. A 1DT model is certainly not capable of simulating the rotations and co-existing updrafts and downdrafts normally found within a convective environment with vertical shear of the horizontal wind. Even without the ice phase and precipitation, Cotton (1975) could not consistently adjust the parameters simulating turbulence to produce model results equivalent to data taken in the field. These numerical experiments, therefore, should be considered mainly sensitivity tests and internal consistency checks of the parameterization.

7.1.0 Control runs and runs without ice

Two runs, one each for the distinctly different precipitation regimes, will be considered controls. They will then be used as a basis of comparison for subsequent runs in which certain parameters (e.g., snow crystal concentration) have been changed. These control

---

*Hereafter, any mention of time will refer to simulated cloud time and not the actual computer time used in running the model.

runs will use the values of parameters given in previous sections as specified under the table of symbols.

7.1.1 Control run for Miami

For this warm-cloud base, maritime simulation, the saturation perturbation is well below the OC isotherm and the ice phase does not play an immediate role in the cloud development. Thus, during the first few moments of the integration, a substantial liquid water field (Figs. 4 and 5 depicting cloud water and rainwater, respectively) and a vertical velocity field (Fig. 6) have built up below the freezing level. Once cloud water advects above the OC isotherm (around eight minutes) snow (Fig. 7) is initiated which, in turn, initiates the graupel production process (Fig. 8) by freezing of raindrops from contacting snow crystals.

Growth of graupel is rapid, mainly due to the large amounts of rainwater present above the freezing level (between ten and fifteen minutes, 77% of the total graupel ice content comes from rainwater accretion and 23% from cloud droplet riming). But with the upward advection of the level of maximum vertical velocity, the bulk of the rainwater field falls below the melting level and, at twenty minutes, increases mainly due to melting graupel. Graupel now loses more ice content than it gains (i.e., the rates of riming and raindrop collection and freezing do not make up for that lost by melting).

Prior to twenty minutes, growth of snow by vapor deposition and to a lesser extent by the riming of cloud droplets, has been slow. Between twenty and twenty-one minutes, ice saturation thermodynamics

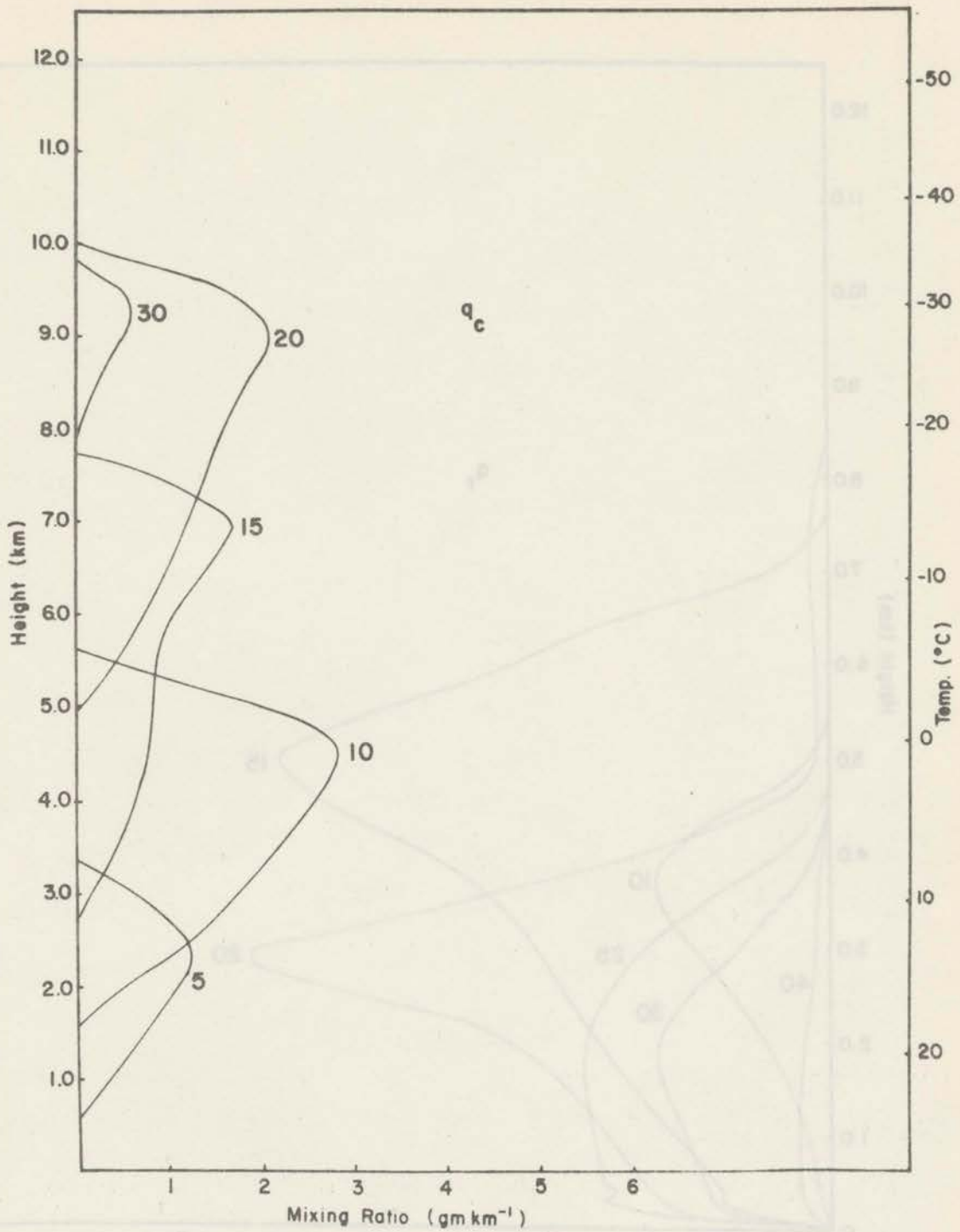

Figure 4. Cloud water mixing ratio in gm kg^{-1} versus MSL height in km as a function of time in minutes for Miami control run. Environmental temperatures in degree centigrade versus height are shown at right.

Figure 5. Same as Fig. 4 for rainwater.

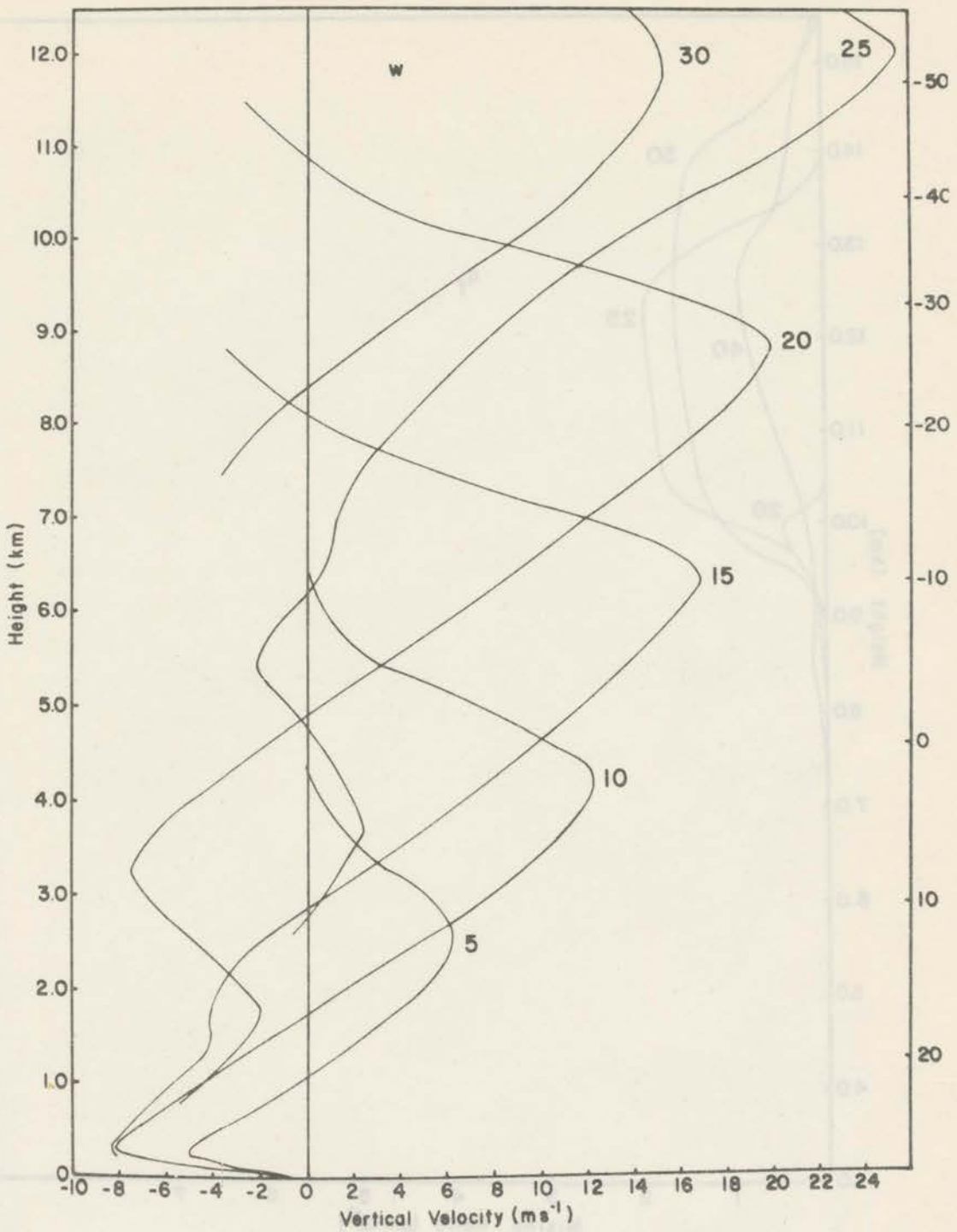

Figure 6. Same as Fig. 4 for vertical velocity in m s^{-1}.

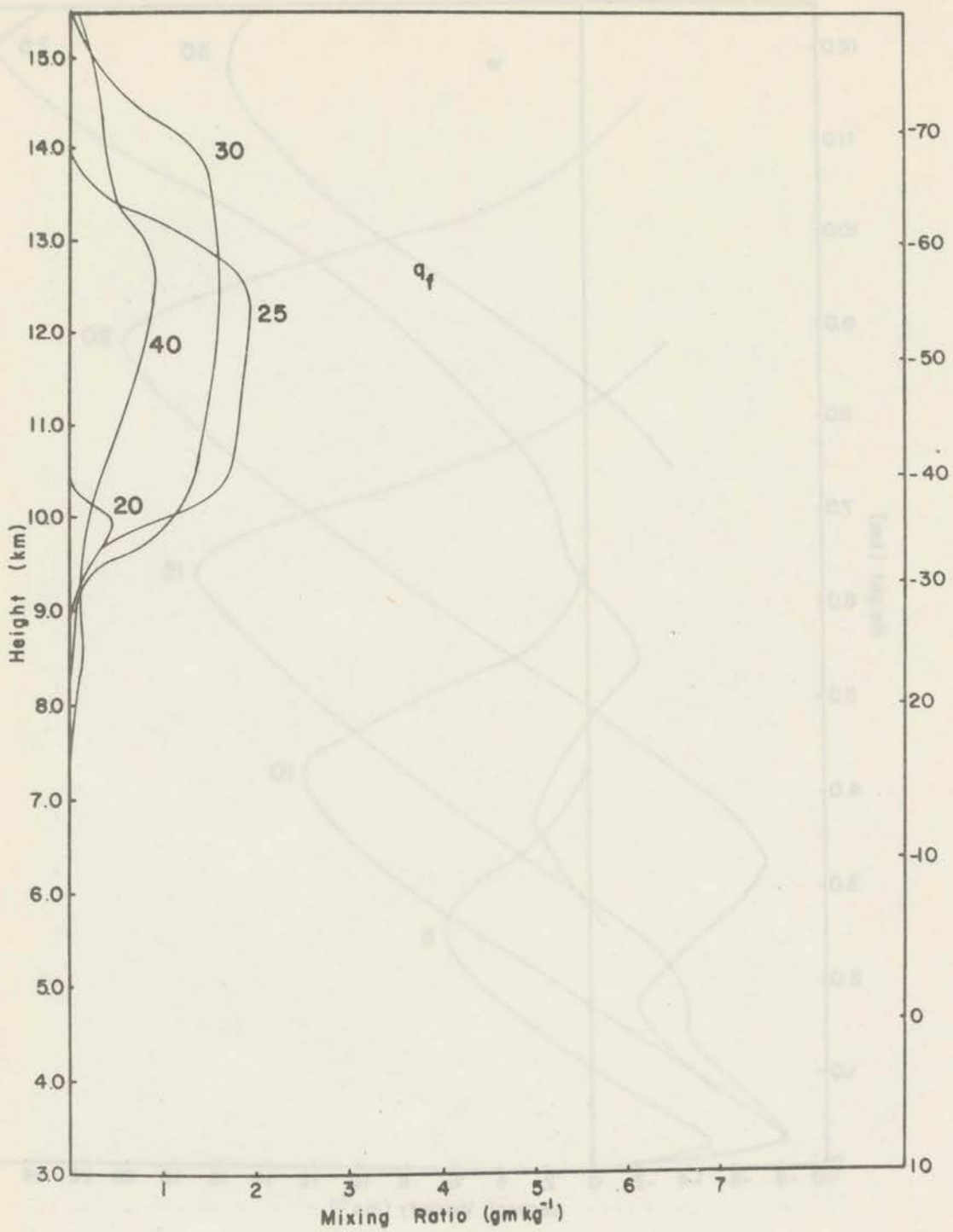

Figure 7. Same as Fig. 4 for snow ice.

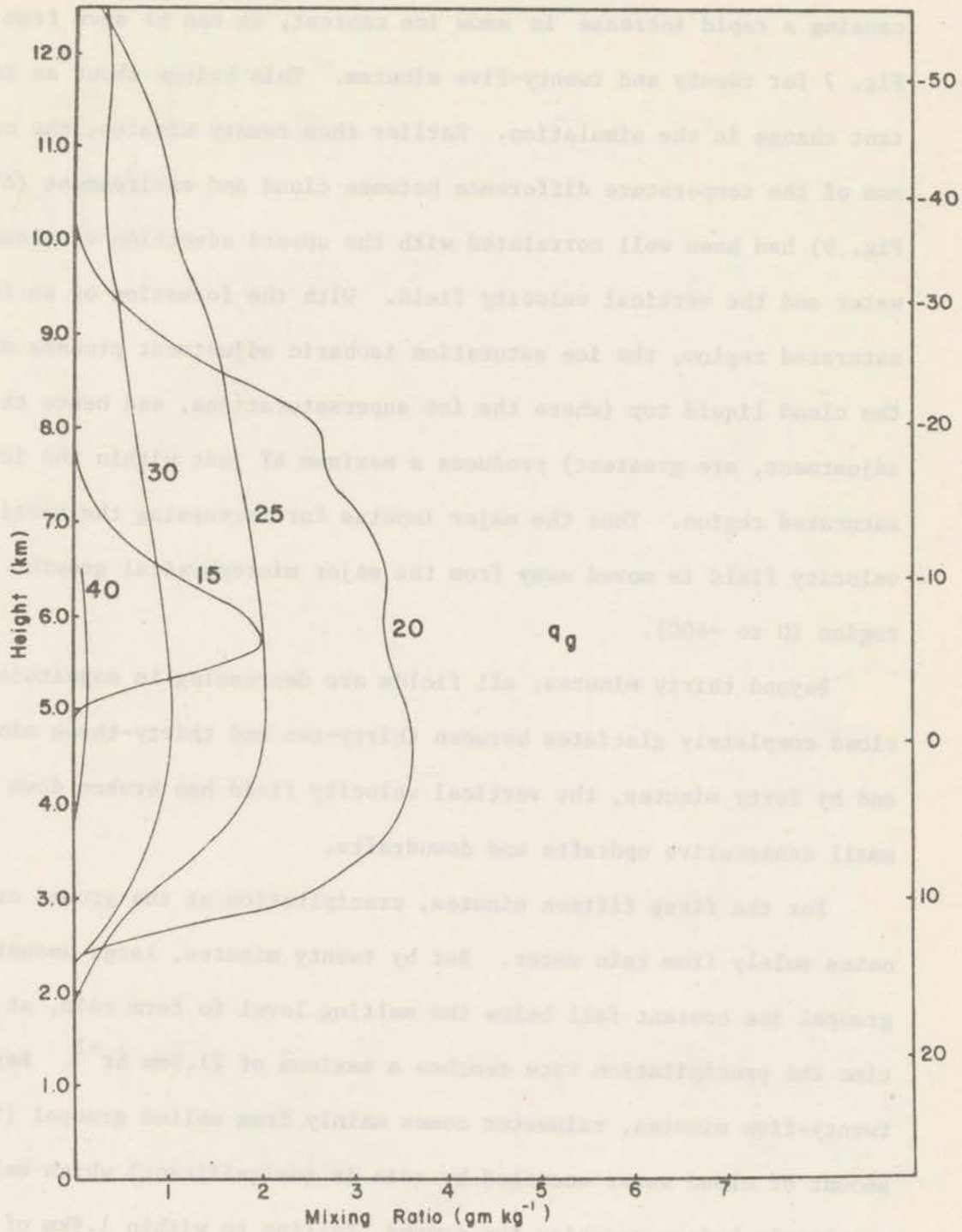

Figure 8. Same as Fig. 4 for graupel ice.

becomes activated (at a height of 10.4km and a temperature of -36.8C) causing a rapid increase in snow ice content, as can be seen from Fig. 7 for twenty and twenty-five minutes. This brings about an important change in the simulation. Earlier than twenty minutes, the maximum of the temperature difference between cloud and environment (ΔT, Fig. 9) had been well correlated with the upward advection of cloud water and the vertical velocity field. With the formation of an ice saturated region, the ice saturation isobaric adjustment process above the cloud liquid top (where the ice supersaturations, and hence the adjustment, are greatest) produces a maximum ΔT just within the ice saturated region. Thus the major impetus for increasing the vertical velocity field is moved away from the major microphysical growth region (0 to -40C).

Beyond thirty minutes, all fields are decreasing in magnitude. The cloud completely glaciates between thirty-two and thirty-three minutes and by forty minutes, the vertical velocity field has broken down into small consecutive updrafts and downdrafts.

For the first fifteen minutes, precipitation at the ground originates solely from rain water. But by twenty minutes, large amounts of graupel ice content fall below the melting level fo form rain, at which time the precipitation rate reaches a maximum of 21.5mm hr^{-1}. Beyond twenty-five minutes, rainwater comes mainly from melted graupel (the amount of cloud water accreted by rain is insignificant) which melts completely before reaching the ground, falling to within 1.9km of the surface. The total amount of water precipitated at sixty minutes is to 6.56mm.

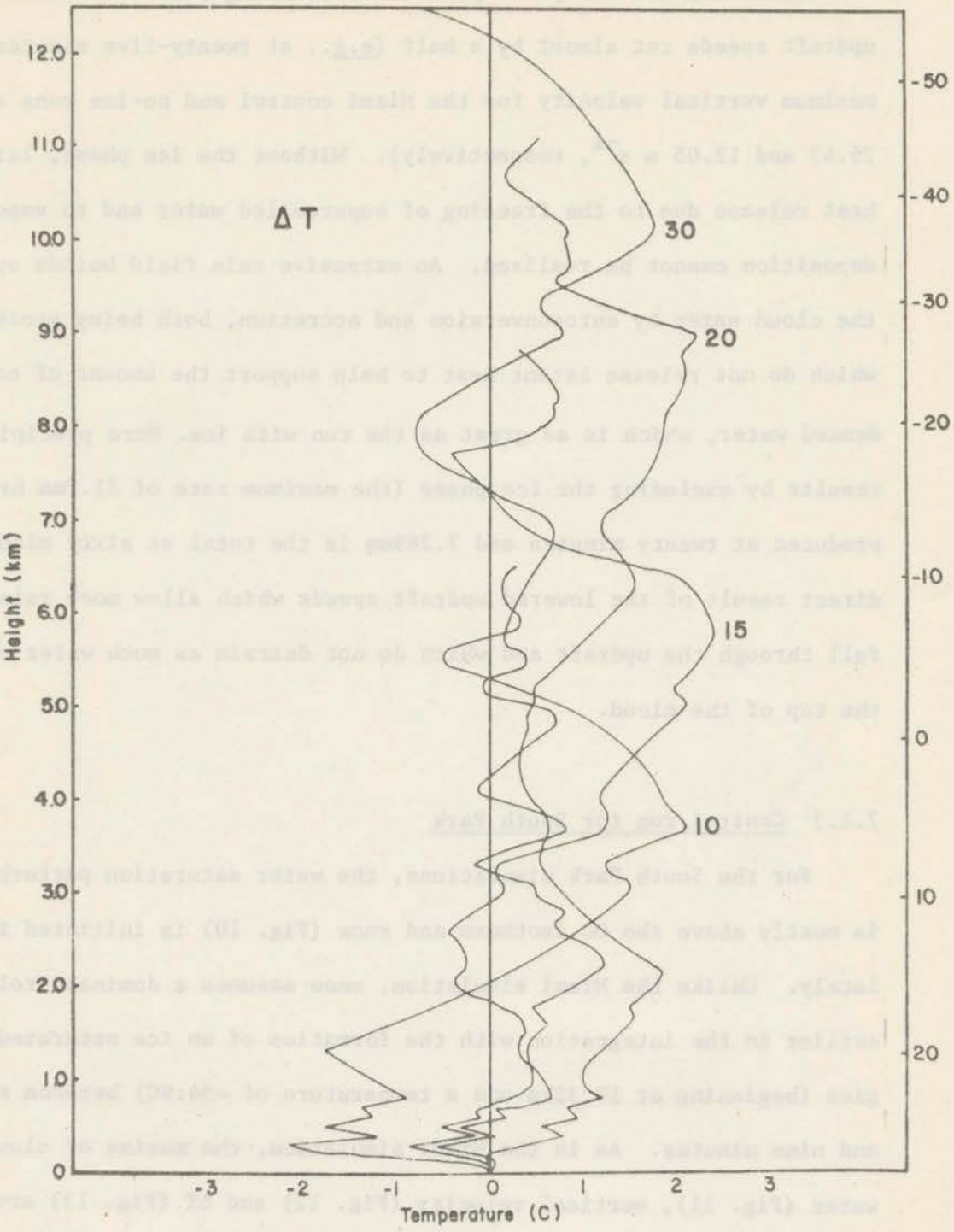

Figure 9. Same as Fig. 4 for temperature difference between cloud and environment (ΔT) in degree centigrade.

7.1.2 Miami simulation without ice

Excluding the ice phase produces a less vigorous cloud with maximum updraft speeds cut almost by a half (e.g., at twenty-five minutes the maximum vertical velocity for the Miami control and no-ice runs are 25.47 and 12.05 m s^{-1}, respectively). Without the ice phase, latent heat release due to the freezing of supercooled water and to vapor deposition cannot be realized. An extensive rain field builds up from the cloud water by autoconversion and accretion, both being processes which do not release latent heat to help support the amount of condensed water, which is as great as the run with ice. More precipitation results by excluding the ice phase (the maximum rate of 21.7mm hr^{-1} is produced at twenty minutes and 7.269mm is the total at sixty minutes), a direct result of the lowered updraft speeds which allow more rain to fall through the updraft and which do not detrain as much water out of the top of the cloud.

7.1.3 Control run for South Park

For the South Park simulations, the water saturation perturbation is mostly above the 0C isotherm and snow (Fig. 10) is initiated immediately. Unlike the Miami simulation, snow assumes a dominant role earlier in the integration with the formation of an ice saturated region (beginning at 10.33km and a temperature of -34.9C) between eight and nine minutes. As in the Miami simulation, the maxima of cloud water (Fig. 11), vertical velocity (Fig. 12) and ΔT (Fig. 13) are all fairly well correlated through ten minutes of integration. At fifteen minutes, condensation of cloud water is still the dominant source of

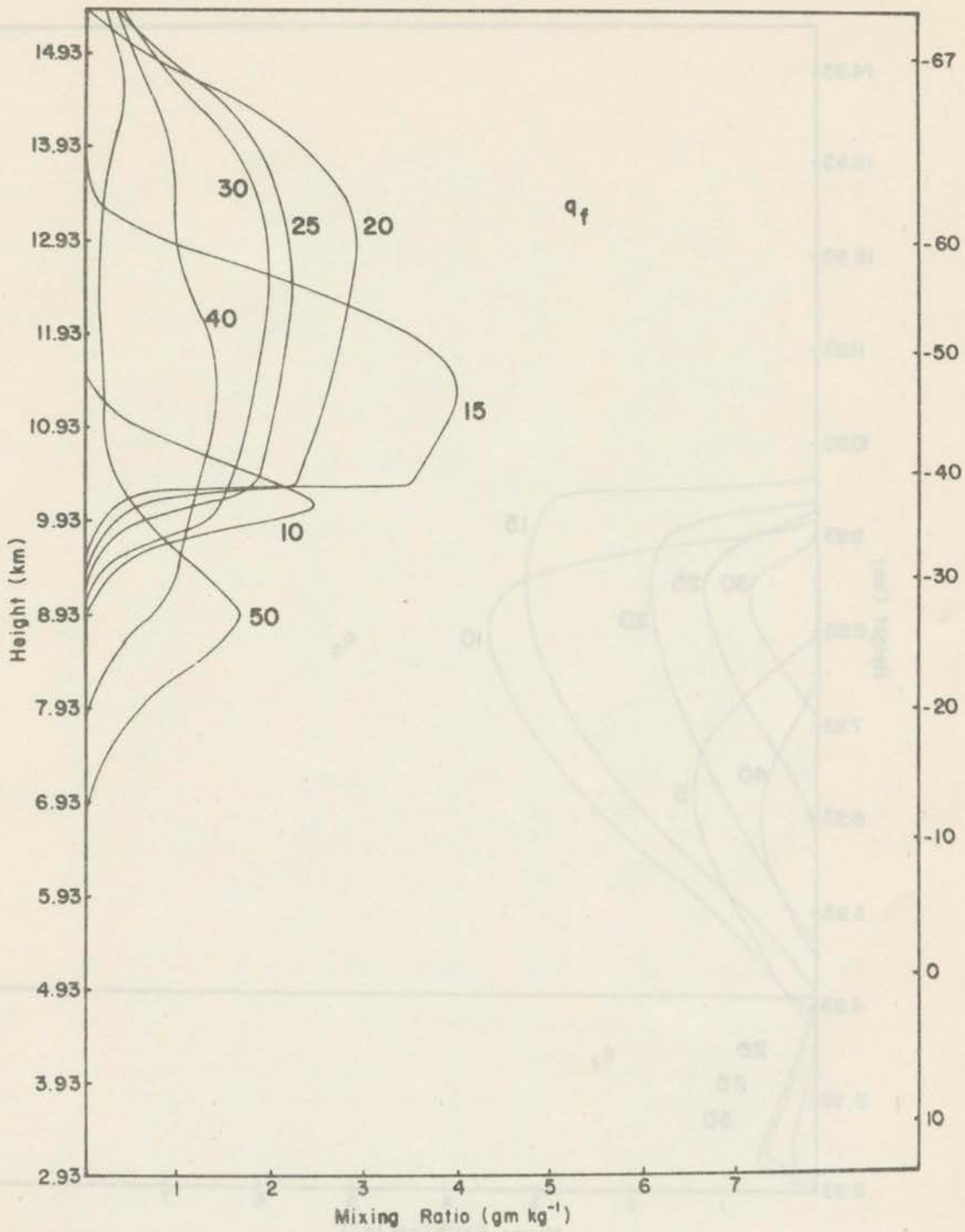

Figure 10. Snow ice mixing ratio in gm kg^{-1} versus MSL height in km as a function of time in minutes for South Park control run. Environmental temperatures in degree centigrade versus height are shown at right.

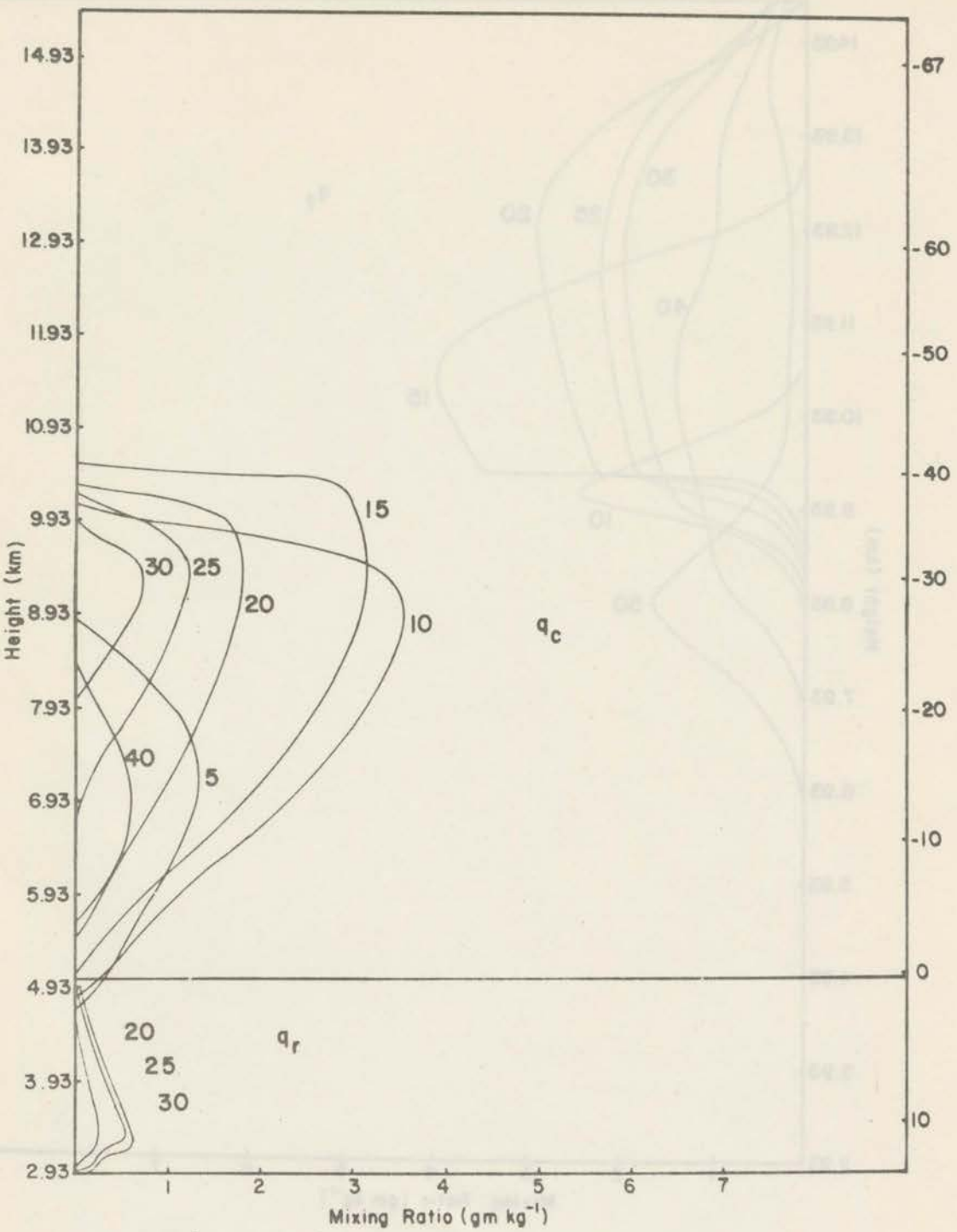

Figure 11. Same as Fig. 10 for cloud water (q_c) and rainwater (q_r).

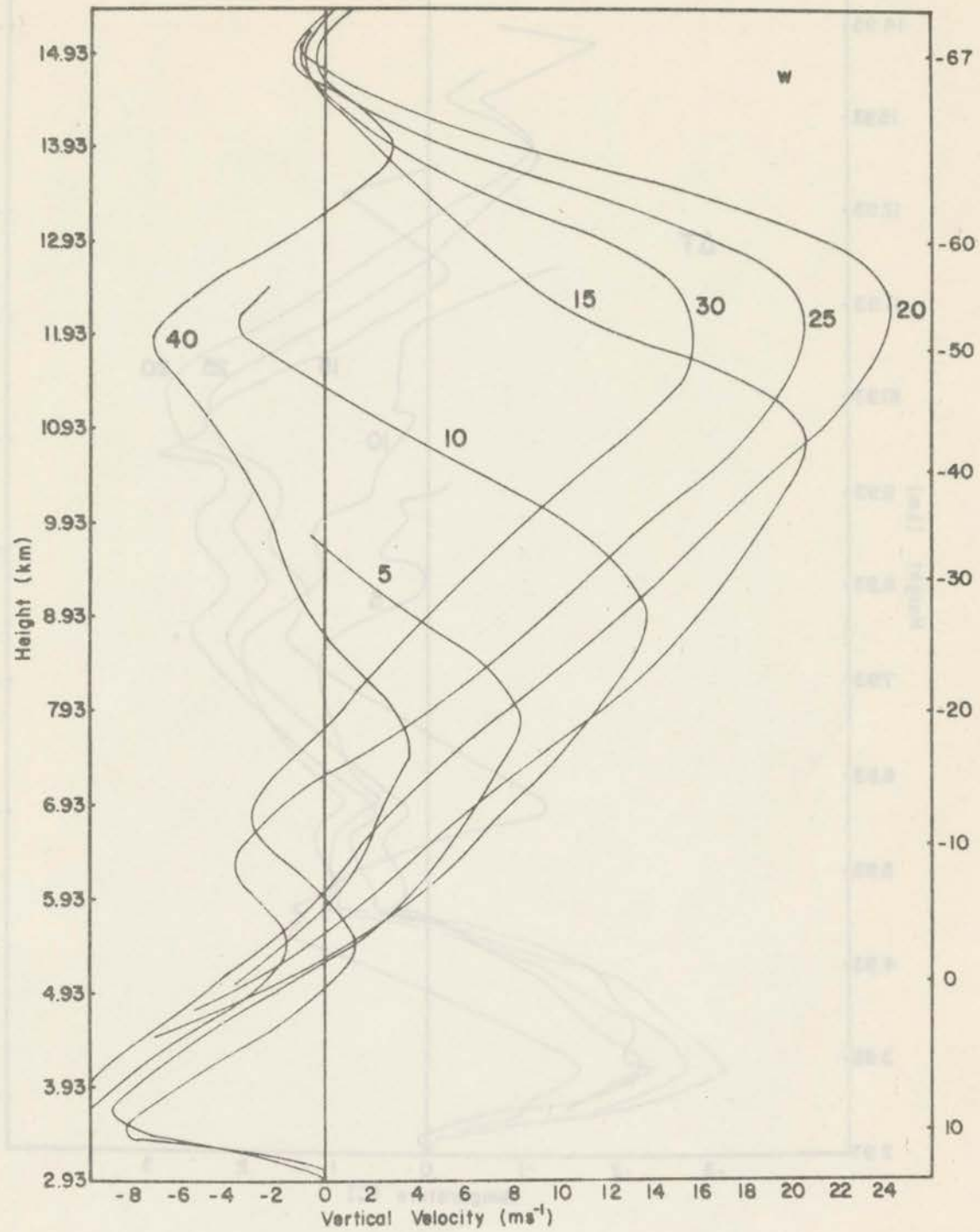

Figure 12. Same as Fig. 10 for vertical velocity field in m s^{-1}.

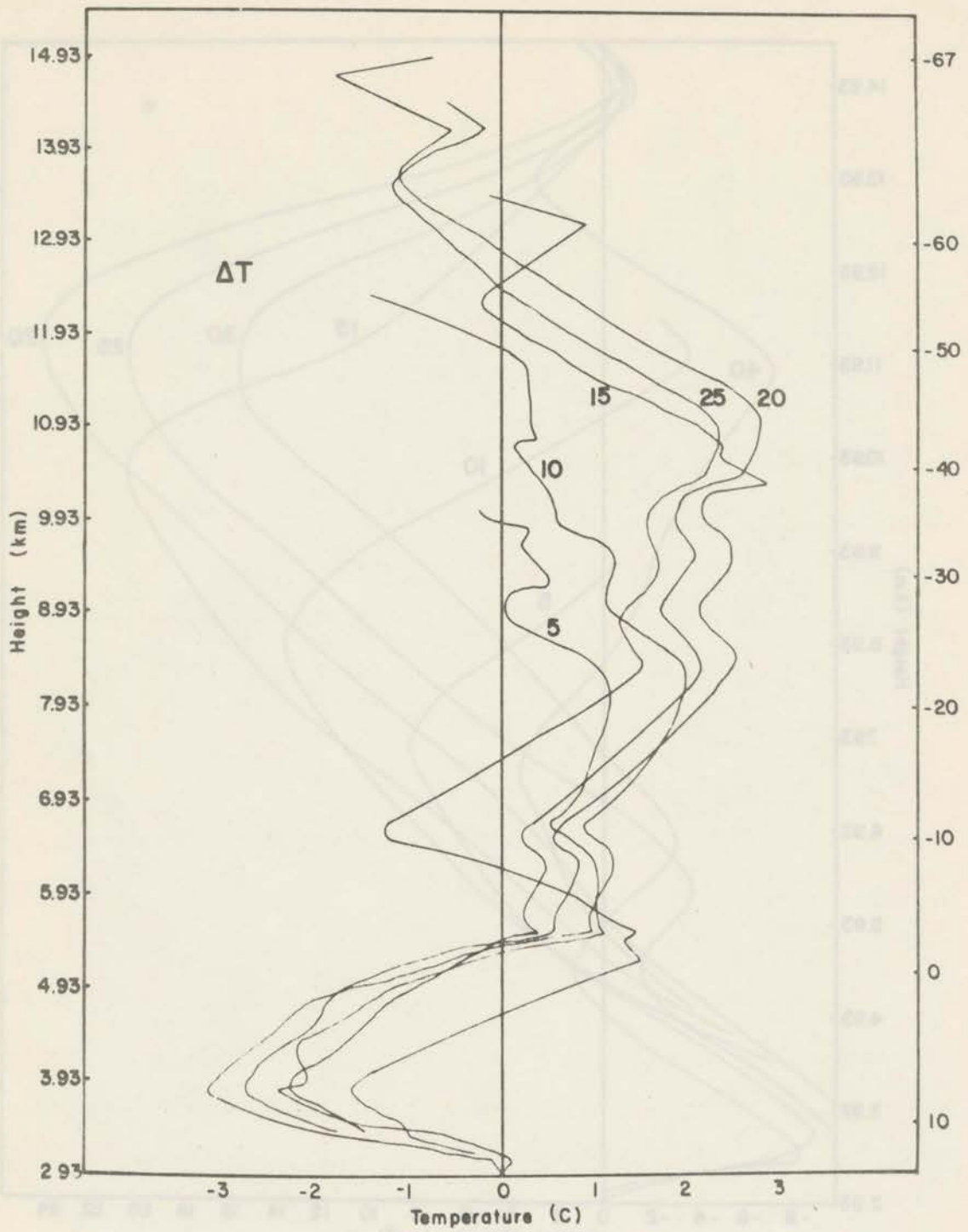

Figure 13. Same as Fig. 10 for temperature difference between cloud and environment (ΔT) in degree centigrade.

latent heat release, but the maximum ΔT is now located within the ice saturated region just above the cloud liquid top. The sharp peak in the ΔT field is a result, not only of the isobaric ice saturation adjustment, but of the isobaric freezing of cloud water advecting into the ice saturated region. The maximum of the vertical velocity field is now just above the -40C isotherm.

Graupel, initialized between six and seven minutes by the riming conversion parameterization, grows by vapor deposition until the mean diameter is large enough to rime cloud droplets. Growth is then rapid as one can see from Fig. 14 at fifteen minutes. Although by this time graupel has begun to fall below the melting level, significant amounts of rainwater begin to be produced at twenty minutes. Indeed, melting graupel is the only source of rain. With the advection of the vertical velocity maximum above the -40C isotherm, the graupel field begins to precipitate rapidly out of the cloud producing a maximum precipitation rate of 6.585mm hr^{-1} at twenty-eight minutes. Although graupel does reach the ground, more precipitation results from melted graupel (i.e., rainwater) than from graupel itself.

Between twenty and thirty minutes, all fields are decaying, but the cloud does not yet completely glaciate. The cloud water field reforms lower down in the domain, as can be seen from Fig. 11 at forty minutes. At this time, the graupel field has been significantly depleted of content and reaches a quasi-steady-state in that approximately as much mass is gained by the riming of cloud droplets as is lost from precipitation below the melting level. The snow content shows a rapid increase above the water saturated region. This is

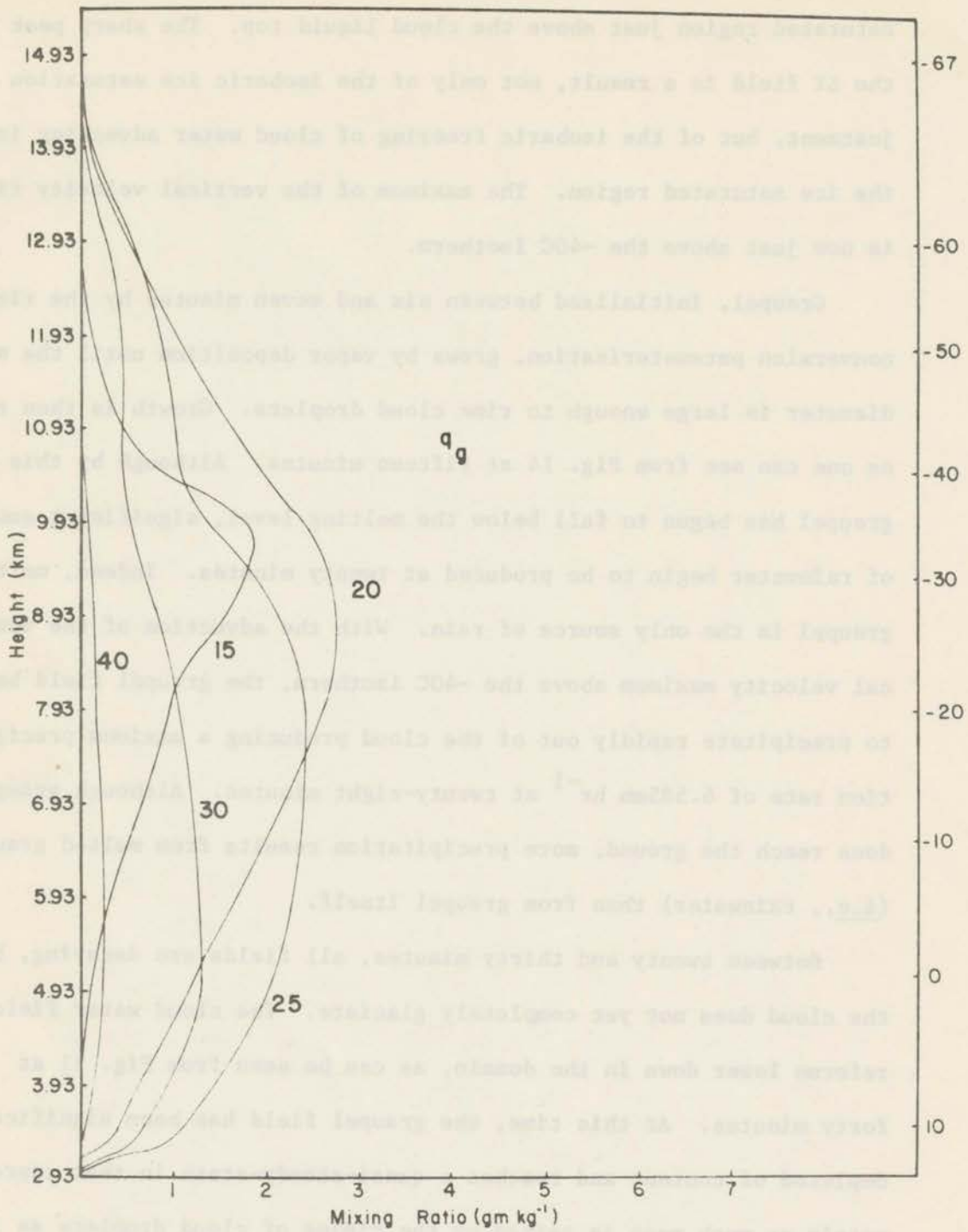

Figure 14. Same as Fig. 10 for graupel ice.

largely due to the upward advection of snow ice content by the weak updraft within the water saturated region and not from ice saturation thermodynamics. The cloud completely glaciates between fifty-four and fifty-six minutes, but again reforms lower down in the domain. Precipitation amounts to 1.56mm at sixty minutes.

7.1.4 South Park simulation without ice

The run in which ice was not allowed produced a much less vigorous circulation (maximum vertical velocity of the run is 13.37m s^{-1}), due to the inability of the cloud to draw into the domain enough water vapor to produce a condensational release of latent heat equivalent to that lost from vapor deposition and riming. Most important is the lack of precipitation (in this case, rain), a direct consequence of the impact of the cold-cloud-base and continentality of the airmass on the conversion formula used to parameterize the formation of rainwater from cloud water. All water vapor in excess of liquid saturation goes into producing an extensive cloud water field which shows a maximum for the run of just under 4.86gm kg^{-1}, and, at thirty minutes, penetrates to a height of 15.73km (-69.6C).

7.2.0 Increase in the concentration of snow

The total snow concentration was increased one order of magnitude by increasing the factor N_{of} (the concentration at 0C) in (3.1). In the following two sections, any reference to a degree of comparison will imply a relation to the control run: e.g., 'greater than' will imply 'greater than the control run'.

7.2.1 South Park

For the cold-cloud-base continental sounding, which does not produce rainwater from cloud water, raising the concentration of snow particles produces two important changes: i) the initial snow ice content is greater and ii) the rate of change of the snow ice content due to vapor deposition and riming are greater. Initially, the mass (or size) of the individual snow crystals is independent of concentration (c.f., section 3.1.3), but since the rate of snow ice content initialization is proportional to this assumed initial mass times the concentration, the initial snow ice content will be higher (in this case one order of magnitude higher). Even though, for the first few moments of the integration, the rate of increase to an individual snow crystal's mass will be independent of concentration, this rate is multiplied by the concentration giving a higher rate of ice content growth the higher the concentration. The greater initial ice content coupled with its more rapid rate of increase, has two important consequences on the dynamic and microphysical properties of the cloud. The greater snow vapor deposition rate allows the formation of an ice saturated region above cloud liquid top sooner and thus provides this important source of latent heat relase earlier to the circulation. Due to the more rapid increase of the snow field from the vapor and, more importantly, from riming, the graupel field is initiated sooner via the riming conversion parameterization which subsequently provides a source of latent heat release earlier to the circulation. Indeed, as one might gather from the above discourse, the higher concentration produces a

more vigorous circulation due to the increased influx of water vapor into the cloud and its subsequent deposition onto snow and condensation onto the cloud water.

The increased vigor of the circulation produced by an increased snow concentration has an enhancing influence on the growth of the snow field from ice saturation thermodynamics. In Fig. 15, one can clearly see the greater mass of snow produced by increasing the snow concentration (although only plotted up to thirty minutes, the snow ice content maintains its greater mass through the integration. As can be seen from Fig. 16, at ten minutes the total graupel ice content is higher. But at fifteen minutes, even though the total amount of graupel ice content is 3.5% greater, the maximum q_g is lowered from 1.83gm kg^{-1} to 1.66gm kg^{-1} due to the effects of the increased circulation (maximum updrafts speeds of 24.57 and 20.57m s^{-1} for high and control concentrations, respectively). After fifteen minutes, the greater updraft speeds advect more graupel ice content into the ice saturated region where the growth rate for graupel is zero due to the absence of supercooled water. This does not permit the initially greater graupel field to gain a greater amount of mass. Consequently, at twenty minutes, more total graupel ice content is obtained in the control experiment.

Similar to the control run, the cloud water field reforms lower down in the domain to bring about an increase to the snow ice content. With higher rates of snow growth, the cloud glaciated sooner (by fifty-one minutes) and the resurgence of the cloud water is delayed, occurring by fifty-six minutes. Due to the lesser graupel ice contents and

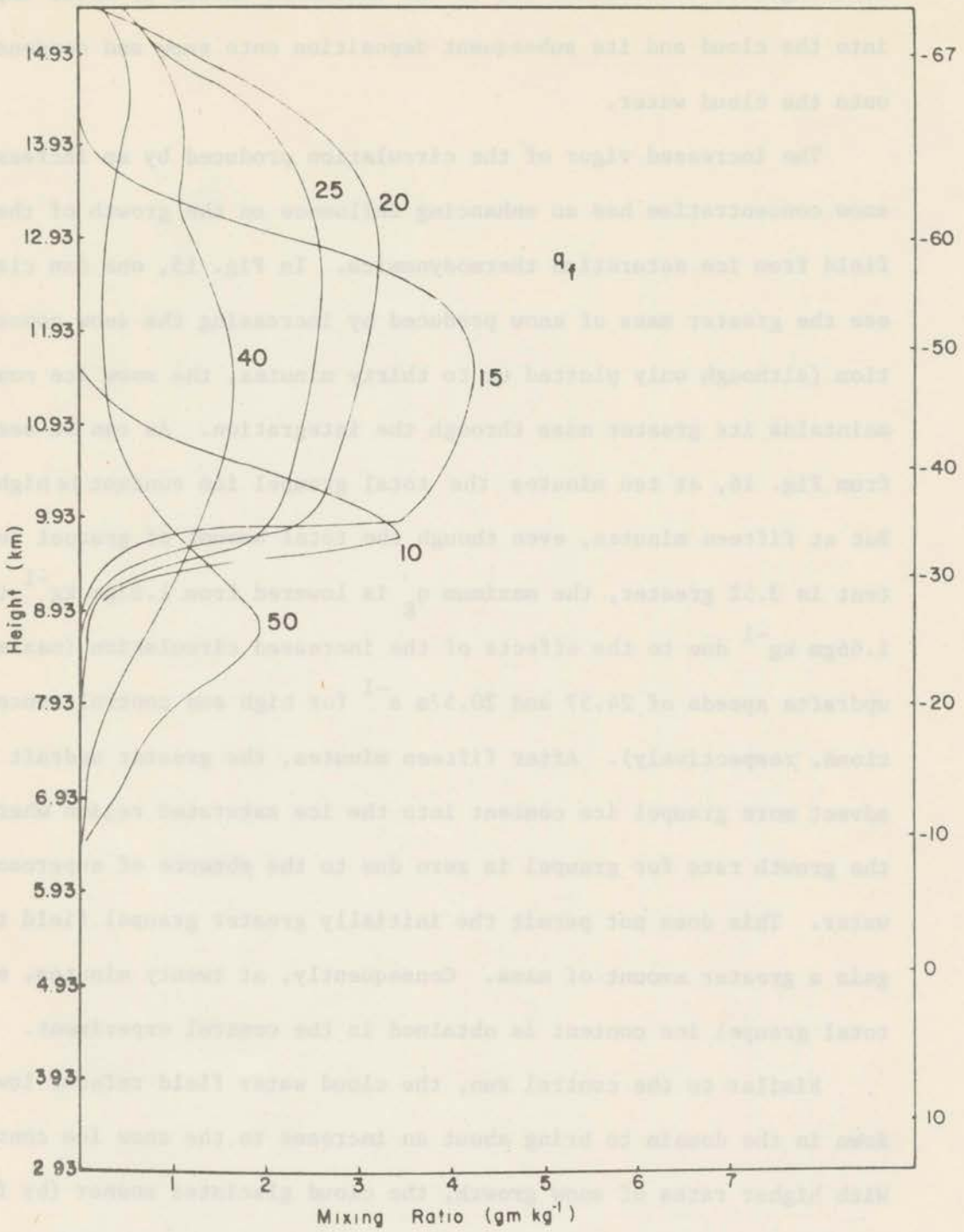

Figure 15. Snow ice mixing ratio in gm kg^{-1} versus MSL height in km as a function of time in minutes for the South Park increased snow crystal concentration ($N_{of} = 10^{-7}$ cm^{-3}) run. Environmental temperatures in degree centigrade versus height are shown at right.

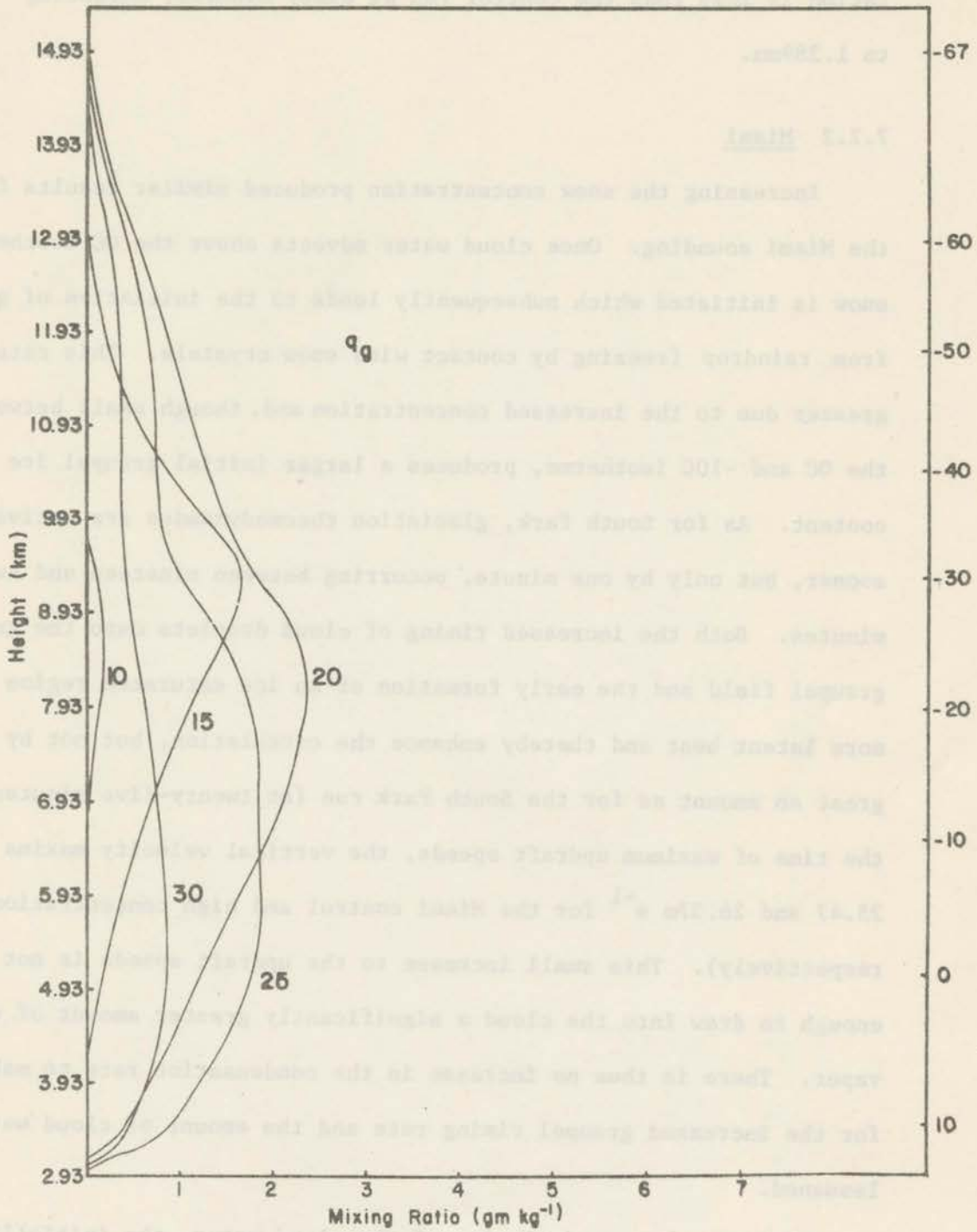

Figure 16. Same as Fig. 15 for graupel ice.

the increased strength of the updraft speeds, the amount of precipitation is less than the control run at sixty minutes, amounting to 1.289mm.

7.2.2 Miami

Increasing the snow concentration produced similar results for the Miami sounding. Once cloud water advects above the 0C isotherm, snow is initiated which subsequently leads to the initiation of graupel from raindrop freezing by contact with snow crystals. This rate is greater due to the increased concentration and, though small between the 0C and -10C isotherms, produces a larger initial graupel ice content. As for South Park, glaciation thermodynamics are activated sooner, but only by one minute, occurring between nineteen and twenty minutes. Both the increased riming of cloud droplets onto the greater graupel field and the early formation of an ice saturated region release more latent heat and thereby enhance the circulation, but not by as great an amount as for the South Park run (at twenty-five minutes, the time of maximum updraft speeds, the vertical velocity maxima are 25.47 and 26.37m s^{-1} for the Miami control and high concentration runs, respectively). This small increase to the updraft speeds is not enough to draw into the cloud a significantly greater amount of water vapor. There is thus no increase in the condensation rate to make up for the increased graupel riming rate and the amount of cloud water is lessened.

With the greater depletion of the cloud water, the initially greater graupel field, after twenty-five minutes begins to decrease.

Graupel is also affected by the decrease of cloud water in that a lesser amount of cloud water is available for accretion by raindrops, lowering the rainwater contents which in turn lower graupel growth from rainwater. Thus the initially greater graupel ice contents are decreased by 7% at twenty-five minutes.

Up to twenty minutes, there is little change in the total precipitation which comes mainly from rainwater formed from cloud water below the freezing level. Past this time, the decreased graupel ice contents affect the amount of water precipitated, which at sixty minutes is decreased by 1.8% to 6.440mm.

7.3.0 Decrease to the total concentration of graupel

The normal total concentration used for graupel, $N_{tg} = 10^{-4}cm^{-3}$, is more closely representative of the smaller spherical ice particles (e.g., rimed snow crystals or rimed frozen raindrops) and not of hail. From the data collected in the field (c.f., section 3.2.2), a total graupel concentration of $10^{-5}cm^{-3}$ (or lower) would place the emphasis on simulating the growth and decay of larger spherical ice particles since the mean mass of the graupel distribution is inversely proportional to the total concentration. This is done by lowering the total graupel concentration by one order of magnitude ($N_{tg} = 10^{-5}cm^{-3}$). Again, any reference to a degree of comparison will imply a relation to the control run.

7.3.1 South Park

All other factors being equal, lowering the total graupel concentration produces two important changes to the simulation of graupel:

i) the riming rate is reduced by 68% (not by one order of magnitude, since the increase to the mean mass compensates, in part, for the decreased concentration) and ii) the characteristic terminal velocity is increased by 147%.

The effects of the reduced riming rate for graupel can be clearly seen in Fig. 17 (compare to Fig. 14). The main difference is that the total graupel ice content is considerably smaller. With the decrease in the major sink of cloud water, this field is greater allowing more riming onto snow crystals, but more important, increasing the snow ice content by isobaric freezing of cloud water at the ice/water saturation interface (Fig. 18) at fifteen minutes. Even though there is a greater isobaric saturation adjustment (66% more at twenty minutes), the reduced riming rate produces a small decrease in the circulation strength, which at twenty minutes amounts to a decrease to the updraft maximum of 1.1m s^{-1}.

The large increase in the characteristic fall speed of graupel, coupled with the lowered rate of melting, increases the value of the graupel mixing ratio at the ground, but decreases the rainwater mixing ratio. The net result is a loss to the amount of water precipitated. At sixty minutes, precipitation is decreased by 31% to 1.076mm.

7.3.2 Miami

Due to the presence of supercooled rainwater, the lower graupel concentration in the Miami run produces substantially different results from the South Park run. At fifteen minutes, there is less total graupel ice content and more total rain content; all other fields remain

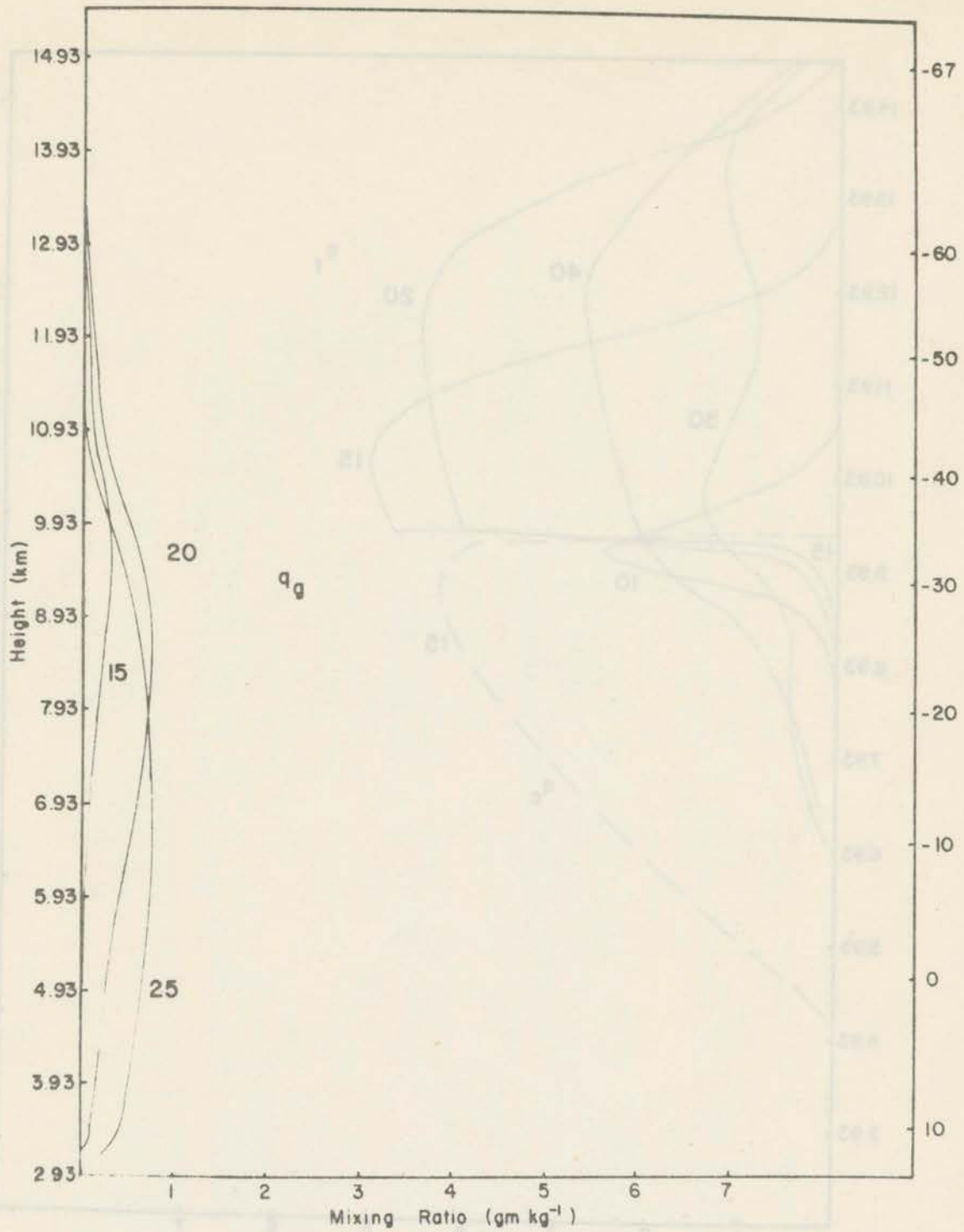

Figure 17. Mixing ratio of graupel ice in gm kg^{-1} versus MSL height in km as a function of time in minutes for the South Park decreased graupel total concentration run. Environmental temperatures in degree centigrade versus height are shown at right.

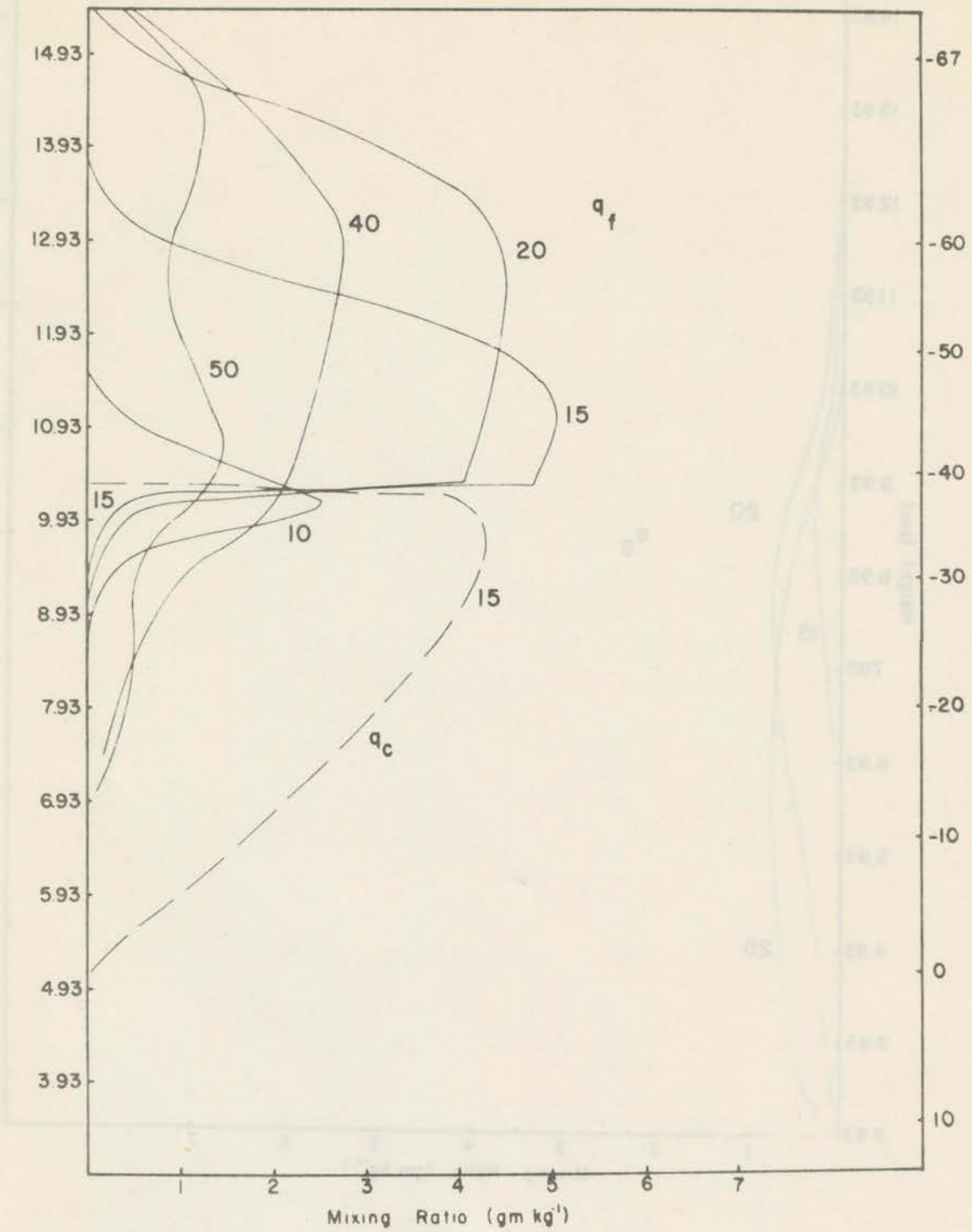

Figure 18. Same as Fig. 17 for snow ice. Also shown is the cloud water field at fifteen minutes (dotted line).

virtually unchanged. But by twenty minutes, the greater cloud water field and the lessened rate of raindrop accretion by graupel have increased the rainwater field above the 0C isotherm substantially (about one order of magnitude increases in the mixing ratios). This tends to compensate for the increased characteristic fallspeed of graupel and the decreased liquid water freezing rate. Also, more rainwater is advected above the -15C isotherm where the rate of raindrop freezing from snow crystal contact becomes significant. Since this rate is unaffected by the graupel ice contents, graupel growth is increased. Indeed, between fifteen and twenty minutes 32.2% more rainwater is frozen into graupel although the total amount of liquid water frozen on to graupel is decreased by 16.6% due to the decreased rate of cloud droplet riming.

At twenty minutes, the circulation strength is much reduced, with an updraft maximum of 15.82m s^{-1} as compared to 20.01m s^{-1} for the control run. The rate of condensation, between fifteen and twenty minutes is decreased by 5.7% and this, along with the 16.6% decrease in liquid water freezing by graupel, may account for this change. By twenty-five minutes, the updraft speeds are about equivalent, although the control run's updraft maximum is 700 meters above that of the decreased total graupel concentration.

At twenty-five minutes, the increased characteristic fallspeed and the decreased melting rate for graupel allow significant amounts of graupel ice content to reach the ground, in contrast to the control run where the graupel field extends to within 1.9km above the surface. In opposition to the results obtained for South Park, precipitation is increased at sixty minutes by 4.4% amounting to 6.850mm.

7.4.0 Decreasing the riming conversion rate

The parameterization of the conversion of snow into graupel by riming assumes that, once the net riming rate for snow has exceeded a pre-specified threshold(c.f., section 3.2.11), the conversion rate equals the snow riming rate. Since this decision is arbitrary, a run is made using the South Park sounding in which one tenth of the net snow riming rate is converted to graupel while the remaining nine tenths increases the snow. This sensitivity experiment did little to change the pattern of the results. The lessened initial amounts of graupel ice contents result in increases in the cloud water and snow ice contents and decreases to the rainwater contents. The vertical velocity field is virtually unchanged. With the lessened graupel field, a decrease in precipitation, at sixty minutes, of 14% results amounting to 1.341mm.

8.0 DISCUSSION

8.1.0 Snow crystal initiation, early growth and snow crystal types

For a warm-cloud-base, maritime precipitation regime, exemplified by the Miami sounding, the liquid water fields (cloud and rain) grow from the start below the OC isotherm. Snow is initiated once the cloud water field advects and/or forms above the OC isotherm and would grow quickly by cloud droplet riming were it not for the already strong updraft speeds produced previously. The updraft advects the small snow crystals and does not allow the rapid growth which could occur from the substantial cloud water field present at the time of snow initiation. For a cold-cloud-base, continental sounding, such as the one from South Park, very little time (compared to Miami) will be spent by the cloud water field below the OC isotherm (for the moisture initiation scheme used, only a small fraction of the cloud field is initiated below the OC isotherm) before advection and/or formation of the field above the freezing level occurs. Thus, snow crystals are initiated while the updraft speeds are low, allowing the accumulation of snow ice content and thereby giving higher riming and vapor deposition rates than for the Miami sounding.

The difference in initial growth rates between the two simulations is also reflected in the amount of time that snow growth is dominated by vapor deposition. For the South Park control run this takes one to two minutes, while for Miami four to five minutes are needed before riming takes place. Both times are within the limits found by other authors. Scott and Hobbs (1977), using a 1DT cloud model, took five

to nine minutes and Hindman and Johnson (1972), who calculated the growth of snow crystals at a constant pressure level, took two to three minutes.

The difference in updraft speeds produced by the two soundings also affects the type of snow crystal. For the active growth phase during the Miami control simulation, the snow field is divided between lightly rimed and unrimed hexagonal plates, with the former predominating at the warmer temperatures. For the active stage in the South Park control simulation, graupel-like snow of a hexagonal type is present at the warmer temperatures, unrimed hexagonal plates dominate the ice saturated region and lightly rimed hexagonal plates are inbetween. The larger, more massive crystals are found at the warmer temperatures due to the increasing snow concentration with height: in general, the snow ice content does not increase with height as rapidly as does the concentration (c.f. (3.2)).

8.2.0 Initiation of graupel and graupel growth

For the Miami sounding, graupel is initiated by raindrop freezing from snow crystal contact and, like snow, occurs as soon as the liquid water fields advect and/or form above the freezing level. The initial graupel ice content is high, compared to that obtained from the riming conversion and tends to simulate the rapid growth of the large frozen raindrops. As found by Cotton (1972), the major role of snow crystals in the supercooled liquid cloud region is the freezing of raindrops.

Since no rain is formed from cloud water for the South Park sounding, graupel initiation depends on the snow riming conversion. This

conversion takes place mainly from riming onto graupel-like snow of hexagonal type (also from a few massive lightly rimed hexagonal plates). Thus initial graupel ice content is small.

The major source of graupel mass for both soundings comes from riming of cloud droplets. For South Park, it is the only source of graupel mass. For Miami, raindrop collection by graupel is also important and even exceeds riming due to the large rainwater field above the freezing level during the first twenty minutes, but does not have as long an effect on graupel. Both soundings produce liquid water accretion rates equal to that of the formation of cloud water from the vapor, but do not have an equal direct effect on the dynamics. The rates being equal, cloud water formation releases one order of magnitude more latent heat to the circulation than do liquid water accretion rates. This is not meant to imply that accretion rates have small influence on the circulation as high accretion rates produce substantial ice contents which indirectly affect the circulation by ice loading. Nor does it mean that the latent heat release itself has insignificant effects on the circulation. For the runs made where the total graupel concentration was lowered, the circulation strength was decreased, primarily due to the loss of latent heat release from riming.

8.3.0 Conversion of snow into graupel

For a cold-cloud-base, continental convective regime, exemplified by the South Park sounding, conversion of snow into graupel is the only means of initializing graupel. In an actual cloud, 'conversion' arises

from a distribution of snow crystals having differing dimensions and masses. By riming cloud droplets, some of the crystals will become heavily rimed graupel particles. Since in this ice parameterization, snow crystals have the same size and mass and are contained in only one variable, it is possible to obtain only an estimate of the conversion process. With only two variables to describe the ice phase and without predictive equations on ice concentrations, the parameterization of the conversion process is constrained to attempt the simulation of the time needed for a snow crystal to become graupel-like and the amount of mass converted. For the South Park control run, the time taken by snow crystals before conversion commences, six to seven minutes, appears satisfactory, within limits found by other authors (Scott and Hobbs, 1977; and Hindman and Johnson, 1972) using less parameterized descriptions of the ice phase. It is harder to judge whether the amount of mass converted is reasonable. When conversion first takes place, it is, of course, the dominant rate of graupel production. Within three minutes, graupel riming becomes much greater than the conversion rate. Thus, during the active stage of cloud growth, the amount of mass converted is only important before graupel riming becomes significant.

Even so, the parameterization does not appear very sensitive to changes in the initial ice contents of graupel, as demonstrated by the decreased riming conversion run. Several factors tend to increase the graupel ice contents to make up for the initial loss in graupel mass. The riming conversion plays a longer role in increasing the graupel ice contents as do the greater rates of riming by snow. The

cloud water field is increased due to the initially small graupel ice contents. Thus, once graupel begins to rime substantially, these greater cloud water contents increase the graupel riming rate (but not above that of the control run) and tend to compensate for the initially lowered graupel ice contents.

A point is reached in the South Park simulations where the amount of cloud water rimed onto snow will not be greater than that fraction of the snow ice mixing ratio used for the threshold, precluding the riming conversion. Thus the snow field can increase until the maximum mass conversion takes place. Between thirty and fifty minutes for the South Park control run, the amount of snow ice content converted into graupel is insignificant when compared with that gained by cloud droplet riming or that lost by melting. But beyond fifty minutes, the conversion rate exceeds that of riming such that the total amount of ice content converted is approximately one order of magnitude greater than that gained from graupel riming. Fortunately, the changes in the graupel field are much smaller at this time than during the active stages of cloud growth. Such is not the case for the South Park lowered riming conversion run in which the maximum mass conversion plays a greater role in increasing the graupel ice contents. More snow ice content is converted by this process sooner in the integration, starting around twenty-five minutes. This is, of course, a direct result of the increased snow ice contents produced by decreasing the rate of riming conversion.

The maximum mass conversion is a necessary artifice to stop the parameterization from producing unrealistic snow crystal dimensions

and fall speeds. It is desirable to place as little emphasis as possible on this conversion. Consequently, no decrease in the riming conversion rate should be made.

That is not to say that the normal conversion parameterization is without its faults. A major problem is that the number of snow crystals is not conserved and consequently neither is the mass of an individual snow crystal. Upward advection of the snow ice content, as is present during riming, takes mass away from that part of the domain where riming is extensive and does not allow a large snow crystal mass to develop. This is made worse by allowing the concentration of snow to increase exponentially with decreasing temperature, in effect giving smaller snow crystal masses with height despite the upward advection of snow ice content. This problem occurs for the South Park control run, but is made more clear from the decreased conversion run, where the amounts of snow ice produced by riming are increased. Another problem is with the conversion parameterization itself. As mentioned before, by comparing the riming rate with a fraction of the snow ice mixing ratio a point is reached where large amounts of snow ice content preclude the riming conversion. High riming rates onto small crystals should produce spherically shaped particles within a short order of time. By lowering the conversion coefficient C_m in (3.2.11) for high snow ice contents, one could alleviate this problem. In order to do this realistically, more field data (and possibly data from detailed computer models of the ice phase) on the formation of graupel-like particles from snow crystals is needed before a better conversion rate can be formulated.

8.4.0 Ice saturation thermodynamics

Ice saturation thermodynamics are the major source of snow ice content and release a significant amount of latent heat. The process by which a cloud model determines whether a water or an ice saturation adiabat is to be followed is therefore an important one.

To make such a decision, the amount of snow mixing ratio gained (or lost) by vapor deposition is compared to the difference between the mixing ratios of water vapor and ice saturation (times a constant of 0.75). Once this decision is made, the rate of change of the snow ice content is determined by an adjustment to ice saturation and the rate of change of ice saturation of an ascending or descending parcel. An ice saturated region was first predicted around the -38.4C and -36.8C isotherms for the South Park and Miami control runs, respectively. This is mainly due to the snow crystal concentration, which, in general, produces a higher vapor deposition rate the colder the temperature. Increasing the snow crystal concentration by one order of magnitude lowers the height at which an ice saturated region first formed, e.g., for South Park, from 10.43km to 9.93km (-33.6C). Concentration also affects the warmest temperature (lowest height) at which the ice saturated region can extend which for both control runs is around the -35C isotherm.

One finds that immediately above the cloud liquid top the domain is not necessarily ice saturated since the net vapor deposition rate may not be great enough to hold the region to ice saturation. Therefore this part of the domain remains supersaturated with respect to ice but subsaturated with respect to water and can divide the ice and

water saturated regions by as much as four hundred meters during the active growth stage of the cloud circulation.

Since for this 1DT model the ice saturation routine is designed to set the water vapor mixing ratio exactly equal to that of ice saturation (thus both the vapor deposition rate and the ice supersaturation will both be zero) once a part of the domain is determined ice saturated it remains at ice saturation until the snow ice content becomes zero. Thus, as for all South Park simulations, cloud water can advect in substantial quantities (q_c > 2gm kg^{-1}) into the ice saturated region. Any cloud water advecting into the ice saturated region is assumed isobarically frozen into snow. This is probably not the correct process as cloud water, when it enters into an ice saturated region, will evaporate to increase the mixing ratio of water vapor and thus the supersaturation with respect to ice. If all of the advected cloud water is not evaporated then the region is water saturated. Judging how much, if any, cloud water remains at the end of a time step should be done in the ice/water saturation decision and will involve a slightly more complicated decision process. In the case of strong advection of cloud water into the ice saturated region, this would move the ice/water saturation interface to the assumed homogeneous nucleation temperature (-40C) and would not produce a great change in the results.

8.5.0 Graupel total concentration

Decreasing the total graupel concentration will produce a decrease in the circulation strength, simply because the rate of liquid water accretion is decreased. Apparently, what effect a change in the concentration has on the precipitation depends on the presence of large

amounts of rainwater. For South Park, decreasing the concentration produces a decrease in the total amount of water precipitated due to the significantly lessened graupel ice contents. Miami, on the other hand, produces more precipitation due to the presence of a rain field formed from cloud water. Since liquid water accretion is lessened, the rain field is not only less affected by collection from graupel but gains water by droplet accretion from the greater cloud water contents. The increase in the rainwater field compensates, in part, for the lessened collection rate by graupel but also allows more upward advection of rainwater which is subsequently frozen by contact with snow crystals, a rate not dependent on the concentration or contents of graupel. Although the contents of graupel are decreased, the greater rain contents, coupled with faster downward advection and lowered melting rate of graupel, increase the precipitation at the ground.

8.6.0 Snow concentration

Both South Park and Miami soundings exhibit similar responses when snow concentration is raised. The snow field grows faster from vapor deposition and riming. Graupel is initiated sooner for South Park allowing more time for graupel to grow by riming and thus creates an initially greater graupel field. Although, for Miami, graupel is initiated through the freezing of raindrops, no sooner than before, the initial graupel mass is higher, creating higher initial riming rates and thereby producing a greater graupel field soon after graupel initiation. Since the snow field and concentration are increased, an ice saturated region is produced sooner and lower in the domain,

simulating the fact that more snow crystals will increase the vapor deposition rate near liquid cloud top and thus create a more extensive ice saturated region. With the increased emphasis on ice saturation thermodynamics and increased rates of snow growth, more latent heat is released to increase the strength of the circulation. Associated with the increase in updraft speeds is a greater upward advection of graupel ice content. The initially greater graupel field cannot overcome the increased updraft speeds and results in a decrease in precipitation. The decrease in precipitation is further enhanced by the early complete glaciation of the cloud.

Some of the effects of seeding as seen in the field are reproduced by the ice parameterization, e.g., increased updraft speeds and early complete glaciation of the cloud. In this case, seeding is done by an increase to the snow crystal concentration over the whole domain and for all time, resulting in a decrease in the total amount of precipitation. In an attempt to bring about an increase in precipitation, runs are made where the concentration is again increased by one order of magnitude for the whole domain, but only for five minute periods, starting at five, ten and fifteen minutes simulated time, for both soundings. Results are similar to the runs made where the concentration is increased for all time, e.g., precipitation decreases, vertical velocity increases, etc.. Apparently, the soundings and model parameters (e.g., cloud radius, turbulent coefficients, etc.) produce a circulation which reaches a height virtually independent of the changes made to the snow crystal concentration. Confirming the results of Simpson and Wiggert (1969), these simulations do not demonstrate high 'seedability' (c.f., section 2.0) and precipitation is reduced.

9.0 SUMMARY AND CONCLUSION

A basic premise of the ice parameterization described herein is that a realistic ice phase simulation be developed without overtaxing computer resources. In order to do this, bulk ice microphysics are used. This, coupled with the use of only two ice variables, emphasizes the simulation of the effects of ice on the dynamics and not the simulation of ice as a means of its own. One can reasonably obtain the characteristic properties of the ice phase within a grid volume (for a three-dimensional cloud model), but not those of the individual ice particles.

The two variables divide the ice phase into small numerous crystals with low terminal velocity (snow) and large spherical ice particles with high terminal velocity (graupel). Snow plays two important roles in convective clouds. Due to its small size and high concentration, it controls the ice saturation thermodynamics, playing a role similar to cloud droplets when the cloud is ice saturated. Snow also initiates precipitating ice (graupel) by riming into spherically-shaped particles or by nucleating supercooled raindrops. Graupel, with its large mass and high fall speeds, is a principal sink of liquid water and plays an important part in precipitation development in both maritime and continental cloud simulations.

The major sources and sinks of the ice phase (vapor deposition, liquid water accretion, raindrop freezing from snow crystal contact, ice saturation thermodynamics and melting) are included and give acceptable results. There are, however, some problems, a major one being the assumption that there is a one-to-one correspondence between the concentration of snow and an externally defined concentration of

depositional ice nuclei. The riming conversion of snow into graupel is not realistically handled due to the advection of snow ice content, and not the individual crystal masses, away from the main riming region. This is compounded by the exponential increase of the concentration with decreasing temperature, giving, for equal snow ice contents, a decrease in crystal mass with height. Carrying the snow crystal concentration as a third ice variable would allow for a more faithful riming conversion as the number, hence crystal mass and size, would be better conserved. Also, the activation of depositional ice nucleants could then be given as a rate of increase in the concentration and not as pre-existing ice crystals having no mass. It is recommended that the snow crystal concentration be added as another ice variable. Unfortunately, this could very well prove too expensive in a three-dimensional simulation; particularly if the turbulence parameterization involves the modeling of variances and covariances of mean quantities.

Without carrying the concentration of snow as a variable, how then to simulate seeding and ice multiplicaton? One cannot, of course, explicitly predict the movement of seeding material or ice splinters within the domain. Rough estimates of the effects of seeding can be obtained by assuming increases to the concentration over a pre-specified region and over a pre-specified period of time. For example, one can simulate an airplane seeding run at the base of a growing tower by an increase in concentration in that region and then decay the concentration to its former value. One might even tie the decay to the turbulent diffusion of some other variable, e.g., of cloud water. Ice multiplication, according to current research, depends on the co-existence of

large supercooled liquid drops and graupel. Recognition of such regions of co-existence would be easy and having done so, they could then be referenced for future use with minimal amounts of computer storage. What might prove difficult is in specifying how much the concentration has been increased. In a similar manner to the simulation of seeding, one could simply increase the concentration by a pre-specified amount when the conditions are right. Such a scheme might give spasmodic jumps in the concentration (and snow crystal growth rates, etc.) should a region fluctuate about the thresholds used to delineate a region of ice multiplication. To solve this problem, the concentration, along with parameters delineating the ice multiplication region, would have to be stored. This might prove feasible if multiplication occurs over a small fraction of the domain, but could prove too much of a drain on computer storage if widespreead. Both the above-mentioned simulations of ice multiplication will give an increase in graupel production due to the increased freezing of raindrops from snow crystal contact as occurred for Koenig (1977). The effects of ice multiplication on increasing the graupel ice content by snow crystal riming, as reported by Takahashi (1976), would not be as valid since the increased number of snow crystals formed by the multiplication process would not be able to advect away from the ice multiplication region.

Aggregation of snow crystals is another ice process in cumulus clouds affecting the snow crystal concentration. Hobbs, et al., (1974) noted that high rates of aggregation occurred for warm temperatures and high crystal concentrations. Aggregation was also increased by the

shape of the crystal, i.e., dendritic type crystals aggregate more than column type crystals. Thus, if seeding can substantially increase the number of snow crystals, an enhancement in the aggregation rate should be expected. Dye, et al., (1976) seeded cold based (-12C) continental clouds and found that stellar dendrites were produced in concentrations of 400 per liter as a direct consequence of the AgI seeding. Aggregates were formed from crystals as small as 400 to 500μm and 50% of all ice particles were aggregates 15 min after seeding. Such a large number of aggregates, with their greater surface area for collection of cloud droplets than an individual crystal of equal mass, would substantially alter the precipitation process. With the current crystal concentration used in this parameterization, no aggregation will occur as the concentration at the warmer temperatures (0 to -10C) is much too small. Thus, modeling of the aggregation process should be considered if the number of crystals at warmer temperatures is increased substantially, e.g. from seeding or an ice multiplication process. Even if the concentration is increased, aggregation will be difficult to include.

Graupel appears to be better represented than does snow; nonetheless, carrying the total graupel concentration would allow for a better simulation of the growth of graupel. Advection of the smaller graupel particles would leave behind the less numerous heavier particles and would better simulate a hail distribution. This would be convenient but not as crucial as carrying the concentration of snow.

Although an economic necessity, the use of a 1DT model restricts the simulation of the ice phase. A steady-state cloud base could not be obtained, even with the addition of water vapor at cloud base for the

first five hundred seconds of the integration. Both cloud water and vertical velocity fields advect upward such that water and ice loading, for most cases, do not cause the demise of the circulation: the cloud water field reaches the -40C isotherm and the vertical velocity field reaches the tropopause. Precipitation development is hampered in that the model cannot produce rotations or simultaneous updrafts and downdrafts. Nonetheless, the model has been useful as a test bed and has shown that the two variable ice phase parameterization should meet with no major problems in higher dimensional time-dependent models.

10.0 IMPLEMENTATION OF THE PARAMETERIZATION IN A 3DT MODEL AND SUGGESTIONS FOR FUTURE TESTING

Implementation of this parameterization in higher dimensional cumulus cloud models will, of course, involve some reformulation of the main program. One will have to allocate storage for a minimum of two ice microphysical variables (snow and graupel), add appropriate equations to simulate the advection and diffusion of ice and include the latent heat release due to the ice phase in the thermodynamics. All variables are defined within their respective subroutines, are made as easily recognizable as possible and are distinct, allowing the use of a text editor to make any changes in variable names necessary to comply with the main program. The most difficult part to implement will be ice saturation thermodynamics, specifically, the decision as to whether a region will be at ice saturation.

Questions which can be best answered using a 3DT cumulus cloud model are:

1. Is recylcing of ice particles important?
2. If recylcing of snow crystals is important, how can one externally specify the concentration in order to reproduce the results found by Takahashi (1976)?
3. If recylcing of graupel is important, does this process increase the mean mass of the distribution so that it can be considered hail (i.e., $\bar{m}_g > 2 \times 10^{-2}$ gm)?
4. What are the effects of the ice phase on downdraft formation?

5. How well do local changes to the snow crystal concentration due to seeding and ice multiplication reproduce the results of Scott and Hobbs (1977), Koenig (1977) and Takahashi(1976)?
6. How close does the parameterization simulate the ice phase as observed in the field?

REFERENCES

Auer, A. H., and D. L. Veal, 1970: The dimensions of ice crystals in natural clouds. J. Atmos. Sci., 27, 919-926.

Bigg, E. K., 1953: The supercooling of water. Proc. Phys. Soc. London, B66, 668-694.

Byers, H. R., 1965: Elements of Cloud Physics. The University of Chicago Press, Chicago, Ill., 191 pp.

Cannon, T. W., J. E. Dye and V. Toutenhoofd, 1974: The mechanism of precipitation formation in NE Colorado cumulus, II. Sail plane measurements. J. Atmos. Sci., 31, 2148-2152.

Charlton, R. B., and R. List, 1972: Hail size distributions and accumulation zones. J. Atmos. Sci., 29, 1182-1193.

Chisholm, A. J., and M. English, 1973: Alberta hailstorms, II. Growth of large hail in the storm. A.M.S. Meteorological Monographs, 14, No. 36, 98pp.

Cooper, W., 1978: Precipitation mechanisms in summertime storms in the Montana Hiplex area. Conference on Cloud Physics and Atmospheric Electricity, A.M.S., Issaquah, Wash., 347-354.

Cotton, W. R., 1970: A numerical simulation of precipitation development in supercooled cumuli, Report No. 17, NSF Contract No. NSF GA-13818, Dept. of Meteorology, The Pennsylvania State Univ., University Park, Penn., 179pp.

_____, 1972: Numerical simulation of precipitation development in supercooled cumuli, I & II. Mon. Wea. Rev., 100, 757-784.

_____, 1975: On parameterization of turbulent transport in cumulus clouds. J. Atmos. Sci., 32, 548-564.

_____, and G. J. Tripoli, 1978: Cumulus convection in shear flow-three-dimensional numerical experiments. J. Atmos. Sci., 35, 1503-1521.

Danielson, E. F., R. Bleck, and D. A. Morris, 1972: Hail growth by stochastic collection in a cumulus model. J. Atmos. Sci., 29, 135-155.

_____, and W. R. Cotton, ed., 1977: Space Log 1977, Dept. of Atmospheric Science, Colorado State Univ., Ft. Collins, Colo., 400pp.

Das, P., 1962: Influence of wind shear on the growth of hail. J. Atmos. Sci., 19, 407-414.

REFERENCES (continued)

Dennis, A. S., and D. J. Musil, 1973: Calculations of hailstone growth and trajectories in a simple cloud model. J. Atmos. Sci., 30, 278-288.

Douglas, R. H., 1964: Size spectra of Alberta hail. National Conference on Physics and Dynamics of Clouds. A.M.S., Chicago, Ill.

Dye, J. E., et al., 1974: The mechanism of precipitation formation in NE Colorado cumulus, III. Coordinated microphysical and radar observations and summary. J. Atmos. Sci., 31, 2152-2159.

Farley, R. D., et al., 1976: Final report on the numerical simulation of hailstorm modification by competing embryos. S. D. School of Mines, Institute of Atmos. Sci. Report 76-5, Rapid City, S. Dak., 56pp.

Federer, B., and A. Waldvogel, 1975: Hail and raindrop size distributions from a Swiss multicell storm. J. Appl. Meteor., 14, 91-97.

Fletcher, N. H., 1969: The Physics of Rain Clouds, Cambridge at the University Press, New York, NY, 390pp.

Gokhale, N. R., and K. M. Rao, 1969: Theory of hail growth. J. Rech. Atmos., 4, 153-178.

Hallett, J., and S. C. Mossop, 1974: Production of secondary ice particles during the riming process. Nature, 249, 26-28.

Hess, S. L., 1959: Introduction to Theoretical Meteorology. Holt, Rinehart and Winston, New York, NY, 362pp.

Heymsfield, A., 1972: Ice crystal terminal velocities. J. Atmos. Sci., 29, 1348-1357.

_____, 1978: The characteristics of graupel particles in northeastern Colorado cumulus congestus clouds. J. Atmos. Sci., 35, 284-295.

Hindman, E. E., and D. B. Johnson, 1972: Numerical simulation of ice particle growth in a cloud of supercooled water droplets. J. Atmos. Sci., 29, 1313-1321.

Hirsch, J. H., 1971: Computer modeling of cumulus clouds during Project Cloud Catcher. S.D.School of Mines, Inst. of Atmos. Sci., Report 71-7, Rapid City, S. Dak., 61pp.

Hobbs, P. V., et al, 1972: Contributions from the cloud physics group, Research report VII. Dept. of Atmos. Sci., Univ. of Wash., Seattle, Wash., 293pp.

_____, S. Chang and J. Locatelli, 1974: The dimensions and aggregation of ice crystals in natural clouds. J. Geophys. Res., 79, 2199-2206.

Iribarne, J. V., and R. G. Pena, 1960: The influence of particle concentration on the evolution of hailstones. Nubila, 5, 7-30.

Jayaweera, K., 1971: Calculations of ice crystal growth. J. Atmos. Sci., 28, 728-736.

Jiusto, J. E., 1971: Crystal development and glaciation of supercooled clouds. J. Rech. Atmos., 5, 69-85.

Jones, R. F., 1960: Size-distribution of ice crystals in cumulonimbus clouds. Quart. J. R. Meteor. Soc., 86, 187-194.

Knight, C. A., et al., 1974: The mechanism of precipitation formation in NE Colorado cumulus, I. Observations of the precipitation itself. J. Atmos. Sci., 31, 2142-2147.

Koenig, L. R., 1971: Numerical modeling of ice deposition. J. Atmos. Sci., 28, 226-237.

_____, 1972: Parameterization of ice growth for numerical calculations of cloud dynamics. Mon. Wea. Rev., 100, 417-423.

_____, and F. W. Murray, 1976: Ice-bearing cumulus cloud evolution: Numerical simulation and general comparison against observations. J. Appl. Meteor., 15, 747-762.

_____, 1977: The rime-splintering hypothesis of cumulus glaciation examined using a field-of-flow cloud model. Quart. J. R. Meteor. Soc., 103, 585-606.

Langmuir, I., 1948: Project Cirrus - The production of rain by a chain reaction in cumulus clouds at temperatures above freezing. General Electric Res. Laboratory Occasional Report No. 1, 26pp.

List, R. J., ed., 1949: Smithsonian Meteorological Tables, Smithsonian Institution Press, Washington, D.C.

_____, R. B. Charlton and P. I. Buttals, 1968: A numerical experiment on the growth and feedback mechanisms of hailstones in a one-dimensional steady-state model cloud. J. Atmos. Sci., 25, 1061-1074.

REFERENCES (continued)

Liu, J. Y., and H. D. Orville, 1968: Numerical modeling effects on a cumulus cloud. Institute of Atmos. Sci., S. D. School of Mines, Rapid City, S. Dak., Report 68-9.

Locatelli, J. D., and P. Hobbs, 1974: Fall speeds and masses of solid precipitation particles. J. Geophys. Res., 79, 2185-2197.

Manton, M., and W. Cotton, 1977: Formulation of approximate equations for modeling moist deep convection on the mesoscale. Dept. of Atmos. Sci., Paper No. 266, Colo. St. Univ., Ft. Collins, Colo., 62pp.

Marshall, J. S., and W. McK. Palmer, 1948: The distribution of raindrops with size. J. Appl. Meteor., 5, 165-166.

Mason, B. J., 1956: On the melting of hailstones. Quart. J. R. Meteor. Soc., 82, 209-216.

_____, 1971: The Physics of Clouds, Oxford Univ. Press, Belfast, N. Ireland, 671pp.

Matsuno, T., 1966: Numerical integrations of the primative equations by a simulated backward difference method. J. Meteor. Soc. Japan, 44, 76-83.

Miller, M. J., 1978: The Hampstead storm: A numerical simulation of a quasi-stationary cumulonimbus system. Quart. J. R. Meteor. Soc., 104, 413-427.

Mossop, S. C., and A. Ono, 1969: Measurements of ice crystal concentrations in clouds. J. Atmos. Sci., 26, 130-137.

Musil, D. J., 1970: Computer modeling of hailstone growth in feeder clouds. J. Atmos. Sci., 27, 474-482.

_____, P. L. Smith, Jr., and A. J. Heymsfield, 1978: Total hydrometeor spectra in a hailstorm and implications for precipitation growth processes. Conference on Cloud Physics and Atmospheric Electricity, A.M.S., Issaquah, Wash., 173-177.

Ogura, Y., and T. Takahashi, 1971: Numerical simulation of the life cycle of a thunderstorm cell. Mon. Wea. Rev., 99, 895-911.

Ono, N., 1969: The shape and riming properties of ice crystals in natural clouds. J. Atmos. Sci., 26, 138-147.

REFERENCES (continued)

Orville, H. D., and K. Hubbard, 1973: On the freezing of liquid water in a cloud. J. Appl. Meteor., 12, 671-676.

_____, and F. J. Kopp, 1977: Numerical simulation of the life history of a hailstorm. J. Atmos. Sci., 34, 1596-1618.

_____, 1978: A review of hailstone-hailstorm numerical simulations. A.M.S. Monograph No. 38, 49-61.

Passarelli, R. E., Jr., 1978: An approximate analytical model of the vapor deposition and aggregation growth of snowflakes. J. Atmos. Sci., 35, 118-124.

Pitter, R. L., and H. R. Pruppacher, 1974: A numerical investigation of collision efficiencies of simple ice plates colliding with supercooled water drops. J. Atmos. Sci., 31, 551-557.

Saunders, P. M., 1957: The thermodynamics of saturated air: a contribution to the classical theory. Quart. J. R. Meteor. Soc., 83, 342-350.

Scott, B. C., and P. V. Hobbs, 1977: A theoretical study of the evolution of mixed-phase cumulus clouds. J. Atmos. Sci., 34, 812-826.

Simpson, J., and V. Wiggert, 1969: 1968 Florida seeding experiment: Numerical model results. Mon. Wea. Rev., 97, 471-489.

Sulkveligze, G. K., et al., 1967: Formation of Precipitation and Modification of Hail Processes. Israel Program for Scientific Translations, Jerusalem, 208pp. (Gidrometeor, Leningrad).

Takahashi, T., 1976: Hail in an axisymmetric cloud model. J. Atmos. Sci., 33, 1579-1601.

_____, 1978: Precipitation mechanisms in a shallow convective cloud model. J. Atmos. Sci., 35, 277-283.

Weinstein, A. I., 1970: A numerical model of cumulus dynamics and microphysics. J. Atmos. Sci., 27, 246-255.

Wisner, C. W., et al., 1972: A numerical model of a hail-bearing cloud. J. Atmos. Sci., 29, 1160-1181.

Vali, G., 1968: Ice nucleation relevant to formation of hail. Sci. Rep. MW-58, Dept. of Meteorology, McGill Univ., 51pp.

REFERENCES (continued)

Vali, G., 1973: Remarks on the mechanism of atmospheric ice nucleation. Proc. 8th International Conf. of Nucleation, Leningrad, 23-29, Sept., I. I. Gaivoronsky, Ed., Gidrometeorjdat, 265-269.

Young, K. C., 1974: The role of contact nucleation in ice phase initiation in clouds. J. Atmos. Sci., 31, 768-776.

_____, 1974: A numerical simulation of wintertime, orographic precipitation: I & II. J. Atmos. Sci., 31, 1735-1767.

_____, 1975: Growth of the ice phase in strong cumulonimbus updrafts. Pure and Applied Geophysics, special issue: Cloud Dynamics, ed. Hans R. Pruppacher, 1005-1017.

Zikmunda, J., and G. Vali, 1972: Fall patterns and fall velocities of rimed ice crystals. J. Atmos. Sci., 29, 1334-1347.

APPENDIX I

Ice Saturation Thermodynamics and Isobaric Adjustment

1.0 Isobaric ice saturation adjustment

The first law of thermodynamics for an isobaric ice saturation adjustment is

$$C_{pd}\, dT = L_{\ell i}\, q_c + L_{vi} \left(q_v - q_{si}\,(T') \right) \tag{1}$$

where the heat capacity of water is assumed negligible, T' is the final temperature after adjustment, q_c is the mixing ratio of cloud water to be frozen, q_v is the mixing ratio of water vapor at the current temperature T and $dT = T' - T$.

The Clausius-Clapeyron equation for an isobaric process is

$$dT = \frac{T^2 R_a}{\varepsilon L_{vi}\, q_{si}} \left(q_{si}(T') - q_{si}(T) \right)$$

which after solving for $q_{si}(T')$ gives

$$q_{si}(T') = q_{si}(T) + \frac{\varepsilon L_{vi}\, q_{si}}{T^2 R_a}\, dT. \tag{2}$$

Substituting (2) into (1) gives

$$C_{pd}\, dT = L_{\ell i}\, q_c + L_{vi}\, (q_v - q_{si}) - \frac{\varepsilon L_{vi}^2\, q_{si}}{T^2 R_a}\, dT$$

where all variables with the exception of dT are at T. Solving for dT gives

$$dT = \frac{L_{\ell i}\, q_c + L_{vi}\, (q_v - q_{si})}{C_{pd} + \dfrac{\varepsilon L_{vi}^2\, q_{si}}{T^2 R_a}} \tag{3}$$

The change in the water vapor mixing ratio

$$dq_v = q_{si}(T') - q_v$$

can be obtained by eliminating dT between (1) and (3):

$$dq_v = - \frac{q_v - q_{si}}{1 + B} + \frac{\frac{L_{\ell i}}{L_{vi}} q_c}{1 + 1/B} \tag{4}$$

where

$$B = \frac{\varepsilon L_{vi}^2 q_{si}}{C_{pd} T^2 R_a} .$$

For this process, the change in the snow mixing ratio will be

$$dq_f = - dq_v + q_c$$

$$= \frac{q_v - q_{si}}{1 + B} - \frac{\frac{L_{\ell i}}{L_{vi}} q_c}{1 + 1/B} + q_c \tag{4}$$

where it has been assumed that all cloud water is frozen into snow.

2.0 Ice saturation thermodynamics

Assuming ice saturation and all heat storage is in the water vapor, the first law of thermodynamics can be written as

$$-L_{vi}\, dq_{si} = C_{pd}\, dT - \frac{dp}{\rho} \tag{5}$$

where ρ is the total density of the air.

From the ideal gas law

$$\rho = \frac{p}{\sigma R_a T} \tag{6}$$

where

$$\sigma = \frac{1 + q_{si} / \varepsilon}{1 + q_{si}} .$$

Replacing ρ in (5) with (6) gives

$$-L_{vi}\, dq_{si} = C_{pd}\, dT - R_a T\, d\ell n\, p.$$

Dividing by temperature and using the Clasius-Claperon equation in the form

$$d\ \ell n\ T = \frac{R_v T}{L_{vi}}\ d\ \ell n\ e_{si}$$

where R_v is the gas constant for water vapor, gives

$$-\frac{L_{vi}}{T}\, dq_{si} = \frac{C_{pd}\, R_v\, T}{L_{vi}}\ d\ \ell n\ e_{si} - \sigma\, R_a\, T\, d\ \ell n\ p. \qquad (7)$$

Now we find an expression for $d\ \ell n\ e_{si}$:

$$e_{si} = R_v\, T\, q_{si}\, \rho_a$$

taking the natural logarithm gives

$$d\ \ell n\ e_{si} = d\ \ell n\ T + d\ \ell n\ q_{si} + d\ \ell n\ \rho_a$$

but $d\ \ell n\ \rho_a + d\ \ell n\ T = d\ \ell n\ p_a$

or $d\ \ell n\ e_{si} = d\ \ell n\ q_{si} + d\ \ell n\ p_a$

since $p_a = p - e_{si}$

$$d\ \ell n\ e_{si} \cong d\ \ell n\ q_{si} + \ell n\ p - d\ (\frac{e_{si}}{p}) \qquad (8)$$

where the series approximation $\ell n(1 - \frac{e_{si}}{p}) \cong -\ell n\ \frac{e_{si}}{p}$ has been used since $e_{si}/p << 1$. Substituting (8) into (7) gives

$$-\frac{L_{vi}}{T}\,dq_{si} = \frac{C_{pd}\,R_v\,T}{L_{vi}}\left[d\,\ell n\,q_{si} + d\,\ell n\,p - d\left(\frac{e_{si}}{p}\right)\right]$$

$$-\sigma\,R_a\,T\,d\,\ell n\,p.$$

After some manipulation, the above equation can be written as

$$\left(\frac{L_{vi}^2\,q_{si}}{C_{pd}\,R_a\,T^2} + 1\right) d\,\ell n\,q_{si} = \frac{e_{si}}{p}\left(d\,\ell n\,e_{si} - d\,\ell n\,p\right) + \left(\frac{\sigma R_a\,L_{vi}}{C_{pd}\,R_v\,T} - 1\right) d\,\ell n\,p.$$

The term $\frac{e_{si}}{p}\,(d\,\ell n\,e_{si} - d\,\ell n\,p)$ is small relative to the others, gives for the above equation

$$d\,\ell n\,q_{si} = \frac{\frac{\sigma R_a\,L_{vi}}{C_{pd}\,R_v\,T} - 1}{1 + \frac{L_{vi}^2\,q_{si}}{C_{pd}\,R_v\,T^2}}\,d\,\ell n\,p. \qquad (9)$$

Assuming the hydrostatic equation in the form

$$d\,\ell n\,p = \frac{-G}{\sigma\,R_a\,T}\,dz$$

and substituting it into (9) gives

$$d\,\ell n\,q_{si} = \frac{G}{\sigma\,R_d\,T}\,\frac{1 - \frac{\sigma R_a\,L_{vi}}{C_{pd}\,R_v\,T}}{1 + \frac{L_{vi}^2\,q_{si}}{C_{pd}\,R_v\,T^2}}\,dz.$$

Dividing by dt and using the fact that $\varepsilon = R_a/R_v$ and $dz/dt = w$ and assuming $\sigma \cong 1$ gives for the above equation

$$\frac{dq_{si}}{dt} = \frac{w\,G}{R_a\,T} \frac{1 - \dfrac{\varepsilon\,L_{vi}}{C_{pd}\,T}}{1 + \dfrac{\varepsilon\,L_{vi}^2\,q_{si}}{C_{pd}\,R_a\,T^2}}\; q_{si} \,. \qquad (10)$$

The change to the snow mixing ratio is simply

$$\frac{dq_f}{dt} = - \frac{dq_{si}}{dt}$$

where $\frac{dq_{si}}{dt}$ is given by (10).

IBLIOGRAPHIC DATA HEET	1. Report No. CSU-ATSP- 319	2.	3. Recipient's Accession No.
. Title and Subtitle A Simple Ice Phase Parameterization			5. Report Date December, 1979 6.
. Author(s) Mark Argyle Stephens			8. Performing Organization Rept. No. CSU-ATSP- 319
. Performing Organization Name and Address Department of Atmospheric Science Colorado State University Fort Collins, Colorado 80523			10. Project/Task/Work Unit No. 11. Contract/Grant No. NSF ATM77-09770
. Sponsoring Organization Name and Address National Science Foundation 1951 Constitution Avenue, N.W. Washington, D.C. 20550			13. Type of Report & Period Covered Masters Thesis 14. June 1976-May 1979

. Supplementary Notes

. Abstracts

A two variable ice parameterization was developed for use in three-dimensional models of cumulonimbus clouds and mesoscale squall lines. Bulk water techniques were employed to simulate the growth and decay of snow crystals and of graupel in order to keep the use of computer resources to a minimum. An externally specified concentration of ice crystals was used to initiate snow. Graupel was assumed to follow the Marshall-Palmer distribution with a constant total concentration. Microphysical growth processes for snow included initiation from the vapor at liquid water saturation, riming, melting, vapor deposition and conversion of rimed crystals into graupel. The graupel microphysical processes that were modeled included raindrop freezing by contact with snow crystals, accretion of raindrops, vapor deposition, riming of cloud droplets and melting. Both types of ice were allowed to precipitate.

Sensitivity tests and internal consistency checks on the parameterization were done using a one-dimensional, time-dependent cloud model. Results suggested that the parameterization should simulate adequately the ice phase evolution in higher dimensional models. The parameterization is most suitable for modeling studies in which the major emphasis is on exploring the dynamic consequences of the ice phase rather than exploratory studies in cloud microphysics. Several deficiencies of the parameterization were commented on, specifically: the use of an externally specified snow concentration and its influence on the conversion of snow into graupel. Comments were also made on how local changes in the snow concentration brought about by seeding, ice multiplication and aggregation could be handled in higher dimensional models.

. Key Words and Document Analysis.

(1) ice phase
(2) convective clouds
(3) numerical modeling
(4) parameterization

. Availability Statement	19. Security Class (This Report) UNCLASSIFIED X	21. No. of Pages 122
	20. Security Class (This Page) UNCLASSIFIED	22. Price

RM NTIS-35 (Rev. 3-72)